2013

A zonal model to aid in the design of household biomass cookstoves

Nordica Ann MacCarty
Iowa State University

A zonal model to aid in the design of household biomass cookstoves

by

Nordica Ann MacCarty

A thesis submitted to the graduate faculty

in partial fulfillment of the requirements for the degree of

MASTER OF SCIENCE

Major: Mechanical Engineering

Program of Study Committee:

Kenneth Mark Bryden, Major Professor

Arne Hallam

Xinwei Wang

Iowa State University

Ames, Iowa

2013

TABLE OF CONTENTS

LIST OF FIGURES

LIST OF TABLES

ACKNOWLEDGEMENTS

I would like to express my gratitude and dedicate this work…

To Odin, my delightful and astonishing son who made his imminent presence on Earth known mere hours after the opportunity to return to graduate school was offered, and whose first three and a half years I was immensely grateful to be able to be present for and cherish throughout this work.

To my enthralling husband Lance, who has always provided the perspective, love and humor needed to create and pursue our dreams and to 'offer our gifts to the world'.

To my parents, Warren and Sharon Hudelson, who instilled the importance of education, nature, and conservation from an early age and whose daily use of rural Minnesotan biomass for cooking, heating and building has no doubt shaped my underlying passions and priorities.

To Dean Still, my mindful mentor in life and cookstoves, and the extended family of Aprovecho Research Center including Damon Ogle, Sandra Moen, Larry Winiarski, Tami Bond, Dale Andreatta and the late Ken Goyer, whose true friendship and kind hearts made magic happen every day; and to all of the global cookstove community whose passion and dedication touch many lives, including my own.

To the United States National Science Foundation, and the taxpayers who support it, for making scientific discoveries a priority and a path forward, and opening opportunities for women.

And to my long-time mentor and advisor Dr. Mark Bryden, who introduced me to a formative adventure in cookstoves over a decade ago, encouraged me to continue my education in order to

share a love of learning and discovery, and whose commitment to helping the poor and living an principled life by example has brought me more inspiration, knowledge, and opportunities than can be expressed.

ABSTRACT

This thesis develops a computational model of a household biomass cookstove for use by the 2.7 billion people currently cooking with biomass in developing countries. This traditional practice results in a number of detrimental effects to health, ecosystems, and global climate, including indoor air pollution, which is responsible for 4 million premature deaths per year and represents the second leading cause of death for women globally. Despite several decades of engineering improved biomass cookstoves, to date there has been relatively little research regarding the computational modeling of such widely used devices. Development of a flexible, comprehensive, computationally inexpensive, and coupled model with detailed experimental validation will allow the design of cookstoves to benefit from the same engineering tools used in design for the developed world.

Through investigation of techniques employed in the literature, a flexible steady-state model is developed for a single pot, natural draft, shielded fire stove burning traditional wood fuel to predict the fluid flow and heat transfer characteristics of the system, which is separated into the (1) bed, (2) flame, and (3) heat transfer zones. The model incorporates 15 design parameters, including 10 geometrical, 2 material, and 3 operating variables spanning the region of interest for household biomass cookstoves. The model is validated from a unified experimental data set developed from three studies in the literature that report thermal performance characteristics in terms of design characteristics. The data set includes 63 data points incorporating variation of all 15 parameters and is shown to be consistent and supportive of qualitative thumb rules regarding the effects of stove geometry, operating variables, and material on overall thermal performance. Several adjustable coefficients and convective heat

transfer correlations are fitted to the data using particle swarm optimization. The model utilizes contracting mapping to predict air flow and temperature profile, resulting in 94% of the data points predicted within 5% of measured thermal efficiency and a L2 norm error of 3%. The model can be used to optimize heat transfer efficiency given local constraints for design and allows for conceptual design and sensitivity analysis without the need for extensive experimentation. In addition, the temperature and velocity profiles, location and magnitude of losses, and heat transfer contributions through various modes and regions of the pot are detailed to lead to greater understanding of the cookstove system.

NOMENCLATURE

A	Area
c_p	Specific heat
D	Diameter
D_h	Hydraulic diameter
F	View factor
f	Friction factor
g	Gravity
H	Height
h	Specific enthalpy
$\tilde{h}$	Convective heat transfer coefficient
h_{fg}	Latent heat of vaporization
i	Counter, species flow in a bed zone
j	Counter, incoming species in a flame zone
k	Counter, total species flow of gases
$\tilde{k}$	Thermal conductivity
l	Counter, pressure losses
K	Pressure loss coefficient
$\dot{m}$	Mass flow
q	Heat transfer rate
r	Radius
R	Thermal resistance
T	Temperature
V	Velocity
W	Width
x	Segment length
β	Fuel bed size factor
ε	Emissivity
λ	Excess air
μ	Viscosity
η	Thermal efficiency
ρ	Density
σ	Stefan-Boltzmann constant
τ	Transmissivity
ϕ	Radiation heat transfer adjustment factor
Nu	Nusselt number
Pr	Prandtl number
Re	Reynolds number
HHV	Higher heating value
LHV	Lower heating value

Subscripts

air2	secondary air
amb	ambient
bed	fuel bed
c	combustion chamber
char	char
cond	conduction
cont	contraction
exp	expansion
ext	exterior wall
flame	flame
int	interior wall
plume	plume
pot	pot
rad	radiation
s	stove
sh	shield
v	volatiles
w	water
wall	wall

CHAPTER 1
INTRODUCTION

Nearly 2.7 billion people use solid biomass fuels for household cooking and heating in open fires and simple stoves (Legros et. al., 2009; Bruce et. al,, 2006; IEA 2010). The users of these stoves live almost entirely in the developing world, and the individual, community, and global impacts of these small biomass cookstoves is significant. It has been estimated that indoor air pollution from solid fuel use is responsible for nearly 4 million deaths annually and approximately 4% of the global burden of disease, representing the second leading cause of death for women globally (Lim et. al, 2012; WHO, 2004). The fine particulate matter, carbon monoxide, polycyclic aromatic hydrocarbons, and other emissions due to incomplete combustion within poorly ventilated spaces contribute to acute lower respiratory infections, pneumonia, and chronic obstructive lung disease; as well as adverse pregnancy outcomes and cataracts (Legros et. al., 2009; Bruce et. al,, 2006; WHO, 2004). In many cases, the use of biomass fuel for household energy is exacerbated by deforestation and desertification around communities, leading to increased time and energy spent in gathering fuel, and it poses a significant opportunity cost to educational, health, and income-generating activities, primarily for women and children (Rehfuess, 2006). In addition, the use of biomass for cooking and heating is a significant source of global black carbon emissions, one source of climate change (Bond et. al., 2013).

The ‘vicious circle’ of energy poverty and environmental deterioration, health degradation, and opportunity costs inhibits the capacity to move from the use of energy for simply meeting basic survival needs to productive or income-generating energy use.

> Poor families spend one-fifth or more of their income on wood and charcoal, devote one-quarter of household labor collecting fuelwood, and then suffer the life-endangering pollution that results from inefficient combustion (Sovacool, 2012).

While cleaner liquid fuels higher on the 'energy ladder' would help to address these individual, community, and global impacts, the cost of such fuels is often prohibitive for these subsistence level families. Recent projections indicate that use of biomass for cooking will increase and remain the dominant energy use in rural, resource-poor households through 2030 (Daioglou, van Ruijven, and van Vuuren, 2012; IEA, 2010), and studies in the West African Sahel found that 98% of household energy needs are met with small household cookstoves (Johnson and Bryden, 2012 a and b). Therefore, a number of groups have focused on the research and development of improved small biomass cookstoves and cookstove replacement programs, with more than 160 stove replacement projects currently operating worldwide (Ruiz-Mercado et. al., 2011). However, few of these efforts have focused on developing numerical models of cookstoves. In the past 30 years more than 500 journal articles have examined various aspects of biomass cookstoves; however, fewer than 30 journal articles have addressed numerical modeling of the heat transfer and combustion processes in traditional biomass fueled stoves, and none of these are flexible, comprehensive, computationally inexpensive, coupled, or provide detailed experimental validation of the computational results.

Because of this, the design of cookstoves today remains a heuristic trial and error process based on previous experience, engineering judgment, thumb rules, and experiment. Beginning with a conceptual design generated from previous models, a prototype is built and tested for performance. Parametric changes are made and tested again. When a sufficient design is found, the stove is brought to the field for further testing, refinement, and eventual dissemination. This iterative process results in greater time and resources spent on prototype development,

construction, and testing, provides less understanding of the coupled processes within the system, and may miss techniques and opportunities for increasing efficiency. Application of the same design and modeling tools used for product design in the developed world would help to address these issues.

Scientific modeling can help researchers to explore design options and their implications using a simplified representation of the world. The purpose of such models is not necessarily to provide designs, but to help ask better questions and make more informed decisions (Hartter and Boston, 2007). Modeling tools for cookstoves would permit examination of complex and coupled heat transfer, fluid flow, and combustion processes within stoves and would support better, faster, more adaptive designs. However, to date there is no dominant design basis or established design algorithm for optimizing the efficiency of these devices, nor are there validated and accepted models or modeling guidelines to support the design process. In addition, there is no standard methodology for stove testing and reporting such that experimental data can be used for model development and validation. This research aims to begin to address these gaps in order to incorporate computational modeling into the cookstove design process.

1.1 Overview

The primary goal of this thesis is to develop a detailed computational zonal model of the heat transfer and fluid flow processes in a natural draft, shielded-fire wood-burning cookstove fitted with a single, flat-bottomed, potentially shielded pot, presented in Chapter 5. This model brings together techniques of previous simplified models from the literature, explored in Chapter 3, to develop a more comprehensive model. Unlike high-fidelity models which use computational fluid dynamics (CFD) software to provide a detailed analysis of a specific region,

this model is flexible and computationally inexpensive, allowing for analysis of the entire stove system under the variation of three operating and 12 physical variables. The model uses a unified set of experimental data from the literature, compiled in Chapter 4, to generate empirical correlations for the heat transfer coefficients for previously uncertain areas in the system.

This research specifically focuses on biomass cookstoves fueled with solid unprocessed biomass ranging in size from 1 to 20 cm, and operated by an individual in a residential setting. Although called cookstoves, depending on local custom and need the primary uses of these stoves include heating water for washing, cooking meals, steeping tea, making medicines, and other household tasks (Johnson and Bryden, 2012a). These types of stoves account for the majority of cookstove designs in use in the developing world today (Jetter et. al, 2012; MacCarty, Still, and Ogle, 2010). Although in some cases the issues are similar, this research does not address charcoal or coal stoves, forced draft stoves, gasifier stoves, pulverized fuel stoves, institutional scale stoves, or stoves used for space heating. Nor does it address the issues associated with fuel processing and fuel pellets. As gaps in the data are identified and further testing is completed, the data set can be expanded to assist in improving and broadening models.

Chapters 3, 4, and 5 present this research in the form of three journal articles that present the required theory, data, and methodology for the development of the model. Chapter 3 reviews the current cookstove modeling literature and the evolution of modeling efforts since the early 1980s. Theory, assumptions, and results of each model are presented and compared. Key methods and equations are highlighted for use in the present and future models.

Chapter 4 provides a unified, consistent data set with sufficient detail and parametric variation spanning the region of interest for validation of the model. Descriptions of the data set design variables, test methods, and experimental results are provided. The data are analyzed to

ensure consistency and to quantitatively confirm known qualitative thumb rules within the design space.

Chapter 5 presents the development and use of the model. Beginning with the methods used in the literature, the equation set is developed for the three zones (fuel bed, flame, and heat transfer) of the system and five geometrical regions of the flow path. Options for various correlations are explored, including friction, pressure loss, and radiation; and coefficients for convective heat transfer correlations are fitted to the data set. Simulations are run to investigate the design lessons that can be learned through use of the model.

The primary researcher and author of the journal articles is Nordica A. MacCarty, graduate student, advised by Kenneth M. Bryden, Associate Professor, Department of Mechanical Engineering, Iowa State University.

1.2 Summary

This research presents a computational model of heat transfer and fluid flow in a small biomass cookstove. Results are presented in three journal articles: (1) a literature review of the current state of cookstove modeling, (2) a unified data set from the literature for verifying thumb rules and validating the model, and (3) the underlying equation set, development, and use of the computational model.

CHAPTER 2

BACKGROUND

2.1 Types of Cookstoves

A traditional biomass cookstove consists of the air intake and transport system, a bed of fuel, a gas phase combustion zone, and a cooking pot. There are three primary types of traditional household biomass cookstoves based on the treatment of the combustion chamber:

1. Open cooking fires—these are traditional cooking fires in which a pot is held atop three stones or other similar support (Fig. 1a). The airflow is uncontrolled and the air is entrained in the system due to buoyancy. Generally a fire grate is not included.
2. Shielded cooking fires—these stoves are often referred to as improved stoves and marketed under a number of names. These devices range from a simple shield of metal or clay around the combustion space to more complex devices with inlets for directed control of primary and secondary air (Fig. 1b). Some include electrically powered fans to control air. In some cases a narrow channel is created around the pot to improve heat transfer from the combustion gases to the pot. There may or may not be a fire grate provided.
3. Enclosed fires with chimneys—these stoves are similar to stoves used for space heating but have high temperature cooking surfaces (Fig. 1c). The fire is fully enclosed within the combustion chamber. The fuel entrance may be open and permit airflow into the system. Alternatively, there may be a tightly sealed fuel door and separate controls for airflow into to the stove. Gases leave the combustion chamber and travel along channels underneath the exposed pot bottoms or a large sealed plate or griddle on which pots are

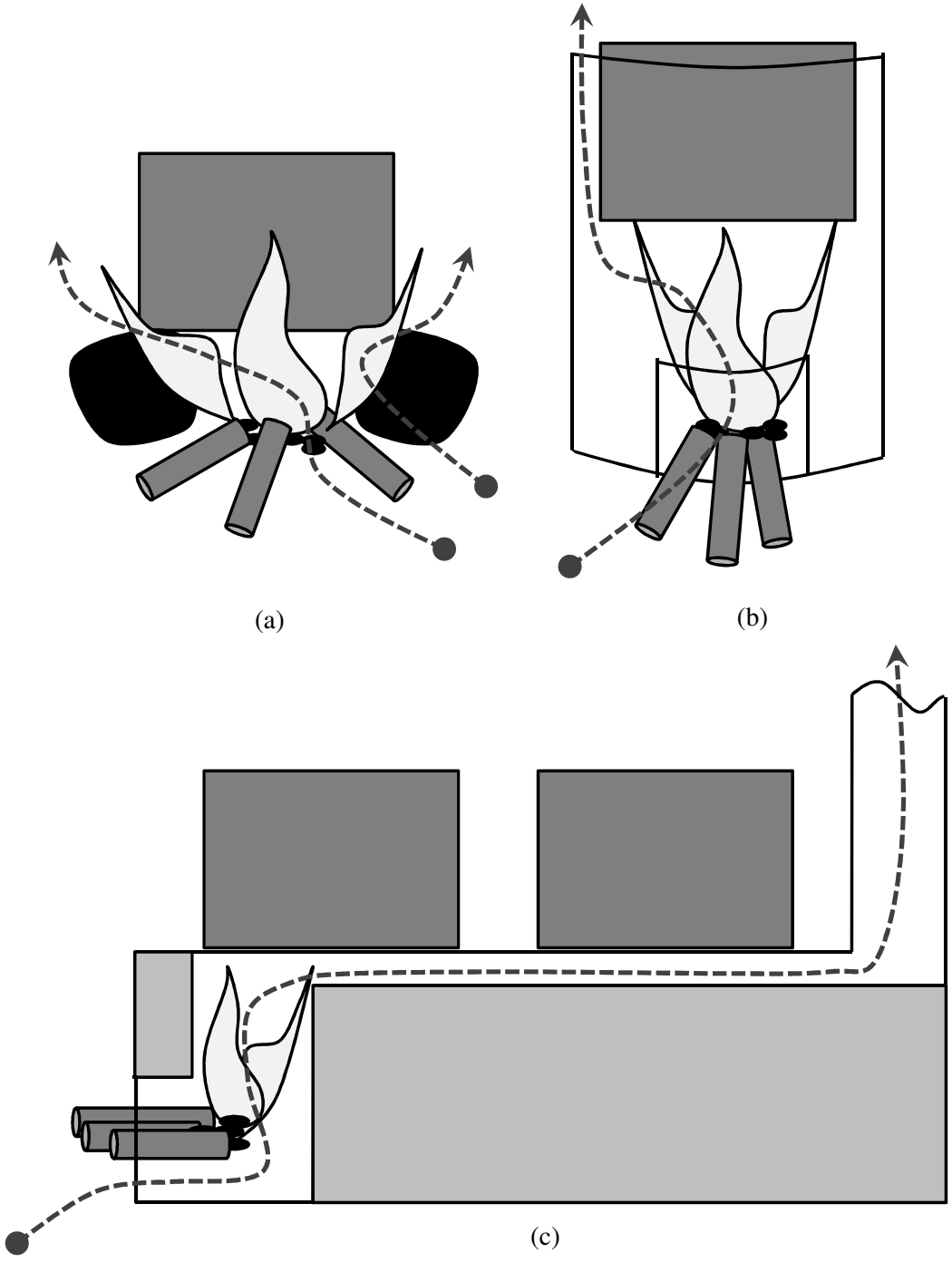

Figure 2.1. Types of cookstoves: (a) Open cooking fire, (b) Shielded cooking fire, (c) Enclosed fire with chimney

heated or food is cooked directly. The combustion gases then exit to the chimney and are exhausted outside of the kitchen.

The basic operation of all three types of stoves is similar. They are fueled with wood or biomaterials (e.g., dung cake or crop residues), ranging in size from small twigs to large un-split branches. The as-received fuel moisture varies in moisture content from 5% to greater than 50% depending on the season, storage availability, harvest method, and curing time (Ragland and Bryden, 2011). Due to limited control of primary and secondary airflow, there is often high excess air resulting in low combustion gas temperatures, short transit times, and incomplete combustion. The challenge for designers of these devices is to create a user-friendly cooking appliance that can utilize a wide array of fuel types, sizes, and moisture contents while maintaining high overall efficiency and low emissions.

2.2 Types of Models

Two types of cookstove models have been developed by researchers. The primary type of model is a zonal model in which conservation of mass, momentum, and energy are applied to various zones within a cookstove. In the second type of model computational fluid dynamics (CFD) is used to examine various aspects of small cookstoves. Initial modeling efforts included algebraic and differential zonal models of open fires, shielded-fire stoves, and enclosed stoves in the 1980s by the Woodburning Stove Group at Eindhoven University. These efforts identified equation sets for fluid flow and heat transfer throughout the system (Bussmann, Visser, and Prasad, 1983; Bussmann and Prasad, 1986). This was followed by investigation of specific regions such as wall losses or heat transfer correlations within a pot shield (Baldwin, 1987), or

models of a specific stove design (Date, 1988; Kumar, Lokras, and Jagadish, 1990). After a dry period in the 1990s, researchers continued to algebraically model specific stove designs (Agenbroad et. al. 2011a, 2011b; Zube, 2010), and some incorporated solid and gas phase combustion rates and efficiency (Shah and Date, 2011). Commercial computational fluid dynamics packages for stove modeling also began to be used for the complete system (Burnham-Slipper, 2007a, 2007b, 2008; Gupta and Mittal, 2010a, 2010b; Ravi, Kohli, and Ray, 2002) or for investigating heat transfer in specific regions of the stove (Wohlgemuth, 2009; Urban, 2002; McCorkle, Bryden, and Carmichael, 2003). The lessons learned through these efforts were valuable for the creation of a zonal model and are reviewed in Chapter 3.

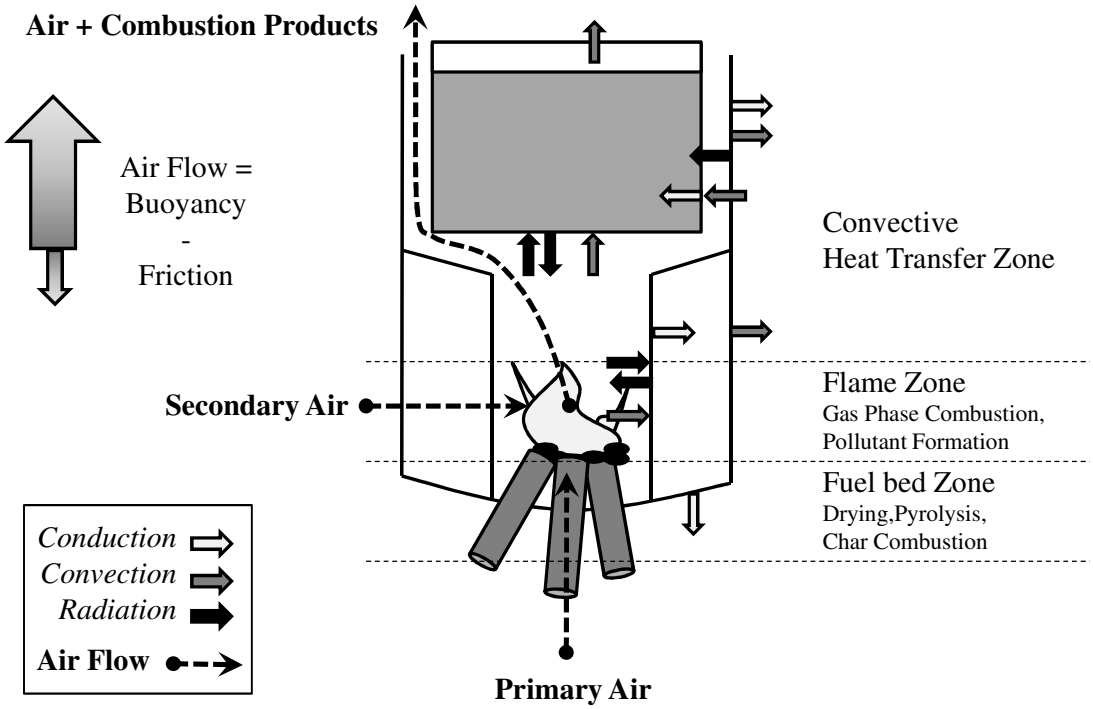

Figure 2.2. The cookstove system

For zonal modeling purposes, the cookstove system can be divided into three zones: the solid phase packed bed zone, the gas phase combustion or flame zone, and the heat transfer zone (Figure 2.2). In the packed bed, solid phase combustion includes heating of the wood and drying of the fuel moisture followed by pyrolysis and char burning with primary air. In the flame zone, secondary air enters, is heated, and is supplied to gas phase combustion. In the heat transfer zone, energy is lost through the stove walls, transferred to the pot via convection and radiation, and exits as sensible losses. Fluid flow and the entrainment of excess air are driven by natural buoyancy, and is slowed by pressure losses due to friction throughout the various geometries of the flow path.

2.3 Design Variables

The design variables required for development of a zonal model include the geometry

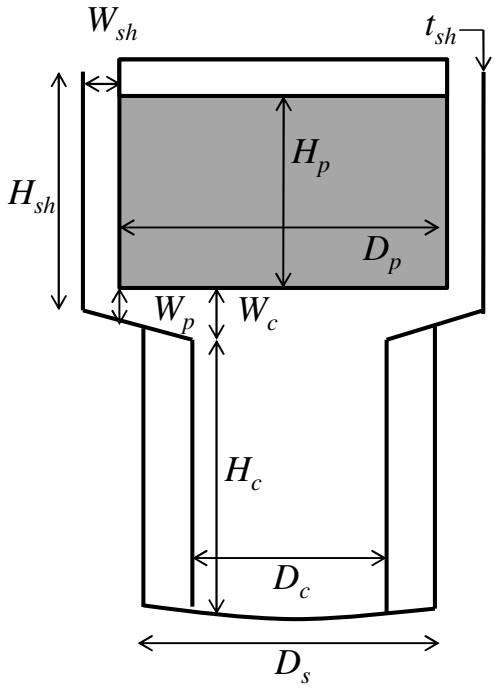

Figure 2.3. Geometrical variables

and materials composing the flow path and the operational variables of the fuel supply. The design outcome of interest is the thermal efficiency, or the energy transferred into the cooking pot as measured by water temperature rise and evaporation divided by the energy released by the fuel as measured by the heating value and mass of fuel burned during the test. Based on this, the following data are needed for input into the model:

1) Operational variables: experimental firepower, fuel moisture content, and lower heating value
2) Geometrical variables: a full description of the flow path, stove body, and cooking pot dimensions (Fig. 2.3) that are subject to the constraints of the model

   D_c – combustion chamber diameter
   H_c – combustion chamber height
   W_c – gap at the edge of the combustion chamber
   W_p – gap at the edge of the pot bottom
   W_{sh} – gap between the shield (if included) and pot
   D_p – pot diameter
   H_p – height of the water in the pot based on its occupied volume
   D_s – stove combustion chamber body diameter
   k_s – stove body material conductivity
   H_{sh} – height of the shield, if included
   t_{sh} – thickness of the shield material
   k_{sh} – shield material conductivity

3) Material variables such that the thermal conductivity of the stove body components can be determined
4) Measured thermal efficiency

2.4 Validation Data

A review of the literature revealed three major categories of stove testing data based on the goals of the study and therefore the data that was collected. (1) Regional in-field testing to generate databanks of fuel use and emissions performance for various stove-fuel combinations, such as (Smith, 1993, 2000; Zhang et. al., 2000; Bhattacharya, Albina, and Khaing, 2002a, 2002b; Bailis, Ezzati, and Kammen, 2003). The goal of this work is to catalogue various cookstove/fuel combinations and extrapolate energy and pollutant data per capita for use in global inventories and policy decisions. (2) In-field testing comparing "improved" to "traditional" stoves as used by community members (Smith et. al, 2007; Johnson et. al, 2008; Roden et. al., 2009). The intent of this type of study was to determine the fuel and emissions savings or indoor air pollution reductions offered by specific stove designs. These studies incorporate the effects of user behavior and report metrics as percent improvement in task-based measures. (3) Stove testing for understanding, comparing, and improving design through measures of thermal performance characteristics in terms of stove design characteristics (Jetter and Kariher, 2009; Jetter et. al., 2012; MacCarty, Still, and Ogle, 2010). The goal of these laboratory based tests is to determine differences in fuel use and/or emissions performance due to stove type, model, or parametric changes to operational, material, or geometrical variables. This third category of data is required for model validation since the focus is the stove design characteristics and resulting thermal performance as opposed to the user or in-field conditions. Laboratory data, though not necessarily predictive of in-field performance (Johnson et. al, 2010), aims to remove the variability of user behavior inherent in field studies and is therefore required for models which assume steady-state operation.

Thus, the criteria for a study to suit the requirements needed for validating zonal models include the following:

1. Report thermal performance characteristics in terms of stove design characteristics, preferably including parametric variation.
2. Provide necessary design variables and thermal efficiency.
3. Include the stove type being modeled. This case models a natural draft, cylindrical, shielded cooking fire fitted with a flat-bottomed metal pot and stove burning wood sticks as fuel.

Include design variables within the design space of the model. For calculation of natural draft due to buoyancy in this case, the pot diameter must be greater than the combustion chamber diameter and the stove must be tall enough or utilize a pot shield such that the height of the flow exit is greater than 13 cm. Three articles were found to contain data points that met criteria 1 and 3 and either provided nearly enough data for criteria 2 that the missing pieces could be estimated, or were recent enough to include physical stove prototypes or primary data that were currently available. These included a parametric study of a shielded fire stove (Bussmann and Prasad, 1986), five of the stoves in a laboratory testing series (MacCarty, Still, and Ogle, 2010), and two of the stoves tested in a second testing series (Jetter et. al., 2012). From these three studies, 63 reported experimental data points were available. As a whole, the group includes variation of every geometrical, material, and operating design variable. Chapter 4 presents a compilation of the design variables values and measured thermal efficiency, and investigates the qualitative design trends observed from the data.

2.5 Equation Set

In the various zones and regions of the cookstove system, processes are evaluated and coupled through standard theory of combustion, heat transfer, and fluid flow.

2.5.1 Fuel Bed and Flame Zones

Within a packed bed, wood fuel is dried and pyrolyzed, and char is combusted at a rate consistent with the size, shape, arrangement, and feed rate of wood and thus firepower along with the diffusion and kinetics of the flow of primary, or underfire, air. The mass flow rate and enthalpy of wood, water vapor from fuel moisture, and gases (including air, pyrolysis, and carbon dioxide from char combustion) are determined such that conservation of energy in the bed zone is used to solve for the temperature of the gases leaving the bed. The hot gases from the fuel bed enter the flame zone where they are mixed with the secondary, or overfire, air. An energy balance in the flame zone is used to determine the gas temperature at the inlet of the combustion chamber. Gas phase combustion can be modeled using reaction mechanisms for major species.

2.5.2 Heat Transfer Zone

Beyond the heat release of the fuel bed and flame zone, the combustion gases flow up through the combustion chamber and around the pot. Energy losses through the stove body and heat transfer to the pot are found by the energy conservation equation for each region. Losses through the stove body are modeled as a thermal resistance analog including convection, conduction and radiation; and convective heat transfer to the walls and bottom and sides of the pot are determined using Nusselt correlations. Radiation heat transfer can be modeled with various methods including assumed fraction of heat release, blackbody radiation between

surfaces, participating or non-participating media, and/or a radiation heat transfer adjustment factor fitted from experimental data.

2.5.3 Fluid Flow

Fluid flow through the system is driven by natural draft due to the buoyancy of hot air and dictates the mass flow rate and excess air through the system. Flow is determined from the pressure due to buoyancy at the stove exit minus the pressure losses due to friction and bends, expansions, and contractions in the path. These loss coefficients are determined from various correlations in the literature.

2.6 Summary

Computational modeling is an informative and illustrative step in the conceptual design of biomass cookstoves, allowing researchers to ask better questions and compare costs and benefits. Such modeling requires (1) an understanding of previous modeling efforts and theories of combustion, heat transfer, and fluid flow; (2) a unified and consistent data set for fitting and validating the model; and (3) a comprehensive and flexible equation set for modeling heat transfer and fluid flow. This thesis addresses these research areas for a cylindrical single pot shielded wood burning cookstove.

CHAPTER 3

MODELING OF HOUSEHOLD BIOMASS COOKSTOVES: A REVIEW

Draft of a paper submitted for publication in *Energy*

Nordica A. MacCarty, Kenneth M. Bryden

Abstract

Computational modeling has the potential to increase the speed, accuracy, and efficiency of the conceptual design of cookstoves, yet relatively little modeling work has been completed to date. This article reviews the cookstove modeling literature for natural draft, wood-fired cookstoves beginning in the early 1980s, including both zonal and high-fidelity models. Nineteen models are presented and compared, including details of assumptions, theory, results and validation. Discussion is organized around the three major zones of the cookstove system: (1) the fuel bed; (2) the flame zone; and (3) the heat transfer zone. Heat transfer and fluid flow correlations are compiled, as are various methods for radiation heat transfer and heat release from combustion. Today's model capability includes steady-state simplified analytic models of packed bed combustion, basic reaction mechanisms for several major species in gas phase combustion, generalized correlations for convection and radiation, and CFD-based models for heat transfer. Future models should be developed to include transient processes; models for combustion of various shapes, sizes and arrangements of fuel; pollutant formation; and flexible geometries and broad data sets for validation.

3.1 Introduction

More than 2.7 billion people use solid fuels for household cooking and heating in open fires and simple stoves (IEA, 2010). The users of these stoves live almost entirely in the developing world and the individual, community, and global impacts of these small biomass cookstoves are significant. It has been estimated that indoor air pollution from solid fuel use is responsible for nearly 4 million deaths annually and approximately 4% of the global burden of disease (Lim et. al, 2012; WHO, 2004). The fine particulate matter, carbon monoxide, polycyclic aromatic hydrocarbons, and other emissions due to incomplete combustion within poorly ventilated spaces contribute to acute lower respiratory infections, pneumonia, and chronic obstructive lung disease; as well as adverse pregnancy outcomes, and cataracts (Legros et. al., 2009; Bruce et. al,, 2006; WHO, 2004). In many cases, the use of biomass fuel for household energy contributes to deforestation and desertification around communities, leading to increased time and energy spent in gathering fuel, and posing a significant opportunity cost to educational, health, and income-generating activities, primarily for women and children (Rehfuess, 2006). In addition, the use of biomass for cooking and heating is a significant source of global black carbon emissions, one source of climate change (Bond, 2013).

Recognizing these individual, community, and global impacts; a number of groups have focused on the research and development of improved small biomass cookstoves. However, few of these efforts have focused on developing numerical models of cookstoves. In the past 30 years more than 500 journal articles have examined various aspects of biomass cookstoves; however, fewer than 30 journal articles have addressed numerical modeling of the heat transfer and combustion processes in traditional biomass fueled stoves. Because of this, today the design of small biomass cookstoves is primarily based on experience and thumb rules.

This paper reviews the current state of numerical modeling of small biomass cookstoves used by more than 2.4 billion households daily. Although in some cases the issues are similar, this article does not address charcoal or coal stoves, forced draft stoves, gasifier stoves, pulverized fuel stoves, institutional scale stoves, or stoves used for space heating. Nor does this article address the issues associated with fuel processing and fuel pellets. Specifically, this article focuses on one- to three-burner biomass cookstoves fueled with solid unprocessed biomass ranging in size from 1 to 20 cm, and operated by an individual in a residential setting. Although called cookstoves, depending on local custom and need the primary uses of these stoves include heating water for washing, cooking meals, steeping tea, making medicines, and other household tasks (Johnson and Bryden, 2012a). These types of stoves account for the majority of cookstove designs in use in the developing world today (Jetter et. al., 2012; MacCarty, Still, and Ogle, 2010).

3.2 Background

A traditional biomass cookstove consists of the air intake and transport system, a bed of fuel, a gas phase combustion zone, and a cooking pot. There are three primary types of traditional household biomass cookstoves based on the treatment of the combustion chamber:

1. Open cooking fires—these are traditional cooking fires in which a pot is held atop three stones or other similar support (Fig. 3.1a). The airflow is uncontrolled and the air is entrained in the system due to buoyancy. Generally a fire grate is not included.
2. Shielded cooking fires—these stoves are often referred to as improved stoves and marketed under a number of names. These devices range from a simple shield of metal or clay around the combustion space to more complex devices with inlets for directed

control of primary and secondary air (Fig. 3.1b). Some include electrically powered fans to control air. In some cases a narrow channel is created around the pot to improve heat transfer from the combustion gases to the pot. There may or may not be a fire grate provided.

3. Enclosed fires with chimneys—these stoves are similar to stoves used for space heating but have high temperature cooking surfaces (Fig. 3.1c). The fire is fully enclosed within the combustion chamber. The fuel entrance may be open and permit airflow into the system. Alternatively, there may be a tightly sealed fuel door and separate controls for airflow into to the stove. Gases leave the combustion chamber and travel along channels underneath exposed pot bottoms or a large sealed plate or griddle on which pots are heated or food is cooked directly. The combustion gases then exit to the chimney and are exhausted outside of the kitchen.

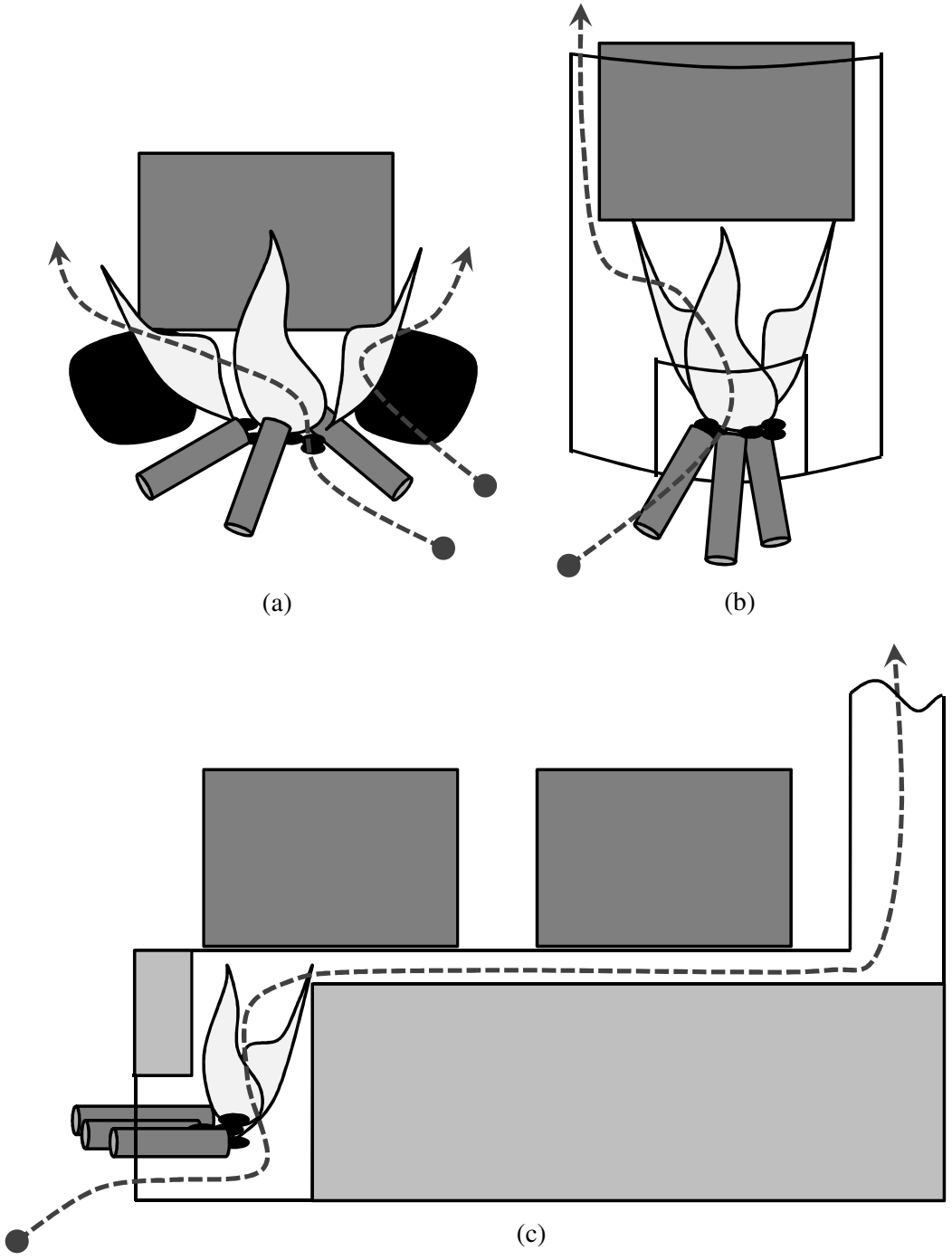

Figure 3.1. Types of cookstoves: (a) Open cooking fire, (b) Shielded cooking fire, (c) Enclosed fire with chimney

The basic operation of all three types of stoves is similar. They are fueled with wood or biomaterials (e.g., dung cake or crop residues), ranging in size from small twigs to large un-split branches. The as-received fuel moisture varies in moisture content from 5% to greater than 50% depending on the season, storage availability, harvest method, and curing time (Ragland and Bryden, 2011). Due to limited control of primary and secondary airflow, there is often high excess air resulting in low combustion gas temperatures, short transit times, and incomplete combustion. The challenge for designers of these devices is to create a user-friendly cooking appliance that can utilize a wide array of fuel types, sizes, and moisture contents while maintaining high overall efficiency and low emissions.

3.3 Cookstove Models

Figure 3.2 provides a schematic of a small biomass cookstove of the type used in nearly all numerical modeling of cookstoves. In general the goal of cookstove modeling has been to improve heat transfer efficiency of the cookstove system by examining the relationships between the combustion rate, excess air, geometry, and heat transfer. In all cases zonal models have been used to describe and couple the processes occurring within the three major zones of the cookstove system—the reacting fuel bed zone, the gas phase combustion zone, and the heat transfer zone around the cooking pot. Table 3.1 provides a chronological summary of published models.

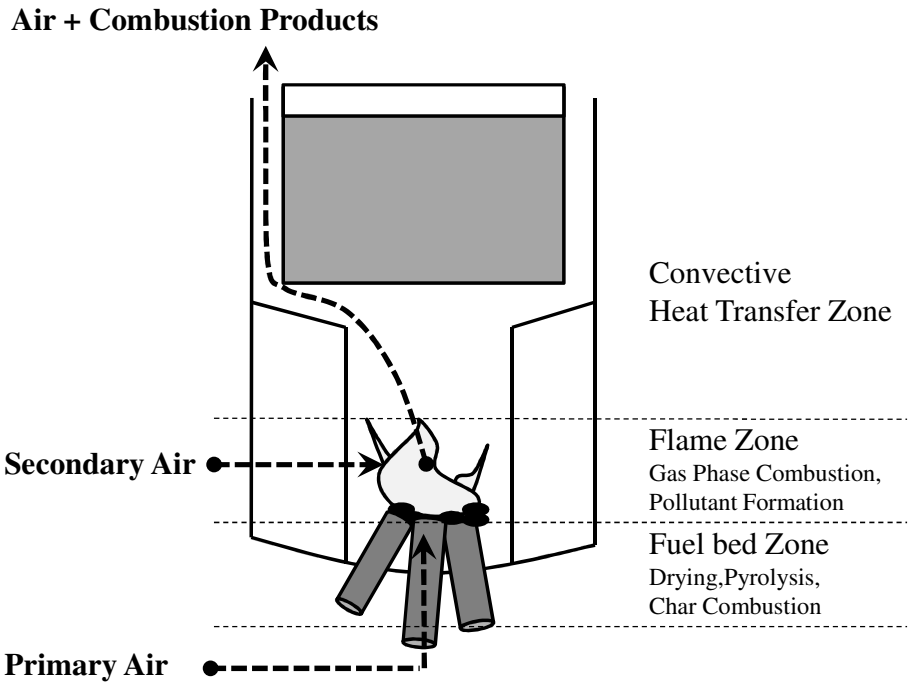

Figure 3.2. Processes within a cookstove

Table 3.1. Chronological summary of cookstove modeling efforts

Reference	Stove Type	Model Characteristics	Validation
De Lepeliere et. al., 1981	Enclosed Stove	Description – Combustion stoichiometry used to determine combustion chamber and primary/secondary air inlet dimensions for given firepower and excess air Packed bed model – no separate packed bed model Gas phase combustion model – no separate gas phase combustion model Heat transfer model – no separate heat transfer model	None
Verhaart, 1982	Enclosed Stove	Description – Empirical velocity of fire penetration used to determine whether heat supplied by char and volatile combustion can sustain a constant firepower Packed bed model – no separate packed bed model Gas phase combustion model – no separate gas phase combustion model Heat transfer model – no separate heat transfer model	None
Bussmann, Visser, and Prasad, 1983	Open Fire	Description – Coupled zonal model to predict temperature, plume width, and velocity for varying firepower, excess air, and volatile fraction Packed Bed Model – Conservation of energy for a control volume with given firepower and volatile fraction Gas phase combustion model – Differential conservation equations including reacting flow with air entrainment Heat transfer model – Local convective heat transfer correlations for bottom and sides of pot, blackbody radiation with nonparticipating media	Quantitative and qualitative experimental
De Lepeliere and Christiaens, 1983	Enclosed Stove	Description – Coupled flow and heat transfer analysis to investigate effects of several geometrical variables Packed bed model – given temperature Gas phase combustion model – no separate gas phase combustion model Heat transfer model – convective heat transfer correlation for short duct with laminar flow	None
Prasad, Sangen and Visser, 1985	Shielded Fire	Description -- Transient wall loss analysis for three body materials Packed bed model – no separate packed bed model Gas phase combustion model – no separate gas phase combustion model Heat transfer model – no separate heat transfer model	None
Bussmann and Prasad, 1986	Shielded Fire	Description – Coupled zonal model to predict efficiency for parametric variation of geometric variables Packed bed model – Same as (Bussmann, Visser, and Prasad, 1983) Gas phase combustion model – Heat addition nplete combustion, non-reacting flow Heat transfer model – Adiabatic wall, local co ve heat transfer correlations for bottom and sides of pot, blackbody radiation with nonparticipating media	Experimental
Baldwin, 1987	Shielded Fire	Description – Discussion and uncoupled models of steady-state and transient combustion and heat transfer processes to investigate effects of design variables Packed bed model – Simplified pyrolysis and 2-step char burning models presented Gas phase combustion model – Assumed temperature and velocity input to heat transfer zone Heat transfer model – Investigated effects of material and geometry on wall losses via thermal resistance analog, global convective heat transfer for the pot side, blackbody radiation using a fuel bed reduction factor of 0.5	Qualitative experimental

Table 3.1 continued

Date, 1988	Shielded Fire	Description – Coupled zonal model to predict efficiency for parametric variation of geometric variables Packed bed model – Time-averaged and temperature dependent char burning and volatile evolution for various wood diameters Gas phase combustion model – Heat addition of complete combustion, reactions added in (Shah and Date, 2011) Heat transfer model – Wall losses as thermal resistance analog, global convective heat transfer correlations from the literature, radiation with participating media as a function of beam length	Experimental
Kumar, Lokras, and Jagadish, 1990	Enclosed Stove	Description – Coupled zonal model to predict heat transfer and flue gas composition for varied firepower Packed bed model – Conservation of energy for a control volume given constant firepower, excess air, and mass of char remaining, no radiative losses Gas phase combustion model – Conservation of energy for a control volume in terms of specific heat of products of complete combustion Heat transfer model – Six well-stirred reactors with convective heat transfer correlations from the literature, cumulative conductive wall losses, and radiation as a function of CO_2, H_2O and beam length	Experimental
hutte et. al., 1991	Enclosed Stove	Description – Presented discussion for predicting flue gas composition in downdraft and traditional combustion with constant firepower Packed bed model – no separate packed bed model Gas phase combustion model – reacting flow using reaction rates from the literature including C, CO, CO_2 and H_2O Heat transfer model – no separate heat transfer model	Experimental
Weerasinghe and Kumara, 2003	Shielded Fire	Description – Coupled CFD model of flaming mode of combustion and heat transfer to determine optimal height Packed bed model – no separate packed bed model Gas phase combustion model – Reaction rate of fuel combustion according to dissipation rates Heat transfer model – CFD analysis	Heat transfer experimental
Bryden et. al., 2003	Enclosed Stove	Description – CFD simulation to optimize baffle placement with empirical inlet conditions Packed bed model – no separate packed bed model Gas phase combustion model – no separate gas phase combustion model Heat transfer model – CFD analysis to optimize heat transfer through griddle with inputs to heat transfer zone determined experimentally	Experimental
Brewster, 2006	Enclosed Stove	Description – Modeled flow conditions from a given heat source to optimize angle of baffle under pot Packed bed model – no separate packed bed model Gas phase combustion model – no separate gas phase combustion model Heat transfer model – CFD to optimize baffle angle	None

Table 3.1 continued

Burnham-Slipper, 2008	Shielded Fire	Description – CFD, analytical, and experimental studies of combustion and heat transfer to a flat plate for design optimization. Packed bed model – Simplified steady-state CFD model developed for a fixed crib of fuel, with pyrolysis limited by heat conduction through char and char combustion limited by oxygen diffusion Gas phase combustion model – CFD model using species transport limited by turbulent mixing Heat transfer model – CFD analysis of impinging jet, radiation as weighted sum of grey gases	Experimental and from literature
Wohlgemuth, Mazumder, and Andreatta, 2009	Shielded Fire	Description – CFD analysis of heat transfer for varying pot shield dimension and material using empirical inlet conditions Packed bed model – no separate packed bed model Gas phase combustion model – no separate gas phase combustion model Heat transfer model – CFD analysis of heat transfer within pot shield, radiation as gray gases with no scattering and tuned absorption coefficient with inputs to a heat transfer zone determined experimentally from detuned gas burner	Experimental used to tune unknown parameters
Gupta and Mittal, 2010a, 2010b	Shielded Fire	Description – CFD simulation of flow and heat transfer for varying operating and geometric variables Packed bed model – Assumed uniform 40% of heat release, permeability expressed through Karman-Cozeny relationship Gas phase combustion model – Assumed uniform 60% of heat release Heat transfer model – CFD analysis	From literature
Agenbroad et. al., 2011	Shielded Fire	Description – Analytical model to predict bulk flow rate, temperature, and excess air as a function of firepower and geometry for an adiabatic combustion chamber with no pot Packed bed model – no separate packed bed model Gas phase combustion model – no separate gas phase combustion model Heat transfer model – no separate heat transfer model	Experimental
Shah and Date, 2011	Shielded Fire	Description – Coupled zonal model to predict efficiency and combustion products for parametric variation of geometric variables Packed bed model – Taken from (Date, 1988) Gas phase combustion model – 4-step Hautmann quasi-global reaction treating stove regions as well-stirred reactors Heat transfer model – Taken from (Date, 1988)	Heat transfer experimental and literature
Joshi et. al, 2012	Shielded Fire	Description – CFD analysis of flow and temperature in pot shield to determine optimal gap Packed bed model – no separate packed bed model Gas phase combustion model – no separate gas phase combustion model Heat transfer model – CFD analysis of heat transfer within pot shield with inputs determined experimentally from an LPG burner	Experimental

3.3.1 Eindhoven models

Throughout the 1980s a group of researchers at Eindhoven University worked to understand small cookstoves. Initially these efforts focused on one or more aspects of small cookstoves including the development of a simplified set of equations to size the combustion chamber and air inlets as a function of combustion stoichiometry for enclosed stoves (De Lepeliere et. al., 1981) and an empirical relationship between the power of the char fire to the power of the volatiles combustion for enclosed stoves (Verhaart, 1982). Bussmann (1982) developed a detailed model of the gas phase region of an open fire above a fixed bed of fuel (i.e., no cook pot). Using differential conservation equations for mass, momentum, and energy, the gas phase combustion zone was modeled as a steady state, two-dimensional axisymmetric cylinder in which the pyrolysis products from the fuel bed form a rising plume that entrains the secondary air. As the plume rises, the diameter of the plume shrinks and the velocity increases. Gas velocities and temperature within the plume were assumed to be a function of height but not diameter. Gas velocity and temperature outside the plume were assumed to be zero and ambient, respectively. Other model assumptions included

- Pressure gradients are negligible.
- Turbulent flow is fully developed.
- Radiation heat transfer is negligible.
- Air, volatiles, and combustion gases are all modeled as a single incompressible ideal gas with constant molecular weight and constant specific heat.

Air entrainment was based on a published correlation (Seward, 1970). Volatile combustion with entrained air was assumed to occur instantaneously and homogeneously over the flame cross-section. The heat release rate per unit volume was a function of height only and was determined

by conservation of energy. Solving the equations analytically resulted in plots of temperature, plume width, and gas velocity as a function of height above the fuel bed for various levels of firepower, excess air, and volatile fraction.

Building from this earlier work Bussmann and Prasad published their first coupled cookstove model in 1983. This model was a steady state, three-zone model of an open cooking fire composed of (1) a reacting fuel bed zone, (2) a gas phase combustion zone, and (3) a heat transfer zone. The reacting fuel bed zone was modeled as a steady state, homogeneous top-fed, fixed bed of wood and char with underfire air using a simplified integral model. The fuel bed height and void fraction; fuel size, type, and moisture content; pyrolysis rate of the fuel; and combustion rate of the char were not considered. Instead the heat release rate of the cooking fire was assumed and used to determine the fuel consumption rate, $\dot{m}_{\mathrm{f}}$. Other assumptions within the fuel bed zone included

- The pyrolysis gases are not combusted within the fixed bed of fuel.
- The air flow through the fuel bed (e.g., primary or underfire air) is stoichiometric based on char combustion to CO_2.
- The char yield, y_{char}, is 20% on a dry basis.
- The specific heat of the reactants and products is equal to air.
- The temperature of the top surface of the fuel bed, T_{bed} is 1100 K.
- The heat of pyrolysis is zero.

The mass flow rate of gases leaving the fuel bed, $\dot{m}_{exit}$, was determined from conservation of mass

$$\dot{m}_{exit} = \left[\left(1 - y_{\text{char}}\right) + y_{\text{char}} \left(\frac{1 + f_{\text{char(s)}}}{f_{\text{char(s)}}} \right) \right] \dot{m}_{\text{f}} \tag{3.1}$$

where $f_{\text{char(s)}}$ is the stoichiometric fuel-air mass ratio for char combustion. The exit temperature of the gases, T_{exit}, is determined from conservation of energy for the reacting bed of fuel

$$y_{\text{char}} \dot{m}_{\text{f}} \text{LHV}_{\text{char}} = \dot{m}_{exit} c_p \left(T_{exit} - T_{amb}\right) + \varepsilon_{bed} \sigma A_{bed} \left(T_{bed}^4 - T_{amb}^4\right) \tag{3.2}$$

The gas phase combustion zone was modeled using the charts developed in (Bussmann and Prasad, 1982). Based on the mass flowrate of gases from the reacting bed of fuel; the temperature, plume width and gas velocity were determined as a function of height above the fuel bed. It was assumed that the presence of the cookpot did not alter the plume of volatiles, and radiant heat transfer to and from the gas phase region was assumed to be negligible. In addition, it was assumed that combustion of volatiles was quenched when reaching the cold pot bottom, resulting in unburned volatiles in the exhaust. In the heat transfer zone, radiant heat transfer from the fuel bed to the pot bottom was modeled assuming black body radiation between the two surfaces. Convective heat transfer to the pot was determined using published correlations (Table 3.2) for three separate regions of the pot, the stagnation region, the bottom beyond the stagnation region, and the sides of the pot. As noted by the authors, the assumption of stoichiometric char combustion led to an overestimation of the temperature of the air leaving the fuel bed. The flame zone model reportedly predicted flame height reasonably well for excess air of 1.5-2.5 without a grate and 2.5-3.5 with a grate based on flame photographs during experiments at varying firepower (Bussmann, 1988; Prasad, Sangen and Visser, 1985). The heat transfer zone model under predicted the heat transfer efficiency. This occurred because

1. it was assumed volatile combustion stopped at the pot bottom;

2. the semi-empirical correlations noted an increasing heat transfer coefficient with increasing fuel bed-to-pot height, which is contrary to experiments, likely due to a smaller Reynolds number and nozzle-to-plate distances than for which the relationships were derived (Bussmann, 1988); and
3. radiation heat transfer from and to the flame zone was neglected.

Table 3.2. Summary of pot heat transfer correlations

Model	Pot bottom	Pot Sides
(De Lepeliere et. al., 1981)	$20 < \tilde{h} < 40$ directly above fire $8 < \tilde{h} < 16$ not directly above fire	$4 < \tilde{h} < 8$
Open Fire (Buss-mann, Visser, and Prasad, 1983; Prasad, Sangen and Visser, 1985)	Within stagnation region $\mathrm{Nu} = \frac{\bar{h} D_{plume}}{k} = 1.03 \mathrm{Pr}^{0.42} \mathrm{Re}_{D_{plume}}^{0.5} \left(\frac{r}{D_{plume}} \right)^{-0.65}$ (3.3)[a] Beyond stagnation region $\mathrm{Nu} = 0.32 \mathrm{Pr}^{0.33} \mathrm{Re}_{D_{plume}}^{0.7} \left(\frac{r}{D_{plume}} \right)^{-1.23}$ (3.4)[b] $\frac{T - T_{amb}}{T_{pot} - T_{amb}} = 0.9 \left(\frac{r}{D_{plume}} \right)^{-1.06}$ (3.5)[c]	$\mathrm{Nu} = 0.25 \mathrm{Pr} \mathrm{Re}^{0.75} \left(\frac{z+12}{W_{jet}} \right)^{-0.6}$ (3.6) $\frac{T}{T_{jet}} = 7.7 \frac{\rho_{jet}}{\rho_a} \left(\frac{z+12}{W_{jet}} \right)^{-0.6}$ (3.7)[d] $W_{jet} = \frac{\dot{m}_{gas}}{\pi R_{pot} \rho V}$ (3.8) $\mathrm{Nu} = 0.664 \sqrt{\mathrm{Re}}$ (3.9)[e]
Shielded fire stove (Buss-mann and Prasad, 1986)	Entirely a stagnation point $\mathrm{Nu}_{D_{plume}} = 1.26 \mathrm{Pr}^{0.42} \mathrm{Re}_{D_{plume}} \left(\frac{D_p}{D_{plume}} \right)^{-0.5}$ (3.10)[f]	Paralell plate with laminar flow: $\mathrm{Nu} = 1.85 \left(\mathrm{Re} \mathrm{Pr} \frac{2W_{sh}}{H_{sh}} \right)^{1/3}$ (3.11)[f]

Table 3.2 continued

(Baldwin, 1987)		Insulated skirt $\mathrm{Nu} = \frac{\tilde{h} \cdot W_{sh}}{\tilde{k}} = 4.861$ (3.12)
Shielded fire stove (Date, 1988)	$\tilde{h} = 0.1214\left(\frac{\dot{m}_g}{A_{gap} D_c}\right)^{1/2}$ (3.13)[g]	Loss from top $\tilde{h}_{top,loss} = 1.3\left(\frac{T_p - T_{amb}}{D_p}\right)^{0.25}$ (3.14) Loss from sides as vertical heated plate $\tilde{h}_{sides,loss} = 1.42\left(\frac{T_p - T_{amb}}{H_p}\right)^{0.25}$ (3.15)
(Shah and Date, 2011)	$\mathrm{Nu} = 0.5\left(1.65\,\mathrm{Re}_D^{0.5} + 2.733\,\mathrm{Re}_D^{0.59}\right)$ (3.16)[g]	$\tilde{h}_{sides,loss} = 1.42\left(\frac{T_p - T_{amb}}{H_p}\right)^{0.25}$ (3.17)
NOTES	[a](Schlunder and Gnielinski, 1967) [b](Hrycak, 1978) [c](Era and Saima, 1976) [d](Seban and Black, 1961) [e](Eckert and Drake, 1972) [f](Shah and London, undated) [g](Bhandari, Gopi, and Date, 1988)	

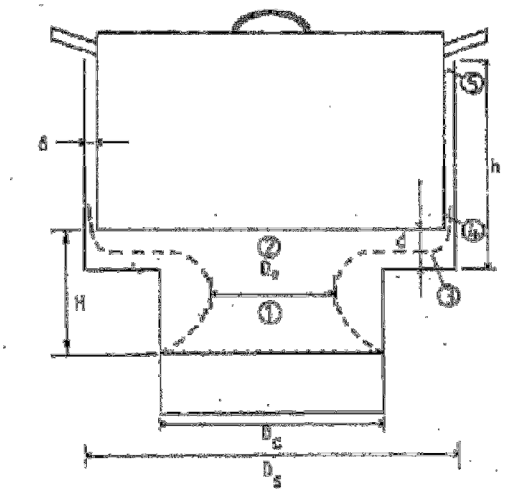

Figure 3.3 Shielded fire stove (Bussmann and Prasad, 1986)

Using the same modeling framework as the open fire model Bussmann (1986) modeled a shielded cooking fire (Fig. 3.3). The flow of air and combustion products through the stove was determined by balancing buoyancy flow and flow losses through the stove. The open fire model was updated as follows:

- Black body radiation heat transfer was assumed between the infinitely thin fuel bed, the stove surfaces, and the pot surfaces.
- The temperature of the stove surfaces was determined from experimental work of Visser (1984).
- The temperatures of the fuel bed and the exiting gases were assumed to be equal.
- Radiation losses from the flames to the stove body were assumed to be 17% of the heating value of the volatiles.
- In the heat transfer zone, the gas-phase flow field was similar to that of the open fire model with air entrainment due to the large secondary air holes, the pot is shielded with a shield of constant temperature equal to the pot temperature, and radiation into the pot was a constant 13% of heat liberated by combustion.

As in the open fire model the fuel consumption rate was determined using the heat release rate. Conservation of mass and conservation of energy were used to determine the mass flow rate of air, and the temperature of the exiting gases, respectively. In the heat transfer zone, the determination of the convective heat transfer to the pot bottom was simplified by assuming that the entire pot bottom was within the stagnation region. Convective heat transfer to the pot sides based on flow between two parallel annular plates of equal temperature (pot and shield) with hydrodynamically developed but thermally developing flow. The resulting set of 14 algebraic equations was solved to calculate excess air, temperature, and heat transfer for varying

geometrical and firepower parameters. Solutions resulting in excess air less than 1 or greater than 10 were rejected. It was found for a given fire power there was an optimum gap between the pot and the stove shield. Gaps smaller than the optimum resulted in fuel rich combustion while gaps larger than the optimum rapidly increase the excess air, decrease combustion temperatures, and decrease thermal efficiency. The model prediction agreed with experiments near the optimum gap width, but over-predicted the sensitivity of efficiency to decreasing and increasing gap width as well as the cut-off of the minimum permissible gap.

To briefly summarize the Eindhoven modeling effort, two separate but related models were developed—an open fire model applicable to three-stone stoves and a shielded cookstove model. In both cases the heat release rate of the cookstove was assumed, and the processes occurring within the three major zones of the cookstove system—the reacting fuel bed zone, the gas phase combustion zone, and the heat transfer zone around the cooking pot--were coupled together. This coupling occurred through heat transfer between the zones and the air flow rate. Specifically, the fuel bed temperature was set by an energy balance that included the combustion rate, airflow rate, and radiation heat transfer from the top surface of the bed. The heat transfer to the pot was based on convection from the flame zone and radiation from the stove body and the reacting fuel. The airflow was based on buoyant flow of gases and flow losses in the stove. It should be noted that in addition to the modeling efforts above, Prasad (1985) modeled the transient heat flow through stove walls of varying materials and found that an insulated stove wall with low thermal capacity increased efficiency by reducing the heat lost due to storage in the thermal mass of the stove.

3.3.2 Baldwin

Baldwin (1987) conducted detailed analysis to examine the effects of geometry and material on the thermal performance of a shielded biomass cookstove. This work focused primarily on heat losses through the stove wall and the heat transfer zone around the cook pot. As a result, only two detailed models were developed. The first one examined the steady-state heat loss through the stove wall as a function of the stove body material and the geometry of the stove. The second was a detailed model of heat transfer to the sides of the pot. Although pyrolysis and combustion of solid biomass fuels in the fuel bed were discussed, no specific model for the fuel bed was developed. Rather, a simplified pyrolysis and char combustion model for a single biomass particle was developed. The results of the single particle were discussed in the context of a packed fuel bed and Baldwin noted the complexity of a reacting bed of biomass fuel precluded development of a detailed model of the fuel bed.

As noted earlier, Baldwin did not model the gas phase combustion zone, and gas phase reactions were not considered. Instead, it was assumed that the gas phase combustion zone was at a uniform gas temperature of 700 K. In addition, the temperature of the top of the fuel bed was assumed to be 1000 K. From this heat transfer through a planar stove wall with convection heat transfer on both sides of the wall is

$$q''_{wall} = \frac{T_g - T_{amb}}{\frac{1}{\tilde{h}_{wall,int,tot}} + \frac{W_{wall}}{\tilde{k}_{wall}} + \frac{1}{\tilde{h}_{wall,ext}}} \tag{3.18}$$

The related equations for cylindrical and spherical geometries were also compared. The heat transfer coefficient on the interior wall was modified to include radiation heat transfer from the fuel bed and pot bottom to the wall of the stove. The fuel and the pot bottom were assumed to be parallel circular disks of equal size.

$$\tilde{h}_{wall,\text{int},tot} = \tilde{h}_{wall,\text{int}} + \sigma\varepsilon_{bed}A_{bed}F\left[\frac{\beta T_{bed}^4 + T_p^4 - 2T_{\text{int}}^4}{T_g - T_{\text{int}}}\right] \tag{3.19}$$

where F is the view factor between the bed and the pot bottom and the wall. To account for the fire not covering the entire area of the fuel bed, the effective size of the fire was reduced by a factor

$$\beta=0.5$$

The convective heat transfer coefficient was generally assumed to be

$$\tilde{h}_{\text{int}} = 10$$

The convection coefficient of the outer wall of the stove was assumed to be the greater of the natural convection correlation for a vertical heated plate

$$\tilde{h}_{wall,ext} = 1.42\left[\frac{T_{ext} - T_{amb}}{H_{stove}}\right]^{0.25} \tag{3.20}$$

or a fixed value to account for cases where the temperature difference between the exterior of the stove and the ambient temperature was small.

$$\tilde{h}_{wall,ext} = 5$$

The conduction term w_{wall}/k_{wall} was expanded to account for various materials such as insulation by adding thermal resistance analog equivalent terms for each layer within the denominator of Eq. (3.18) (Incropera et. al., 2007). The effect of a double metal wall with dead air space was calculated by applying the above equations to each wall separately with the effective convective heat transfer coefficient for the interior dead air space determined empirically from the literature.

$$\tilde{h}_{airspace} = 3.93\delta^{-0.1389}H_c^{-0.111}\left[\frac{\left(T_1 - T_2\right)^{0.25}}{\left(T_1 + T_2\right)^{0.317}}\right] \tag{3.21}$$

In the heat transfer zone, heat transfer to the pot was divided into the pot bottom and the shielded pot side. The radiation and convection heat transfer to the pot bottom was assumed to be 20% of the total energy released from combustion of the fuel. Convective heat transfer to the shielded pot side was determined by a uniform, one-dimensional discretization along the vertical axis of the channel between the pot side and the pot shield and performing an integral energy balance.

$$\Delta z\left(h_{side}\right)\left(T_i - T_{side}\right) + \Delta z\left(h_{shield}\right)\left(T_i - T_{shield}\right) = \Delta r\left(V_i \rho_i c_{p(i)}\right)\left(T_{i+1} - T_i\right) \tag{3.22}$$

for segment $i = 1$ to n. The inlet temperature to the channel was assumed to be

$$T_1 = 900 \text{ K}$$

where heat transfer coefficients were calculated using empirical Nusselt values for various geometry and flow schemes for fully developed laminar flow, with a baseline Nusselt number of 4.861 for the sides of the pot and zero for the Nusselt number inside the insulated shield. Variation of these and other parameters verified the robustness of the model. The velocity was found by balancing the buoyancy due to the density difference of combustion products and friction loss in the channel for each segment. The combustion product gases were assumed to be the same as air and were a function of temperature. The model was run with baseline parameters of $Nu_p = 4.86$, $Nu_{wall} = 0$ (varied up to 4.86) and pot and shield temperatures constant at 373 K. As shown in Table 3.3, efficiency is particularly sensitive to channel gap width, and increases in channel length become less and less effective as gases release their heat although increases in channel length can be used to offset increases in gap width necessary for increasing firepower limited by narrow gaps. These results are similar to those of Bussmann (1986) showing that narrower gaps and longer pot shields increase thermal efficiency. A simple analysis of radiation heat transfer from the fuel bed to the pot bottom was also performed, and it was found that

lowering the pot or increasing the pot diameter would generally increase thermal efficiency. It was also noted that higher wall temperatures increase thermal efficiency.

Table 3.3 – Stove efficiency (%) as a function of channel length and gap (Baldwin, 1987)

Length (cm) Gap (mm)	5	10	15	20
6	38	45	47	48
8	30	35	38	42
10	25	28	32	34
12	23	25	27	29
14	22	23	24	25

While the Baldwin models were primarily steady state, transient heat loss through the combustion chamber wall construction schemes was examined. In this case the transient heat conduction equation

$$\rho c_p \forall \frac{\partial T}{\partial t} = \tilde{h}_{\text{int}} A_{\text{int}} \left(T_{\text{int}} - T \right) - \tilde{h}_{ext} A_{ext} \left(T - T_{ext} \right) \tag{3.23}$$

was numerically solved for the combustion chamber using the assumptions developed for the steady state case for various wall material/construction, thickness, and emissivities. The conclusions were similar to those of Prasad (1985) who found that a lightweight metal wall with 1-cm insulation or dead air space resulted in the lowest heat losses through the cylindrical combustion chamber wall, followed by fired clay, bare metal, and a massive stove. The massive stove began to lose less heat than the bare metal after about 90 minutes of operation.

3.3.3 Date, Shah and Kumar

Using similar assumptions to the Eindhoven models, Date (1988) developed a detailed zonal model of heat transfer in a shielded-fire stove with a "nozzle" above the fuel bed and primary and secondary air (Figure 3.4). The model was based on three coupled zones (1) a reacting fuel bed zone, (2) a gas phase combustion zone, and (3) a heat transfer zone. The fuel bed was modeled using time-averaged rates of pyrolysis and char burning accounting for fuel diameter and moisture content. Gas flow was modeled via buoyancy and pressure losses. The effect of swirl was investigated by introducing a factor $K_{swirl}>1$ to the coefficient of heat transfer to the pot and the pressure loss coefficients. In comparison to earlier models, this model incorporated additional geometrical complexity, losses through the walls, participating media (Date, 1988), and gas phase combustion was incorporated into the model with a few other changes by Shah (2011). The effects of 9 geometrical design variables and 3 operational parameters on steady-state thermal efficiency, combustion efficiency, and volatiles evolution was investigated.

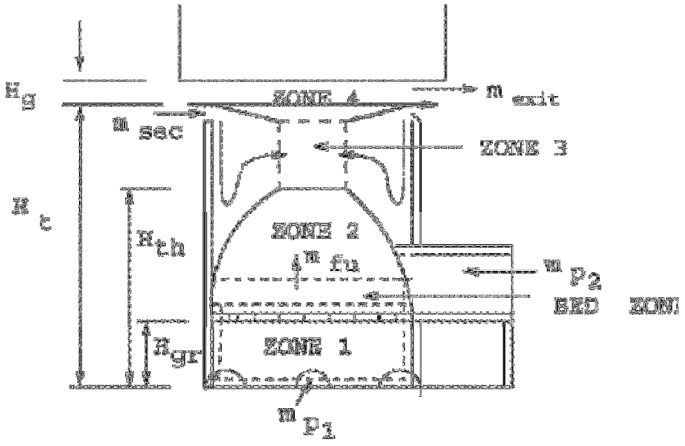

Figure 3.4. Shielded fire stove (Date, 1988; Shah and Date, 2011)

In the fuel bed zone, a simplified packed model was introduced. the steady state solid phase combustion was modeled for burning large (0.5-5 cm diameter wood) by determining the time-averaged outputs of pyrolysis and char burning based on the wood surface temperature, T_{wood}, and energy balance at the wood surface assuming:

- The wood was fed into the stove at its exact burning rate with a constant given burning surface area, A_f, typically 400 cm^2, and steady-state operation.
- Volatiles evolution dominated at lower temperature $T_{vol}=T_{wood}-50$ for 40% of the time, and char burning dominated at higher temperature $T_{char}=T_{wood}+50$ for the remaining 60% of the time, per published experiments by (Tinney, 1965) and (Blackshear and Murthy, 1965).
- Radiation at the wood surface was calculated per enclosure theory.
- The latent heat of the wood which mimics wood burning as volatile liquid fuel burning was taken from the literature as $10.47(4926D_{wood}+38)$ kJ/kg from (Simmons and Lee, 1965).
- The mass fraction of volatiles was varied from 0.6-0.9.

The kinetically-controlled mass burning flux of wood (Eq. 3.24) was determined through the time-averaged steady-state burning of volatiles and char expressed using the Arrhenius rate relationship with constants evaluated in terms of wood diameter, as listed with updated units in Table 3.4 for wood pyrolysis and Table 3.5 for char.

$$\dot{m}_f'' \simeq \frac{\rho_{wood} D_{wood}}{4}\left(\frac{0.4\, y_v k_{0,pyr} e^{-E_{pyr}/\hat{R}T_{pyr}} + 0.6\, y_{char} k_{0,char} e^{-E_{char}/\hat{R}T_{char}}}{2}\right) \tag{3.24}$$

Table 3.4. Summary of Arrhenius rate constants for pyrolysis

Model	$k_{0,pyr}$ (s^{-1})	E_{pyr} (kcal/gmol)
Prasad, Sangen and Visser, 1985	7×10^{7}	30.1
Baldwin, 1987 (1)	$A=5\times10^{9}$ g/cm^{3}s	35
Baldwin, 1987 (2)	$A=3\times10^{17}$ g/cm^{3}s	55
Baldwin, 1987 (3)	$A=5\times10^{7}$ s^{-1}	30
Baldwin, 1987 (4)	$A=2.5\times10^{4}$ g/cm^{3}s	18
Baldwin, 1987 (5)	$A=5\times10^{8}$ g/cm^{3}s	33
Date, 1988 – 2.54 cm dia wood	6×10^{7}	29.8
Date, 1988 – 1.26 cm dia wood	3.5×10^{8}	29.8
Date, 1988 – 0.63 cm dia wood	7.5×10^{8}	29.8
Shah and Date, 2011 – curve fit from Date, 1988	$(3541.2D_{wood}-13.625)\times10^{7}$	29.8
Ragland and Baker, 1991; Ragland and Bryden, 2011	7×10^{7}	31.0

Table 3.5. Summary of Arrhenius rate constants for char combustion

Model	$k_{0,char}$ (s^{-1})	E_{char} (kcal/gmol)
Date, 1988 – 2.54 cm dia wood	4×10^{8}	42.7
Date, 1988 – 1.26 cm dia wood	1.2×10^{9}	39.5
Date, 1988 – 0.63 cm dia wood	2×10^{9}	36.3
Shah and Date, 2011—curve fit from Date, 1988	$(8071.94D_{wood}-0.619)\times10^{7}$	$332.9D_{wood}+34.26$
Khummongkol, Wibulswas, and Bhattacharya, 1988	$7{,}84\times10^{11}\sqrt{T}$	44
Ragland and Baker, 1991	1.71×10^{7} kg/m^{2}hr	238

A physically-controlled energy balance at the wood surface (Eq. 3.25) conducted through balance of heat transfer by convection and radiation to the enthalpy change of the material

transferred to the surface from deep inside the wood at average temperature T_{wood}-150 per (Evans and Emmons, 1977) was used to determine the wood surface temperature.

$$\dot{m}_f^{"}\left(c_{p,g}\left(T_{wood}-T_{amb}\right)-c_{p,wood}\left(T_{wood}-150-T_{amb}\right)-h_{fg,wood}\right)=q_{rad,wood}+q_{conv,wood} \tag{3.25}$$

where $q_{rad,wood}$ and other radiative transfers were determined with view factors and a nonparticipating media in (Date, 1988), later updated to a participating media in (Shah and Date, 2011) where transmissivities and emissivities are evaluated as functions of mean beam length and temperature evaluated at 700K (Eq. 3.26-2.28).

$$\tau_{i\to j}=1-\varepsilon_{i\to j} \tag{3.26}$$

$$\varepsilon_{i\to j}=\exp\left[\left(0.848+9.02\times10^{-4}T\right)+\left(0.9589+4.8\times10^{-6}T\right)\ln\left(0.2L_{beam}\right)\right] \tag{3.27}$$

$$L_{beam}=3.6\frac{V}{A_s} \tag{3.28}$$

In the earlier model (Date, 1988), a heated cylinder correlation from (Hollman, 1975) was used to determine $q_{conv,wood}$ is taken per the average of wood surface and ambient temperatures, (Eq. 3.29), but it is unclear which method was used in the later model.

$$\tilde{h}_{wood}=1.32\left(\frac{T_{amb}-T_{wood}}{2D_{wood}}\right)^{0.25} \tag{3.29}$$

In the Date model, total heat release was calculated as the product of the fuel burning rate and calorific value of fuel, with non-reacting volatile flow. In the flame zone of the Shah model, gas phase combustion processes were incorporated by treating the five geometrical zones of the stove as well-stirred reactors: the primary air inlets under and through the grate, the bed zone, the nozzle-shaped area above the bed zone, the cylinder with secondary air holes, and the expansion under the pot. In the bed zone, a generic formula for wood composition was used assuming the

volatiles consist of CO_2, CO, H_2, H_2O and C_7H_{16} to represent both light and heavy hydrocarbons (soot and tar). From an element balance it was assumed that the mass fraction of CO/CO_2=1.591 and H_2O/CO_2 is 2.174 in the volatiles (Ragland and Baker, 1991). The rate of flow of each gas is then

$$\dot{m}_{j,v} = \dot{m}_v \left(n_j \frac{M_j}{M_v} \right) \tag{3.30}$$

A single-step char surface reaction ($C+O_2 \rightarrow CO_2$) was assumed due to low surface temperatures resulting in the production of CO_2 dominating that of CO. These flow rates were added to the gas phase along with the unbound moisture.

$$\dot{m}_{CO_2} = \dot{m}_{\text{char}} \left(\frac{M_{CO_2}}{M_{\text{char}}} \right) \tag{3.31}$$

$$\dot{m}_{O_2} = -\dot{m}_{\text{char}} \left(\frac{M_{O_2}}{M_{\text{char}}} \right) \tag{3.32}$$

Combustion of volatiles was modeled using four-step Hautman qausi-global reaction mechanism with coefficients per (Turns, 1996). In each geometrical zone (i), species (j) and energy were balanced between inlet and exit, incorporating gas phase reaction rate and secondary air flow.

$$\omega_{j,i} = \frac{\dot{m}_{i-1}\omega_{j,i-1} + \dot{m}_{air,\text{sec}ondary}\omega_{j,amb} + \hat{r}_j\left(T_i, \omega_{j,i}\right)\forall_i}{\dot{m}_{g,i}} \tag{3.33}$$

$$q_{v,i} = \sum \hat{r}_{j,i}\left(T_i, \omega_{j,i}\right)\forall_i LHV_j \tag{3.34}$$

The combustion efficiency is then evaluated as the sum of char and volatile heat release in each zone divided by the firepower, and emission factors are reported as the mass flow rate at the exit of each species divided by the mass flow rate of fuel.

In the pot heat transfer zone of both models, heat transfer correlations from the pot bottom were taken from experiments of the stove in the literature (Bhandari, 1988), and the sides of the pot represented convective losses per a vertical heated plate at a pot temperature T_p= 343 ± 5K. In the Date model the top of the pot also represented a loss. Convective heat transfer correlations around the pot are listed in Table 3.2.

Flow rates through various specific stove geometries including primary and secondary air were calculated using pressure drop equations tabulated in Table 3.6, including air inlet holes, expansions, and bends. Excess air was determined from the sum of inlet air flow rates. Heat losses through the stove walls were calculated using a thermal resistance analog similar to (Baldwin, 1987) including conduction, convection, and radiation where convective heat transfer coefficients were taken as 5 or 6 W/m^2K, depending on location. Temperatures were predicted by energy balance in each zone of the stove.

Table 3.6. Equations for pressure losses and fluid flow through stove geometry (Date, 1988) and (Shah and Date, 2011)

Pressure losses through stove geometries	$\Delta p_{loss} = \sum_i \rho_i \frac{V_i^2}{2}\left(\frac{f_D L}{D_h} + K_i\right)$	(3.35)
Friction factor in contraction, $f_{D,c}$	[a,b] $K_{cont} = 0.5\sin\phi\left(1 - \frac{A_{i+1}}{A_i}\right)$	(3.36)
Friction factor of expansion, $f_{D,e}$	$K_{\exp} = \left(1 - \frac{A_i}{A_{i+1}}\right)^2$	(3.37)
Pressure loss in bend	$K_{bend} = 1.0$	
Entry resistance in primary air holes	$K_{in} = 0.6$	
Resistance through fuel grate of spacing w_{grate} and rod diameter D_{rod}	[b] $K_{grate} = 0.75\left(\frac{W_{grate} + D_{rod}}{D_{rod}} - 1\right)^{1.33}$	(3.38)
Resistance through fuel bed	$K_{bed} = 1.12\left(0.66 N_{row} + 0.5\right)$ $K_{bed}=1.3$	(3.39)
Resistance under pot bottom with gap A_{gap}	[c] $K_{pot,bottom} = \left[\left(\frac{A_{pot}}{A_{gap}}\right)^2 - 1\right] + \left[\left(\frac{A_{pot}}{A_{gap}}\right) - 1\right]^2$	(3.40)

[a] ϕ is the half-angle of the contraction

[b] Kazantsev, 1977

[c] Bussmann and Prasad, 1986

Results from the Date model predicted efficiency 0.36% less than was measured in concurrent experiment (Bhandari, 1988) and published fuel burning rate by Blackshear & Murthy 1965. The Shah model predicted efficiency of 1.2% greater than the same experiment, excess air and stove power nearly corroborated with experiment, CO/CO_2 ratio was predicted at 0.17 compared to 0.12-0.16 measured in (Bussmann and Prasad, 1986), and air flow rate and wood surface temperature agreed with (Kausley and Pandit, 2010).

The steady-state heat transfer in a three-pot enclosed stove was modeled in (Kumar, Lokras, and Jagadish, 1990) through energy balances on a series of six stirred vessels in order to predict the effects of geometry on efficiency and to compare the heat flow to the pots versus body and exhaust losses using the following assumptions:

- Steady state with constant wood burning and charcoal production rates, and excess air
- Complete combustion
- The spaces under each pot represented as hemispherical chambers and the channels between pots and to the chimney as rectangular ducts, each modeled as stirred vessels with instant mixing, uniform velocity, and uniform gas temperature equal to the exit and wall temperatures

Heat release of the dry wood release rate minus that of the unburned charcoal was equated to the energy used to evaporate the fuel moisture and heat the gas components as expected from compete combustion of wood with the given excess air and used to determine the gas temperature leaving the fuel bed as an input to the series of reactors. Convective heat transfer to the pot bottoms was modeled using correlations for laminar flow through a rectangular duct of given geometry where Nu_∞ is the asymptotic value available as a curve fit as a function of the width, *W*, and height, *H*, of the duct for air (Clark and Kays, 1953):

$$\frac{\overline{\mathrm{Nu}}}{\mathrm{Nu}_\infty} = 1 + \left(0.003 + 0.039 \frac{W}{H} \right) \frac{D_H}{L} \mathrm{Re}\,\mathrm{Pr} \tag{3.41}$$

Radiative transfer from gas to pot was modeled using the partial pressure fraction of CO_2 and H_2O, temperature, and beam length as a radiative heat transfer coefficient taken from charts in the literature, including a factor of 1.1 when the gas is luminous. Radiation from wall to pot was modeled assuming view factors of two gray concentric spheres. Conductive losses to the

spherical mud walls were modeled as cumulative loss per small time elements to represent steady-state through solution of the radial conduction equation with constant combined convective and radiative heat transfer coefficients at the inner surface. Sensible energy leaving each vessel was the sum of the specific heat of each gas component.

The pressure drop method was used to equate the chimney draft to the pressure drop through the flow path for determination of excess air. The chimney temperature distribution was determined from overall energy balance in the chimney using thermal resistance method with interior heat transfer coefficient calculated per empirical correlation for turbulent flow, $\mathrm{Nu} = 0.023\,\mathrm{Re}^{0.8}\,\mathrm{Pr}^{0.3}$. Pressure losses through geometries were evaluated per standard pressure drop methods.

3.3.5 CFD-Based Coupled Models

(Weerasinghe and Kumara, 2003) modeled gas phase combustion in addition to heat transfer in a cylindrical combustion chamber below a flat cooking plate. The source term of energy release due to gas phase combustion was approximated by the reaction rate of fuel combustion taken as the slowest of the dissipation rates of fuel, oxygen, and products (Eq. 3.42).

$$R_{wood} = -\rho \frac{\varepsilon}{k} \min\left[C_R m_{wood}, C_R \frac{m_{O_2}}{s}, C_R^{'} \frac{m_{prod}}{1+s} \right] \tag{3.42}$$

The flaming power output was assumed 3 kW, representing 75% of the total stove firepower. Predicted temperature was lower than experiment.

(Gupta and Mittal, 2010a) analyzed the 2D heat transfer in the wood-burning Janta stove including approximations for the packed bed and flame zones. Flow through the fuel bed was modeled as a porous medium through the Darcy-Brinkman law with effective bed thermal

conductivity as a weighted average per porosity. It was assumed 40% of heat release is in the bed zone and the remaining 60% in the flame zone, treated as a uniformly distributed source term. The permeability of the fuel bed was expressed through the Karman-Cozeny relationship. Pyrolysis rates were determined experimentally as a pseudo-first order reaction as a function of temperture in (Gupta and Mittal, 2010b), but modeled as a uniform heat release rate. The model was validated with two cases in the literature.

The doctoral dissertation of (Burnham-Slipper, 2008) incorporated two articles detailing analytic models for jet impingement heat transfer to a flat plate (Burnham-Slipper, 2007a) and simplified wood combustion (Burnham-Slipper, 2007b) and utilized CFD to optimize an African rocket-type griddle stove using genetic algorithms.

The packed bed model for thermally thick wood combustion (Burnham-Slipper, 2007b) assumed pyrolysis is limited by heat transfer through the fuel, and char combustion is limited by oxygen diffusion. Rates were based on experimental determination of the burn rate and temperature field in a crib of stacked cylindrical fuel with varying volume, void fraction, and specific area, introducing a lumpiness function to incorporate mixing of discrete streams of volatiles and oxidants.

Char combustion to CO_2 was modeled using oxygen diffusion through the species boundary layer according to Fick's law and assuming O_2 is fully consumed and experimentally shown to be limited by diffusion resulting in the simplified oxygen consumption rate (Eq. 3.43) in terms of the mass transfer coefficient for flow through an inert packed bed from (Cussler, 1997) (Eq. 3.44), which is simplified as approximately proportional to the square root of the superficial velocity, V_0. Here a is the fuel specific area (m^2/m^3), v is the normalized crib volume,

and units of volume specific mass flow are kg/m^{3}s. The simplified char combustion model is then shown in equations 3.45-3.47.

$$m'''_{O_2} = -\frac{a}{v}\tilde{h}_D \rho_{O_2,\infty} \tag{3.43}$$

$$\frac{\tilde{h}_D}{V_0} = 1.17\left(\frac{DV_0}{\upsilon}\right)^{-0.42}\left(\frac{D_{AB}}{\upsilon}\right)^{0.66} \tag{3.44}$$

$$m'''_{char} = \frac{12}{32}\frac{a}{v}\tilde{h}_D V_0^{0.5}\rho_{O_2,\infty} \tag{3.45}$$

$$m'''_{CO_2} = \frac{44}{32}\frac{a}{v}\tilde{h}_D V_0^{0.5}\rho_{O_2,\infty} \tag{3.46}$$

$$q'''_{char} = HHV_{char} m'''_{char} \tag{3.47}$$

Pyrolysis was modeled with drying and volatile release as a superimposed single thermal decomposition wave per (Bryden, Ragland, and Rutland, 2002), assuming a constant pyrolysis temperature of 550K from (Demirbas, 2004) and pyrolysis wave separating char and virgin wood surfaces at varying radius *r* for fuel of radius *R*. The heat conducted through the char layer is shown by Eq. 3.48 and the resulting mass flow of volatiles is calculated as this divided by the enthalpy of pyrolysis, including sensible energy from the temperature rise, estimated as 2.5 MJ/kg$_v$ per experimental values. The mass flow of water and volatiles are then calculated per their mass fraction from proximate analysis.

$$q'''_{pyr} = \frac{\tilde{k}_{char} a\left(T - T_{pyr}\right)}{vR\ln\left(\frac{R}{r}\right)H_{pyr}} \tag{3.48}$$

Values of inertial flow resistance coefficient for the crib were calculated from the Ergun equation and verified experimentally.

In the flame region, chemistry was modeled using the species-transport model of Fluent where the reaction between wood volatiles and oxygen took place according to Eq. 3.49 and was limited by turbulent mixing according to the eddy-dissipation model.

$$CH_2O+O_2 \rightarrow CO_2+H_2O \tag{3.49}$$

Radiation was included by the Discrete Ordinates model and weighed-sum-of-grey-gases model of Fluent, though the effect of soot was not included due to the availability of diesel fuel soot models only. The model was validated experimentally and from the literature.

Convective heat transfer to the griddle plate was modeled as a steady-state axisymmetric impinging jet neglecting the effects of buoyancy and radiation with turbulence, and was validated experimentally. The zones were then coupled and optimized with genetic algorithm.

3.4 Conclusions and Future Work

As discussed earlier, cookstoves that reduce fuel use and emissions can help to improve the health and livelihoods of over 2.7 billion people currently cooking with biomass each day. Because of this, a complete, validated model of household cookstoves suitable for design is needed. To date progress has been made in developing these models but more work is needed. Today's model capability includes steady-state simplified analytic models of packed bed combustion, basic reaction mechanisms for several major species in gas phase combustion, generalized correlations for convection and radiation, and CFD-based models for heat transfer.

These models should be extended to include transient processes including the addition of fuel charges, start-up and cool-down. Current models are specific to a given stove geometry, and flexibility in geometry and primary/secondary air flow is necessary. In the packed bed zone, models of drying, pyrolysis, and char combustion for various fuel sizes, shapes, and

arrangements should be addressed. In the gas phase zone, detailed models of heat release and pollutant formation specific to biomass combustion, especially that of PAH and soot, are needed. In the heat transfer zone, radiation with a participating medium including gas composition and particle concentration within the gas and luminous flames is needed, as are validated convective heat transfer correlations specific to the flow and temperature regimes for the various regions within the stove body and cooking surfaces. Additionally, overall performance should be validated from a broad data set while recognizing that performance in the field is different than performance in the laboratory.

Acknowledgements

The authors gratefully acknowledge the financial support of Nordica MacCarty by the United States National Science Foundation Graduate Research Fellowship Program.

CHAPTER 4

AN EXPERIMENTAL DATA SET OF SINGLE-POT SHIELDED-FIRE WOOD-BURNING COOKSTOVES FOR VALIDATION OF ZONAL MODELS

Draft of a paper to be submitted for publication in *Energy*

Nordica A. MacCarty, Kenneth M. Bryden

Abstract

The use of computational modeling tools for conceptual design of biomass cookstoves would permit understanding of heat transfer and flow processes within stoves and would support better, faster, more adaptive designs. For development of such models, experimental data sets that report thermal performance characteristics in terms of design characteristics are required for model validation. This article presents a unified data set from the literature, including all necessary design variables and outcomes with parametric variation spanning the region of interest for cylindrical, natural draft, shielded, wood burning cookstoves fitted with a single flat-bottomed shielded or unshielded pot. The data set includes 63 unique points compiled from three laboratory studies and is shown to be consistent and supportive of qualitative conclusions and thumb rules regarding the effects of stove geometry, operating variables, and material on overall thermal performance.

4.1 Introduction

The design and dissemination of improved cookstoves for the 2.7 billion people worldwide (IEA, 2010) currently cooking with traditional biomass fuels each day has been gaining increasing global attention due to the number of health, safety, and environmental risks from this age-old tradition and hallmark of energy poverty. Recent projections indicate that use of biomass for cooking will continue to be the dominant energy use in rural, resource-poor households through 2030 (Diaoglou, 2012) where 98% of household energy needs are met with small household cookstoves (Johnson and Bryden, 2012 a and b). For these subsistence-level families, the cost of acquiring this fuel represents a significant fraction of household time and income. Cookstove replacement programs aim to promote high efficiency, clean-burning cookstoves which have the potential to reduce deforestation and desertification, improve health and livelihoods, and slow global climate change (Rehfuess, 2006), and the design of such cookstoves remains an engineering challenge.

While the use of computational modeling for cookstove design remains largely absent, modeling tools for cookstoves would permit examination of complex and coupled heat transfer, fluid flow, and combustion processes within stoves and would support better, faster, more adaptive designs. Some limited algebraic and computational modeling work has occurred, yet today the design of small biomass fueled cookstoves is primarily a heuristic trial and error process based on previous experience, engineering judgment, thumb rules, and experiment. Beginning with a conceptual design generated from previous models, a prototype is built and tested for performance. Parametric changes are made and tested again. When a sufficient design is found, the stove is brought to the field for further testing, refinement, and eventual dissemination. To date there is no dominant design basis or established design algorithm for

optimizing the efficiency of these devices. Nor are there validated and accepted models or modeling guidelines to support the design process although much of the necessary data, experience, and equations are available.

There are two types of numerical models that have been developed for cookstoves. Zonal models break the system into zones in which processes are lumped and coupled with other zones to predict efficiency, excess air flow, and average temperatures throughout the system and may provide an indication of emissions. Zonal models are fast and flexible within the prescribed design space, and there are a number of measurements available for validation. Detailed high-fidelity models use differential equations of mass, momentum, and energy within a 3-dimensional mesh and are appropriate for examining complex temperature profiles, heat transfer coefficients, and combustion. High fidelity models are more computationally expensive than zonal models but can provide a complete history of temperature, velocity, and species in the flow path to assist in determining flow behavior and pollutant formation. Detailed measurements of temperature, velocity, and species within the flow field are required to validate these high fidelity models. In both cases, unified sets of data for validation are not presently available in the literature.

In order to develop such a computational model for a given type of cookstove, a unified and consistent data set with sufficient detail and parametric variation spanning the region of interest is required for validation. Such a data set can also be used to extract and quantitatively confirm known qualitative thumb rules (Bryden et. al., 2005) within a prescribed design space. This article examines the stove testing literature to develop a unified set of data to support development and validation of zonal models for predicting heat transfer efficiency as a function of operational and geometrical variables for a natural draft, shielded-fire wood-burning

cookstove fitted with a single, flat-bottomed shielded or un-shielded pot. As gaps in the data are identified and further testing is completed, the data set can be expanded to assist in improving and broadening models.

4.2 Background

A biomass cookstove (Fig. 4.1) is fundamentally composed of the air handling system, the combustion chamber, the convective hear transfer region, the cooking pot, and the support structure and insulation. The air handling system directs the flow of primary and secondary air. The combustion chamber encloses the solid phase and gas phase combustion region and provides for radiant heat transfer from combustion to the cooking pot. The convective heat transfer system transfers energy from the combustion products to the cooking pot, and the cooking pot holds the food or water. The support structure and insulation provide the structural support to hold the other components together, limit energy loss from the stove, and protect the user from the heat and flame. A traditional stove such as the three-stone fire may have only one or two components, whereas a highly engineered stove may have complex designs for each of the components.

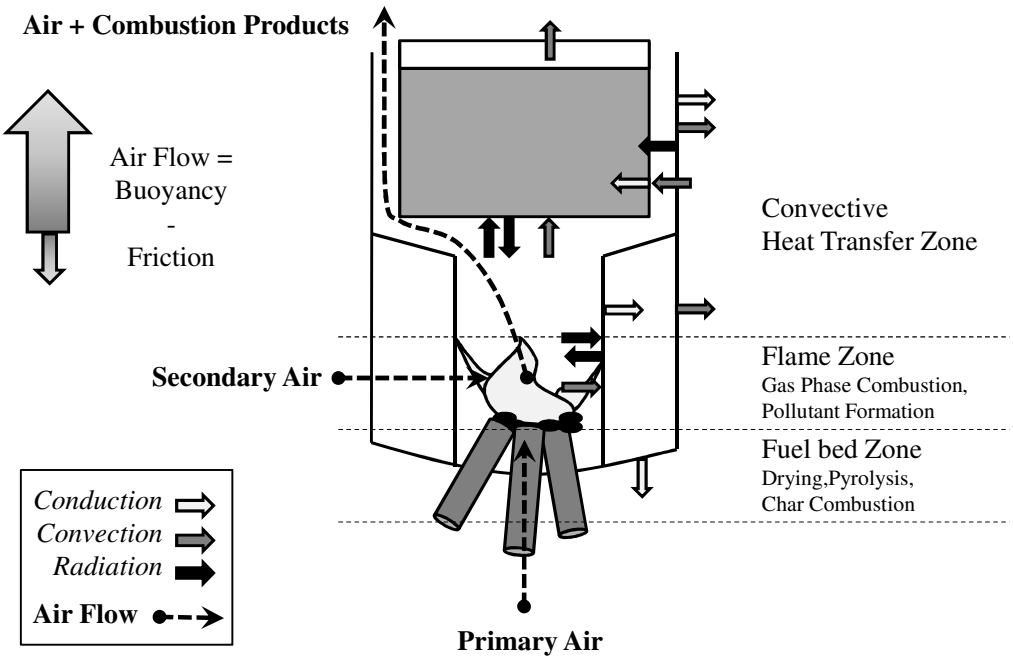

Figure 4.1. A typical cookstove

There are three primary types of biomass cookstoves based on the treatment of the combustion chamber. These are 1) An open cooking fire in which a pot is held atop 3 stones or other similar support where the airflow is uncontrolled and entrained throughout the system due to buoyancy, and heat transfer efficiency is primarily a function of the fuel bed diameter, distance to the pot, and fuel size; 2) A shielded cooking fire, often referred to as improved stoves and marketed under a number of names (e.g., rocket stoves, VITA stoves, jikos) which vary in complexity from a simple shield of metal or clay around the combustion space to more complex devices with inlets for directed control of primary and secondary air and a narrow channel around the pot to encourage combustion gases to pass closely to the pot sides; and 3) An enclosed fire with chimney, similar to stoves used for space heating but with high temperature

cooking surfaces underneath which gases pass from the combustion chamber along channels and then exit to a chimney to exhaust outside, posing less health risk to the user.

The cylindrical shielded cooking fire type is most frequently designed for use in households as indicated by a review of published stove testing data (MacCarty, Still, and Ogle, 2010; Jetter and Kariher, 2009; Jetter et. al., 2012), and is therefore the focus of this article and subsequent model. Due to the different combustion behavior and therefore alternate modeling techniques required for variations from the traditional wood fueled stoves, stoves which require specialized fuel, such as charcoal, chips, or pellets; or those incorporating an electric fan, are not included. Nor are those with non-cylindrical combustion chambers or round-bottomed pots.

The design variables required for development of a zonal model include a) the geometry and b) materials composing the flow path, as well as c) the operational variables of the fuel supply and firepower. The design outcome of interest is the thermal efficiency, that is, the energy transferred into the cooking pot as measured by water temperature rise and evaporation divided by the energy released by the fuel as measured by the lower heating value and mass of fuel burned during the test. Based on this, the following data are needed for input into the model:

1) *Operational variables*, including experimental firepower, fuel moisture content, and lower heating value
2) *Geometrical variables* providing a full description of the flow path, stove body, and cooking pot dimensions (Fig. 4.2) subject to the constraints of the model

D_c – combustion chamber diameter
H_c – combustion chamber height
W_c – gap at the edge of the combustion chamber
W_p – gap at the edge of the pot bottom
W_{sh} – gap between the shield (if included) and pot

D_p – pot diameter
H_p – height of the water in the pot based on its occupied volume
D_s – stove combustion chamber body diameter
k_s – stove body material conductivity
H_{sh} – height of the shield, if included
t_{sh} – thickness of the shield material
k_{sh} – shield material conductivity

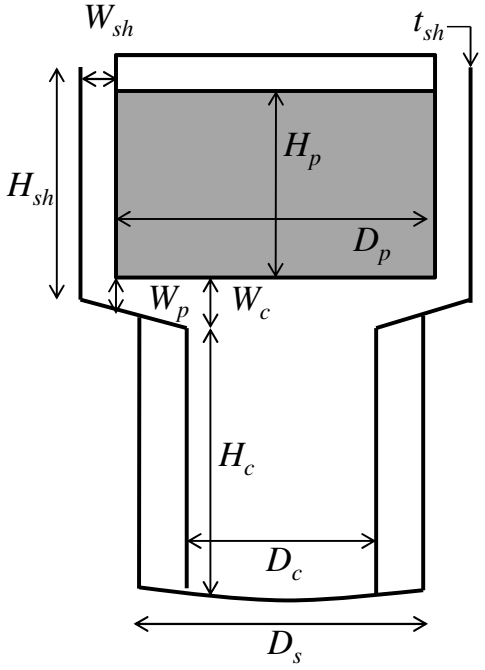

Figure 4.2. Geometrical variables

3) *Material variables* such that the thermal conductivity of the stove body components can be determined

4) *Thermal efficiency* as measured

This article presents a compilation of these design variables and measured thermal efficiency for a natural draft, shielded-fire wood-burning cookstove fitted with a single, flat-bottomed shielded or un-shielded pot, and investigates the trends observed from the data.

4.3 Data Set

A review of the literature revealed three major categories of stove testing data based on the goals of the research and therefore the data that was collected. 1) Regional in-field testing to generate databanks of fuel use and emissions performance for various stove-fuel combinations, such as (Smith, 1993, 2000; Zhang et. al., 2000; Bailis, Ezzati, and Kammen, 2003). The goal of this work is to catalogue various regional stove/fuel combinations in order to extrapolate energy and pollutant data per capita for use in global inventories and policy decisions. 2) In-field testing comparing "improved" to "traditional" stoves as used by community members (Smith et. al, 2007; Johnson et. al, 2008; Roden et. al., 2009). The intent of this type of study was to determine the fuel and emissions savings or indoor air pollution reductions offered by specific stove designs in a specific community. These studies incorporate the effects of user behavior and report metrics as percent improvement in task-based measures. 3) Stove testing for understanding, comparing, and improving design through measures of thermal performance characteristics in terms of stove design characteristics (Jetter and Kariher, 2009; Jetter et. al., 2012; MacCarty, Still, and Ogle, 2010). The goal of these laboratory based tests is to determine differences in fuel use and/or emissions performance due to stove type, model, or parametric changes to operational, material, or geometrical variables. This third category of data is required for model validation because the focus is the stove design characteristics and resulting thermal performance, as opposed to the user or in-field conditions. Laboratory data, though not necessarily predictive of in-field performance (Johnson et. al, 2010), aims to remove the variability of user behavior inherent in field studies and is therefore required for models which assume steady-state operation.

The criteria for such a laboratory-based study to suit the requirements needed for validating zonal models include the following:

1. Report necessary design variables and thermal efficiency.
2. Include the stove type being modeled. In this case, a cylindrical, natural draft, shielded, cookstove fitted with a single flat-bottomed shielded or unshielded pot and burning wood sticks as fuel.
3. Encompass design variables within the design space of the model. For calculation of natural draft due to buoyancy in this case, the pot diameter must be greater than the combustion chamber diameter, and the stove must be tall enough or utilize a pot shield such that the height of the flow exit is greater than 13 cm.
4. Examine thermal performance characteristics in terms of stove design characteristics, preferably including parametric variation.

Three articles were identified to contain data points that met criteria 2-4 and either provided nearly enough data for criteria 1 that the missing pieces could be estimated, or were recent enough to include physical stove prototypes or primary data that were currently available. These are summarized in Table 1. These included a parametric study of a shielded fire stove (Bussmann and Prasad, 1986), five of the stoves in a laboratory testing series (MacCarty, Still, and Ogle, 2010), and two of the stoves tested in a second testing series (Jetter et. al., 2012). These are shown in Figure 3. Several other studies that may provide additional data points but are not incorporated here include (Bhattacharya, Albina, and Khaing, 2002a) which presented a parametric study of fuel moisture, firepower, and pot size for a single suitable stove but was missing details regarding the other constant variants, and the stove was likely too short for the buoyant flow model. A concurrent emission factor study (Bhattacharya, Albina, and Khaing,

2002b) included a taller version of that stove but included no parametric variation, nor was experimental firepower reported. The predecessor to the selected stove comparison by Jetter (Jetter and Kariher, 2009) provided testing of two stoves that were duplicated in (MacCarty, Still, and Ogle, 2010) and did not include parameter variations and are thus not included.

Table 4.1. Data set[d]

Stove	Eff.	D_c	H_c	W	W_p	W_{sh}	V_w	D_p	H_p	H_{sh}	D_{stove}	k_{stove}	t_{sh}	k_{sh}	LHV_f	MC_f	q
	%	cm	cm	cm	cm	cm	L	cm	cm	cm	cm	W/mK	cm	W/mK	MJ/kg		kW
Vary W_{sh}, r_p[a]	0.35	18.0	10.0	3.5	3.5	0.4	5	20.0	15.9	17.8	18.10	26.2	0.05	26.2	18.60	0%	4.0
	0.37	18.0	10.0	3.5	3.5	0.7	5	20.0	15.9	17.8	18.10	26.2	0.05	26.2	18.60	0%	4.0
	0.33	18.0	10.0	3.5	3.5	1.0	5	20.0	15.9	17.8	18.10	26.2	0.05	26.2	18.60	0%	4.0
	0.30	18.0	10.0	3.5	3.5	1.3	5	20.0	15.9	17.8	18.10	26.2	0.05	26.2	18.60	0%	4.0
	0.27	18.0	10.0	3.5	3.5	1.6	5	20.0	15.9	17.8	18.10	26.2	0.05	26.2	18.60	0%	4.0
	0.39	18.0	10.0	3.5	3.5	0.4	5	24.0	11.1	17.8	18.10	26.2	0.05	26.2	18.60	0%	4.0
	0.40	18.0	10.0	3.5	3.5	0.7	5	24.0	11.1	17.8	18.10	26.2	0.05	26.2	18.60	0%	4.0
	0.37	18.0	10.0	3.5	3.5	1.0	5	24.0	11.1	17.8	18.10	26.2	0.05	26.2	18.60	0%	4.0
	0.33	18.0	10.0	3.5	3.5	1.3	5	24.0	11.1	17.8	18.10	26.2	0.05	26.2	18.60	0%	4.0
	0.30	18.0	10.0	3.5	3.5	1.6	5	24.0	11.1	17.8	18.10	26.2	0.05	26.2	18.60	0%	4.0
	0.47	18.0	10.0	3.5	3.5	0.4	7.5	28.0	12.2	17.8	18.10	26.2	0.05	26.2	18.60	0%	4.0
	0.42	18.0	10.0	3.5	3.5	0.7	7.5	28.0	12.2	17.8	18.10	26.2	0.05	26.2	18.60	0%	4.0
	0.39	18.0	10.0	3.5	3.5	1.0	7.5	28.0	12.2	17.8	18.10	26.2	0.05	26.2	18.60	0%	4.0
	0.36	18.0	10.0	3.5	3.5	1.3	7.5	28.0	12.2	17.8	18.10	26.2	0.05	26.2	18.60	0%	4.0
	0.33	18.0	10.0	3.5	3.5	1.6	7.5	28.0	12.2	17.8	18.10	26.2	0.05	26.2	18.60	0%	4.0
Vary W_c[a]	0.36	18.0	13.0	0.5	0.5	1.0	7.5	28.0	12.2	17.8	18.10	26.2	0.05	26.2	18.60	0%	4.0
	0.38	18.0	12.5	1.0	1.0	1.0	7.5	28.0	12.2	17.8	18.10	26.2	0.05	26.2	18.60	0%	4.0
	0.37	18.0	12.0	1.5	1.5	1.0	7.5	28.0	12.2	17.8	18.10	26.2	0.05	26.2	18.60	0%	4.0
	0.35	18.0	11.0	2.5	2.5	1.0	7.5	28.0	12.2	17.8	18.10	26.2	0.05	26.2	18.60	0%	4.0
	0.32	18.0	10.0	3.5	3.5	1.0	7.5	28.0	12.2	17.8	18.10	26.2	0.05	26.2	18.60	0%	4.0
Vary H_{sh}[a]	0.33	18.0	12.5	1.0	1.0	1.0	7.5	28.0	12.2	1.0	18.10	26.2	0.05	26.2	18.60	0%	4.0
	0.36	18.0	12.5	1.0	1.0	1.0	7.5	28.0	12.2	2.0	18.10	26.2	0.05	26.2	18.60	0%	4.0
	0.39	18.0	12.5	1.0	1.0	1.0	7.5	28.0	12.2	4.0	18.10	26.2	0.05	26.2	18.60	0%	4.0
	0.41	18.0	12.5	1.0	1.0	1.0	7.5	28.0	12.2	8.0	18.10	26.2	0.05	26.2	18.60	0%	4.0
	0.42	18.0	12.5	1.0	1.0	1.0	7.5	28.0	12.2	12.0	18.10	26.2	0.05	26.2	18.60	0%	4.0
	0.42	18.0	12.5	1.0	1.0	1.0	7.5	28.0	12.2	16.0	18.10	26.2	0.05	26.2	18.60	0%	4.0
Vary H_c, No Ins[a]	0.40	18.0	10.0	1.0	1.0	1.0	7.5	28.0	12.2	1.0	18.10	26.2	0.05	26.2	18.60	0%	4.0
	0.37	18.0	17.5	1.0	1.0	1.0	7.5	28.0	12.2	1.0	18.10	26.2	0.05	26.2	18.60	0%	4.0
	0.35	18.0	22.5	1.0	1.0	1.0	7.5	28.0	12.2	1.0	18.10	26.2	0.05	26.2	18.60	0%	4.0
	0.30	18.0	26.0	1.0	1.0	1.0	7.5	28.0	12.2	1.0	18.10	26.2	0.05	26.2	18.60	0%	4.0
Vary H_c, Ins[a]	0.42	18.0	10.0	1.0	1.0	1.0	7.5	28.0	12.2	1.0	20.10	0.038	0.05	26.2	18.60	0%	4.0
	0.41	18.0	17.5	1.0	1.0	1.0	7.5	28.0	12.2	1.0	20.10	0.038	0.05	26.2	18.60	0%	4.0
	0.39	18.0	22.5	1.0	1.0	1.0	7.5	28.0	12.2	1.0	20.10	0.038	0.05	26.2	18.60	0%	4.0
	0.38	18.0	26.0	1.0	1.0	1.0	7.5	28.0	12.2	1.0	20.10	0.038	0.05	26.2	18.60	0%	4.0

Table 4.1 continued

Stovetec 2D[b]	0.27	10.0	20.0	2.5	1.0	0.8	5	24.0	11.1		26.0	1			19.26	12%	4.1
	0.36	10.0	20.0	2.5	1.0	0.8	5	24.0	11.1	8.0	26.0	1	0.05	26.2	19.26	12%	3.9
	0.20	10.0	20.0	2.5	1.0	0.8	5	24.0	11.1		26.0	1			19.26	12%	2.2
	0.30	10.0	20.0	2.5	1.0	0.8	5	24.0	11.1	8.0	26.0	1	0.05	26.2	19.26	12%	2.0
Stovetec 1D[b]	0.24	10.0	23.3	2.5	1.0	0.8	5	24.0	11.1		26.0	1			19.26	14%	3.8
	0.33	10.0	23.3	2.5	1.0	0.8	5	24.0	11.1	8.0	26.0	1	0.05	26.2	19.26	14%	4.0
	0.20	10.0	23.3	2.5	1.0	0.8	5	24.0	11.1		26.0	1			19.26	14%	2.2
	0.30	10.0	23.3	2.5	1.0	0.8	5	24.0	11.1	8.0	26.0	1	0.05	26.2	19.26	14%	2.0
WFP[b]	0.37	12.0	28.0	3.0	1.5	1.0	5	24.0	11.1	12.3	32.0	0.18	0.05	26.2	19.26	11%	5.5
	0.33	12.0	28.0	3.0	1.5	1.0	5	24.0	11.1	12.3	32.0	0.18	0.05	26.2	19.26	11%	6.3
	0.26	12.0	28.0	3.0	1.5	1.0	5	24.0	11.1	12.3	32.0	0.18	0.05	26.2	19.26	11%	2.2
Mauritania[b]	0.18	12.0	36.0	3.0	3.0	1.6	5	24.0	11.1	14.1	28.0	1.7	0.05	26.2	19.26	5%	4.1
	0.20	12.0	36.0	3.0	3.0	1.6	5	24.0	11.1	14.1	28.0	1.7	0.05	26.2	19.26	5%	4.6
	0.18	12.0	36.0	3.0	3.0	1.6	5	24.0	11.1	14.1	28.0	1.7	0.05	26.2	19.26	5%	3.3
UCODEA[b]	0.30	12.4	29.0	2.7	1.2	1.2	5	31.0	6.6	7.6	23.0	0.6	0.05	26.2	19.26	7%	5.8
	0.31	12.4	29.0	2.7	1.2	1.2	5	31.0	6.6	7.6	23.0	0.6	0.05	26.2	19.26	7%	5.6
	0.27	12.4	29.0	2.7	1.2	1.2	5	31.0	6.6	7.6	23.0	0.6	0.05	26.2	19.26	7%	3.7
Stovetec 1D[c]	0.35	10.0	23.3	2.5	1.0	0.8	5	24.0	11.1	8.0	26.0	1	0.05	26.2	17.74	9%	3.9
	0.33	10.0	23.3	2.5	1.0	0.8	5	24.0	11.1	8.0	26.0	1	0.05	26.2	17.74	10%	5.1
	0.35	10.0	23.3	2.5	1.0	0.8	5	24.0	11.1	8.0	26.0	1	0.05	26.2	17.74	21%	2.8
	0.36	10.0	23.3	2.5	1.0	0.8	5	24.0	11.1	8.0	26.0	1	0.05	26.2	17.74	20%	3.6
	0.37	10.0	23.3	2.5	1.0	0.8	5	24.0	11.1	8.0	26.0	1	0.05	26.2	17.74	9%	2.8
	0.35	10.0	23.3	2.5	1.0	0.8	5	24.0	11.1	8.0	26.0	1	0.05	26.2	17.74	9%	3.8
Envirofit[c]	0.38	9.5	19.6	3.2	1.2	1.0	5	24.0	11.1	8.0	25.0	0.05	0.05	26.2	17.74	9%	4.4
	0.41	9.5	19.6	3.2	1.2	1.0	5	24.0	11.1	8.0	25.0	0.05	0.05	26.2	17.74	9%	4.9
	0.37	9.5	19.6	3.2	1.2	1.0	5	24.0	11.1	8.0	25.0	0.05	0.05	26.2	17.74	22%	2.7
	0.41	9.5	19.6	3.2	1.2	1.0	5	24.0	11.1	8.0	25.0	0.05	0.05	26.2	17.74	22%	3.3
	0.36	9.5	19.6	3.2	1.2	1.0	5	24.0	11.1	8.0	25.0	0.05	0.05	26.2	17.74	9%	2.9
	0.40	9.5	19.6	3.2	1.2	1.0	5	24.0	11.1	8.0	25.0	0.05	0.05	26.2	17.74	10%	3.8
Minmum	0.18	9.5	10.0	0.5	0.5	0.4	5.0	20.0	6.6	1.0	18.10	0.04	0.05	26.2	17.74	0%	2.0
Maximum	0.47	18.0	36.0	3.5	3.5	1.6	7.5	31.0	15.9	17.8	32.00	26.20	0.05	26.2	19.26	22%	6.3
Average	0.34	14.6	18.2	2.5	1.8	1.0	6.0	25.5	11.7	10.8	22.01	12.82	0.05	26.2	18.61	5%	3.9

[a](Bussmann and Prasad, 1986), [b](MacCarty, Still, and Ogle, 2010), [c](Jetter et. al., 2012)
[d]shaded cells denote estimates

In (Bussmann and Prasad, 1986), a shielded fire cookstove prototype with primary and secondary air constructed of sheet metal was modeled and experimentally validated through parametric variations of design variables under constant operating conditions. Geometrical variations included steps of D_p, H_c, W_c, W_p, W_{sh}, H_{sh}, as well as the insulation of the combustion chamber (D_s and k_s), for a total of 34 data points. The test protocol sought to operate the stove at a constant 4 kW firepower for about 1 hour with the covered pot holding an unspecified amount of water although concurrent publications (Prasad, Sangen and Visser, 1985) indicated the pots were filled 2/3 full. The water quantity was estimated as 5 liters for the 20 and 24 cm diameter pots, and 7.5 liters for the 28 cm pot. Thermal efficiency was reported; however, the variation or number of tests were not. In some of the parametric variations, the default values of several constant variables were not specified explicitly but were inferred by comparison to results and variables in other variations, indicated by grey shaded cells in Table 4.1. There is no indication of the moisture content or heating value of the fuel, so these are assumed as 0% for dry fuel and 18.6 $MJ/kg_{as\text{-}recd}$ as the default per (Ragland and Baker, 1991), and it was assumed the reported constant 4 kW firepower accounts for these. The thermal conductivity of the sheet metal, assumed 0.5 mm thick, and added fiberglass insulation were not specified but were determined from the literature per Table 4.2.

Table 4.2. Thermal conductivity

Material	Thermal Conductivity
Sheet Metal[a]	26.2
Concrete[a]	1.7
Fireclay Brick[b]	1
Pumice Brick[b]	0.6
Wood Ash[a]	0.18
Perlite[b]	0.05
Fiberglass[b]	0.04

[a](Avallone, Baumeister, and Sadegh, 2007), [b](Incropera et. al., 2007)

The laboratory stove testing report of (MacCarty, Still, and Ogle, 2010) presented laboratory test results of fifty cookstoves, including those with chimney, electric fan, and prepared or liquid fuels in addition to the single-pot shielded fire of interest here. Of these, several did not meet the criteria of the model due to a combustion chamber that was a) too short, b) of a diameter larger than that of the pot, or c) not cylindrical. However, five stoves were suitable, including two that were tested both with and without a pot shield. These stoves included the StoveTec fireclay brick one- and two-door stoves with and without a pot shield, the Mauritania stove with a heavy concrete-like combustion chamber, the World Food Program (WFP) stove with a wood ash filled combustion chamber, and the UCODEA stove with a pumice brick combustion chamber. These provided a total of 17 data points which used the Water Boiling Test (WBT) (Bailis et. al., 2007) to bring five liters of water with no lid from room temperature to boiling at high power, or to maintain the water at a simmer at low firepower. The firepower was not prescribed or controlled, but the average firepower was determined by the feed rate of fuel required to bring the water to boil as quickly as possible without being excessively wasteful of fuel, or to maintain the water 3˚C below boiling during simmer, as

indicated by the test protocol. Specific consumption was reported in lieu of thermal efficiency, however thermal efficiency measurements were available from the primary data incorporating the average of three to nine WBT results for cold start, hot start and simmer. Stove geometry details were not provided, but the physical stove models were available for measurement. Thermal conductivity of the materials was not reported but determined per Table 2, and the thickness of the sheet metal pot shields was assumed to be 0.5 mm.

The (Jetter et. al., 2012) study reported laboratory fuel and emissions performance of twenty-three stoves, also including stove designs and fuels not applicable to this data set. Two stoves met the criteria, including the StoveTec fireclay brick one-door (also tested in (MacCarty, Still, and Ogle, 2010)) and the Envirofit perlite-filled stove. These were evaluated at medium and high firepower and two levels of fuel moisture content for a total of 12 data points. The WBT was used to bring five liters of water with no lid from room temperature to boiling at medium or high power, where firepower was not prescribed or held constant but calculated from fuel consumption. The average and standard deviation of thermal efficiency from three WBTs was reported, with the exception of low power tests. Stove geometry details were not provided, but the physical stove models were available for measurement. Thermal conductivity of the materials was not reported but determined per Table 2, and the thickness of the sheet metal pot shields was assumed to be 0.5 mm.

From the three selected studies, 63 reported experimental data points were available. As a whole, the group includes variation of each geometrical, material, and operating design variable. Figure 4.3 shows the cookstove models and Table 1 provides a collection of the measured thermal efficiency and 15 design variables for the 63 data points. Table 4.3 shows the range and averages of each variable, indicating the design space covered by the data set.

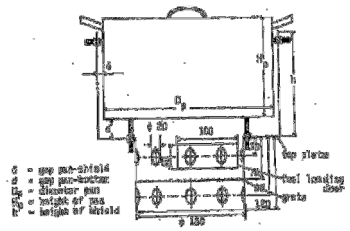

Fig. 1. Standard configuration of the stove.

Bussmann Stove

Sheet metal body, fiberglass insulation added

34 variations of H_c, g_c, g_p, g_{sh}, H_{sh}, k_s
(Bussmann and Prasad, 1986)

StoveTec Two-Door

Fireclay brick combustion chamber
with and without pot shield

Cold Start, Hot Start, Simmer (MacCarty, Still, and Ogle, 2010)

StoveTec One-Door

Fireclay brick combustion chamber
with and without pot shield

Cold Start, Hot Start, Simmer (MacCarty, Still, and Ogle, 2010)
Low moisture content fuel at 4 firepower levels,
High moisture content fuel at 2 firepower levels
(Jetter et. al., 2012)

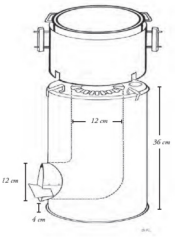

WFP Rocket

Wood ash-filled metal combustion chamber
Pot shield

Cold Start, Hot Start, Simmer
(MacCarty, Still, and Ogle, 2010)

Mauritania Rocket

Mud/cement combustion chamber
Pot shield

Cold Start, Hot Start, Simmer (MacCarty, Still, and Ogle, 2010)

Figure 4.3. Stoves and variations

UCODEA Rocket

Pumice combustion chamber
Integral pot shield

Cold Start, Hot Start, Simmer (MacCarty, Still, and Ogle, 2010)

Envirofit G3300

Perlite-filled metal combustion chamber
Pot shield

Low moisture content fuel at 4 firepower levels,
high moisture content fuel at 2 firepower levels
(Jetter et. al., 2012)

Figure 4.3 continued

Table 4.3. Range of variables in data set

			Minimum	Maximum	Average
Geometrical Variables					
Combustion chamber diameter	D_c	cm	9.5	18.0	14.6
Combustion chamber height	H_c	cm	10.0	36.0	18.2
Gap at combustion chamber	W_c	cm	0.5	3.5	2.5
Gap at pot corner	W_p	cm	0.5	3.5	1.8
Shield gap[a]	W_{sh}	cm	0.4	1.6	1.0
Stove diameter	D_{stove}	cm	18.10	32.0	22.0
Shield height[a]	H_{sh}	cm	1.0	17.8	10.8
Shield thickness[a]	t_{sh}	cm	0.05	0.05	0.05
Pot diameter	D_p	cm	20.0	31.0	25.5
Pot water height	H_p	cm	6.6	15.9	11.7
Pot volume	V_p	L	5.0	7.5	6.0
Operational Variables					
Fuel Heating Value	LHV_f	MJ/kg	17.74	19.26	18.61
Fuel Moisture Content	MC_f		0%	22%	5%
Firepower	q	kW	2.0	6.3	3.9

[a]Does not include unshielded pot data points

4.4 Analysis

Investigation of the data set as a whole indicates the consistency and thus reliability of the results, trends in performance and design variables, and any gaps in the data. Incorporating results from all studies in such a way increases the richness of the findings from each individual study, quantitatively confirming qualitative knowledge and thumb rules (Bryden et. al., 2005). It should be noted that the (Bussmann and Prasad, 1986) study analyzed the effects of variation on heat transfer only, and it is likely that some of the highest efficiency data points occurred at the expense of increased pollutant emissions. The (MacCarty, Still, and Ogle, 2010) and (Jetter et. al., 2012) studies analyzed cookstoves that had been designed to optimize both heat transfer and combustion efficiencies, thus generally present only designs that do not result in excessive emissions.

4.1.1 Minimizing the gaps around the pot while maintaining flow increases convective heat transfer efficiency.

In Figures 4.4-4.5, efficiency clearly increases with decreasing pot shield gap. Cross-sectional flow area is accounted for in Fig. 4.4 by the shield gap to pot radius ratio, including stoves with no pot shield positioned at the maximum x-axis of the chart. This figure shows a clear trend for all stoves of increasing heat transfer as this ratio is decreased, with the dataset maximum efficiency of 47% occurring at the dataset minimum shield gap to pot radius ratio. Some of the lowest efficiency values of the data set occur at the four data points with no pot shield, confirming that the presence of a shield is one of the most important factors in increased efficiency. However, when the cross-sectional flow area is reduced too severely, as shown by the two points for small shield gaps (8mm) paired with small diameter pots from (Bussmann and

Prasad, 1986) highlighted in Fig. 4.5, efficiency decreases due to reduced flow velocity. The same effects are shown by a parametrically decreasing pot bottom gap in (Bussmann and Prasad, 1986) shown Table 4.1.

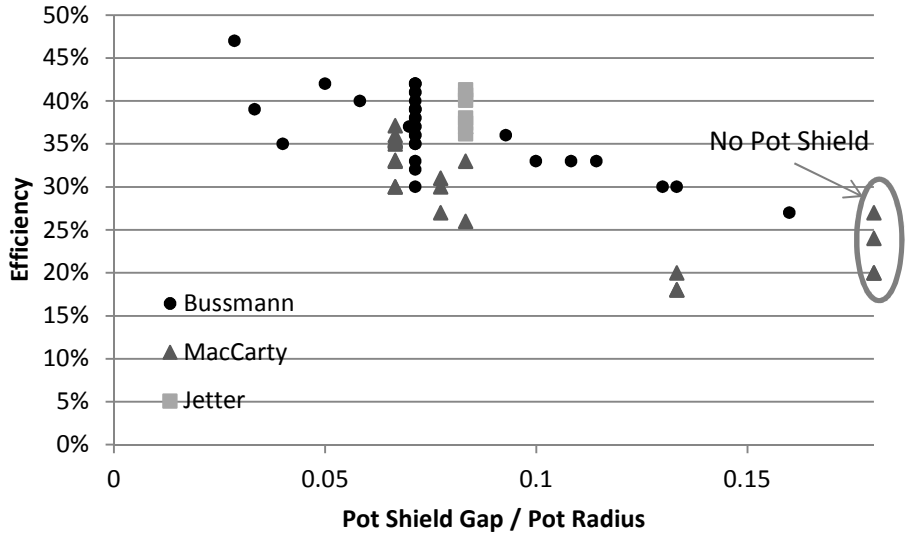

Figure 4.4. Efficiency vs. dimensionless pot shield gap to pot radius ratio

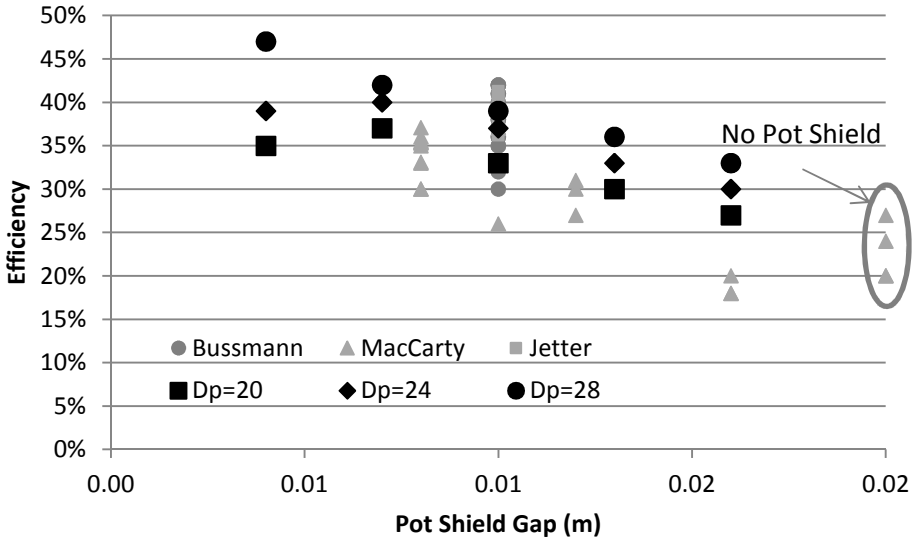

Figure 4.5. Efficiency vs. pot shield gap, highlighted for various pot diameters (cm)

4.4.2 Use of a pot shield increases heat transfer into the pot sides, with diminishing returns as shield height increases.

While the confounding effects of other variables obscure trends in shield height within the data set as a whole, the parametric shield height study from (Bussmann and Prasad, 1986) clearly indicates this relationship (Fig 4.6), predicted by (Baldwin, 1987).

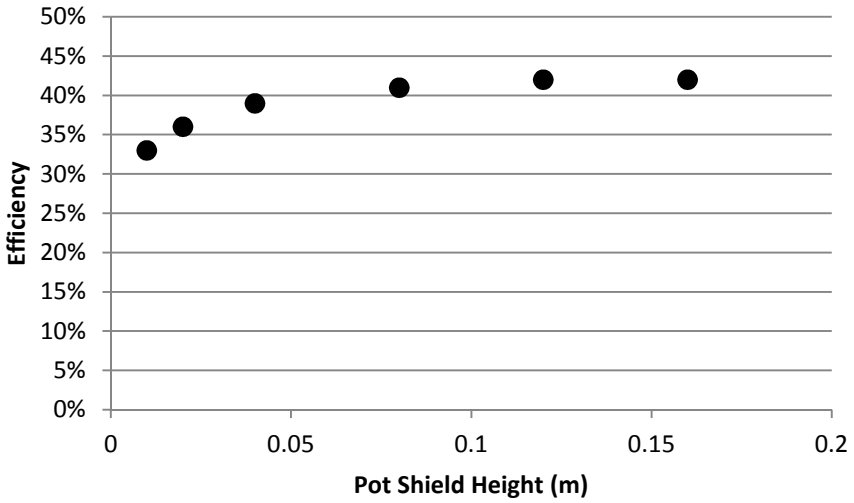

Figure 4.6. Efficiency vs. pot shield height (Bussmann and Prasad, 1986)

4.4.3 A shorter combustion chamber is more efficient.

A shorter combustion chamber places the pot in closer proximity to the fuel bed, resulting in greater radiation heat transfer and higher temperatures for convective heat transfer into the pot. This is illustrated by the downward trend in efficiency from the dataset maximum of 47% at 10 cm combustion chamber height to the dataset minimum of 18% at 36 cm combustion chamber height (Fig. 4.7). As was demonstrated by the parametric study of (Bussmann and Prasad, 1986), highlighted in the figure, this effect is less pronounced when the combustion chamber is

insulated. As shown by the broad range of this trend, other geometrical and design variables also play a significant role in overall efficiency.

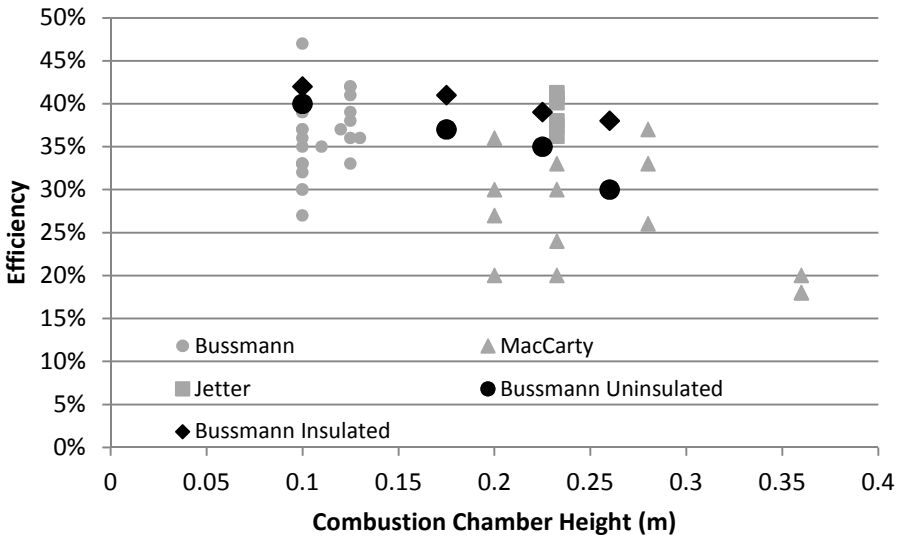

Figure 4.7. Efficiency vs. combustion chamber height

4.4.4 An insulated combustion chamber is more efficient

Thumb rules, previous models (Baldwin, 1987), and common sense indicate that an insulated combustion chamber improves efficiency of heat transfer to the pot by reducing losses. This is clearly indicated by the efficiency vs. thermal resistance (R-value, stove wall thickness divided by material thermal conductivity) shown in Fig. 4.8. Here some of the highest efficiencies occur at the highest resistance (R) values. The (Bussmann and Prasad, 1986) study evaluated a single metal wall stove of low R value with varying geometries, which indicates the potential range of performance for a given R-value.

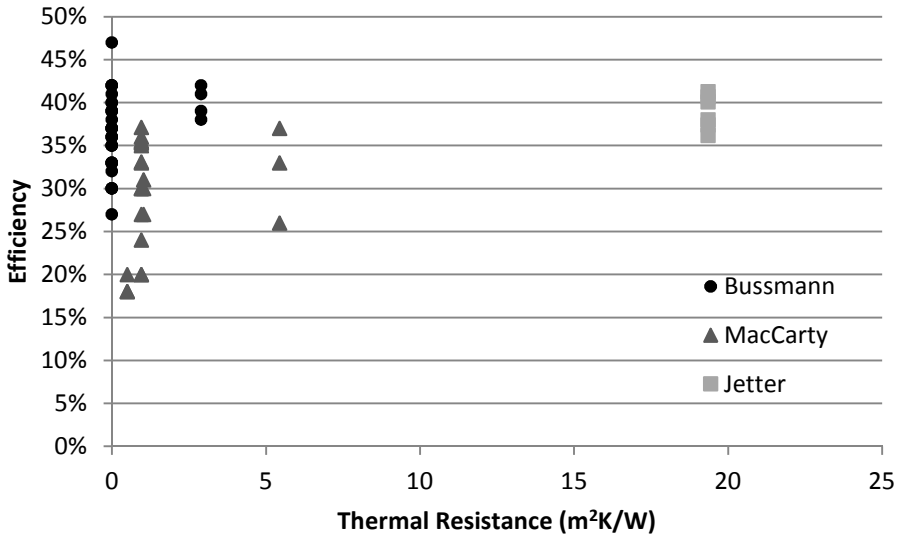

Figure 4.8. Efficiency vs. stove body thermal resistance (R-value)

4.4.5 A greater fire intensity generates greater efficiency.

A higher firepower for a given combustion chamber volume (Fig. 4.9) or plan area (Fig. 4.10) shows a slight trend in increased efficiency throughout the data set. The firepower and combustion chamber diameter were held constant in (Bussmann and Prasad, 1986), illustrating the lower sensitivity of the fire intensity metrics in comparison to other variables.

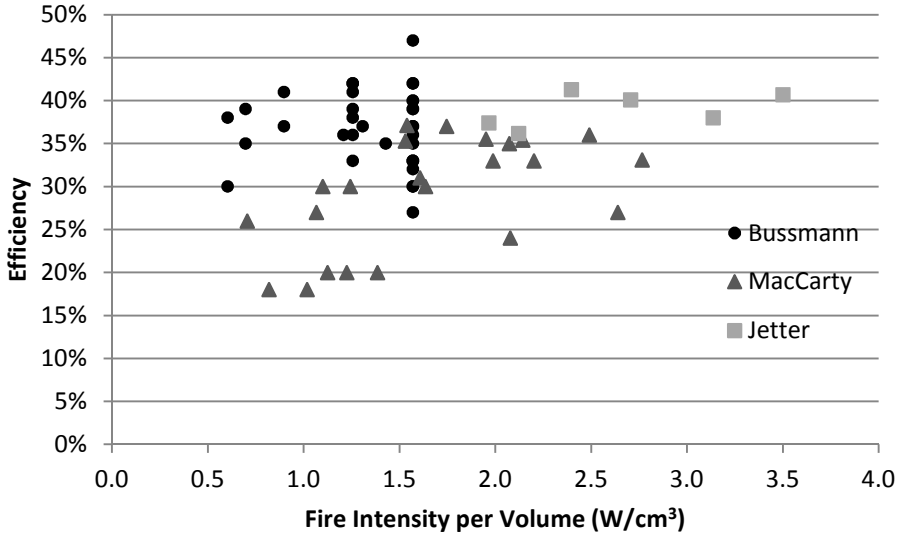

Figure 4.9. Efficiency vs. fire intensity per combustion chamber volume

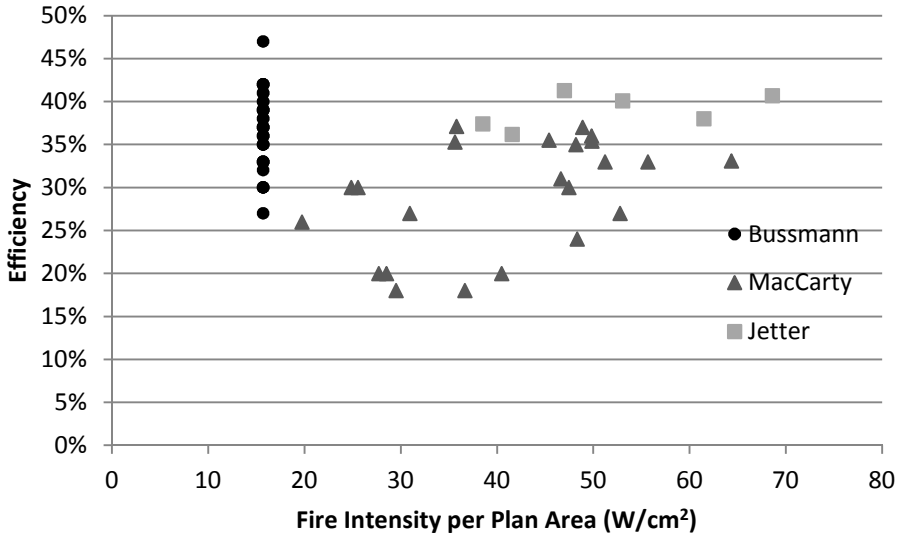

Figure 4.10. Efficiency vs. fire intensity per combustion chamber plan area

4.5 Conclusions

This article provided a unified data set useful for validating zonal models of single pot, cylindrical, shielded fire, wood burning cookstoves. The data set includes 63 data points of

empirical efficiency encompassing parametric variation of 15 operating, geometrical, and material design variables. The data set is shown to be consistent as evidenced by banded data with no outliers that follow known trends and quantitatively support qualitative thumb rules.

The compilation of this data set from the few available articles which offered nearly all of the information required illustrates the need for more detailed experimental reporting which should include thorough descriptions of all physical and operational variables involved in the experiment. In order to be useful to the development of zonal models, a cookstove testing study should compare and report the thermal performance characteristics in terms of design characteristics, including sufficient detail of geometry and operation.

Future work should involve expansion and broadening of the data set and stove types covered. While several variations of each design variable were included in this study, additional data points for unshielded pots, variation of fuel moisture content, and an overall expansion of the design space for this stove type would be useful. In addition, similar data sets should be created for round bottomed pots, and for stoves which utilize charcoal, prepared fuels, and/or forced draft.

Acknowledgements

The authors gratefully acknowledge the financial support of Nordica MacCarty by the United States National Science Foundation Graduate Research Fellowship Program. In addition, the authors thank the Aprovecho Research Center for access to their past experimental data.

CHAPTER 5

A GENERALIZED ZONAL HEAT-TRANSFER MODEL FOR SHIELDED-FIRE HOUSEHOLD COOKSTOVES

Draft of a paper to be submitted for publication in *Energy*

Nordica A. MacCarty, Kenneth M. Bryden

Abstract

Despite several decades of engineering improved biomass cookstoves, to date there is no existing dominant design basis or accepted heat transfer model and equation set for these widely used household devices. This paper presents a steady-state heat transfer model of a shielded-fire, natural-draft biomass cookstove suitable for conceptual design of the small household cookstoves used in developing countries. This model was validated using data from three previously published studies and included 63 geometric and operating variations of 15 design variables. The input variables included 10 geometrical design variables, 2 material design variables, and 3 operating conditions, any of which can be considered as design constraints as user preferences dictate. The thermal efficiency of 59 of the 63 designs was predicted within 5.0% of the reported cookstove value with an L2 norm error of 3.0%. Parametric variations of design variables within the model can assist in the conceptual phase of design. In addition, the temperature and velocity profiles, location and magnitude of losses, and heat transfer contributions through various modes and regions of the pot are detailed to lead to greater understanding of the cookstove system.

5.1 Introduction and Background

Approximately 2.7 billion people use solid biomass fuel in small stoves and three-stone fires to meet their household energy needs for cooking each day (IEA, 2010). This results in a number of adverse health, safety, community, and environmental effects including 4 million premature deaths per year (Lim et. al, 2012), deforestation, and climate-changing emissions (Rehfuess, 2006; IEA, 2010; Bond and Sun, 2005). Recent projections indicate that use of biomass for cooking will increase and continue to be the dominant energy use in rural households through 2030 (IEA, 2010; Diaoglou, 2012) and studies in the West African Sahel found that 98% of household energy needs are met with small household cookstoves (Johnson and Bryden, 2012 a and b). For these subsistence-level families, the cost of acquiring this fuel represents a significant fraction of household time and income (Rehfuess, 2006). As a result the design, manufacture, and distribution of clean, low cost, high efficiency household cookstoves has identified by many governmental and non-governmental organizations as a critical need to improve the lives of the resource-poor while concurrently addressing millennium development goals and slowing climate change.

To meet this need a number groups have over the past thirty years worked to design household cookstoves, with more than 160 stove projects currently operating worldwide (Ruiz-Mercado et. al., 2011). Yet the design of cookstoves today is a heuristic trial and error process based on previous experience, engineering judgment, thumb rules, and experiment. To date there is no dominant design basis or established design algorithm for optimizing the efficiency of these devices, nor are there validated and accepted models or modeling guidelines to support the design process. In addition, there is no standard methodology for stove testing and reporting such that experimental data can be used for model development and validation. Over the past 30 years

fewer than 30 journal articles have been written on the computational modeling of household biomass cookstoves, with the majority focusing on a single stove design, and few of these provide detailed experimental validation of the computational results. This paper addresses the need for a flexible and robust equation set for computational modeling of the heat transfer processes occurring within a typical cooking stove to assist in the conceptual design process.

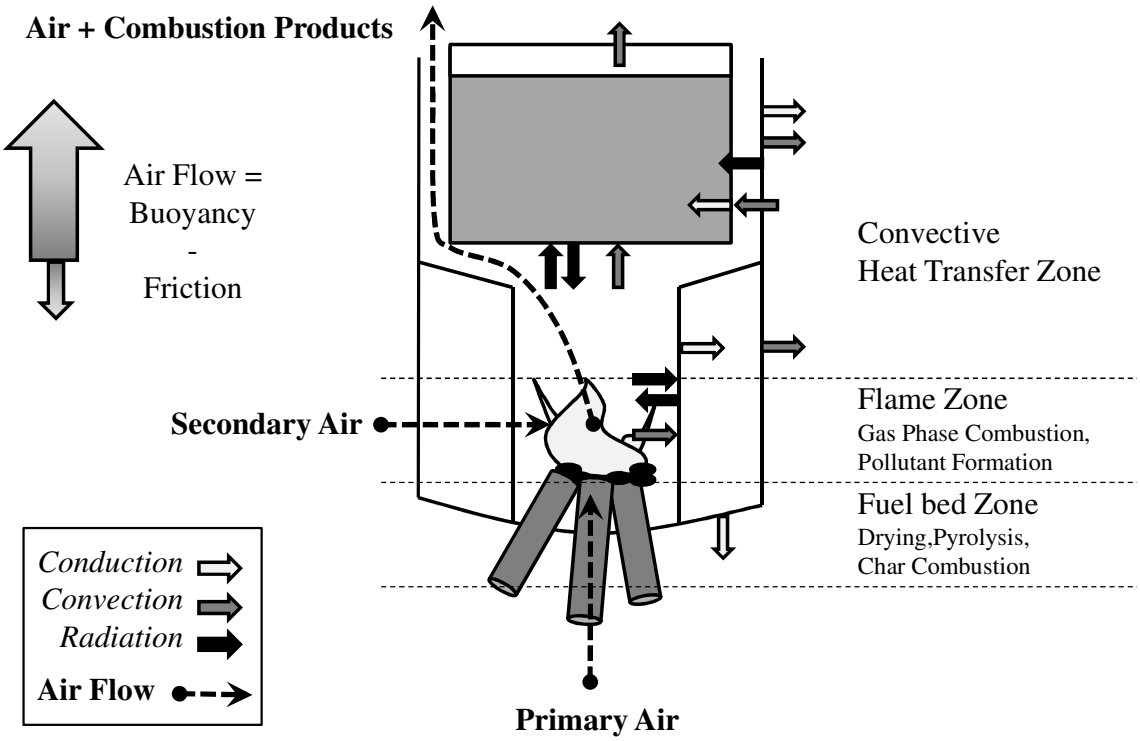

Figure 5.1. Combustion, flow, and heat transfer processes

As shown in Figure 5.1, a biomass cooking stove can be conceptualized as being composed of the air handling system, the combustion chamber, the convective hear transfer region, the cooking pot, and the support structure and insulation. The air handling system directs

the flow of primary and secondary air. The combustion chamber encloses the solid phase and gas phase combustion region and provides for radiant heat transfer from combustion to the cooking pot. The convective heat transfer system transfers energy from the combustion products to the cooking pot, and the cooking pot holds the food or water. The support structure and insulation provide the structural support to hold the other components together, limit energy loss from the stove, and protect the user from the heat and flame. A traditional stove such as the three-stone fire may have only one or two components, whereas a highly engineered stove may have complex designs for each of the components.

For modeling purposes, this system can be divided into three zones: the solid phase packed bed zone, the gas phase combustion or flame zone, and the heat transfer zone. In the packed bed, solid phase combustion includes heating of the wood and drying of the fuel moisture followed by pyrolysis and char burning with primary air. In the flame zone, secondary air enters, is heated, and is supplied to gas phase combustion. In the heat transfer zone, energy is lost through the stove walls, transferred to the pot via convection and radiation, and exits as sensible losses. Fluid flow and the entrainment of excess air are driven by natural buoyancy, and is slowed by pressure losses due to friction throughout the various geometries of the flow path.

Two types of cookstove models have developed by researchers. The primary type of model is a zonal model in which conservation of mass, momentum, and energy are applied to various zones within a cookstove. In the second type model of computational fluid dynamics (CFD) is used to examine various aspects of small cookstoves. Initial modeling efforts included algebraic and differential zonal models of open fires, shielded-fire stoves, and enclosed stoves in the 1980s by the Woodburning Stove Group at Eindhoven University, identifying equation sets for fluid flow and heat transfer throughout the system (De Lepeliere et. al., 1981; Bussmann and

Prasad, 1982; Bussmann, Visser, and Prasad, 1983; Bussmann and Prasad, 1986; Prasad, Sangen, and Visser, 1985). This was followed by investigation of specific regions such as wall losses or heat transfer correlations within a pot shield (Baldwin, 1987), or models of a specific stove design (Date, 1988; Kumar, Lokras, and Jagadish, 1990). After a dry period in the 1990s, researchers continued to algebraically model specific stove designs (Agenbroad et. al., 2011a and b, Zube, 2010) and some incorporated solid and gas phase combustion rates and efficiency (Shah and Date, 2011). Use of commercial computational fluid dynamics packages for stove modeling also began to be used for the complete system (Burnham-Slipper 2007a and b, 2008; Gupta and Mittal, 2010a and b; Joshi et. al, 2012; Ravi, Kohli, and Ray, 2002; Ravi, Sinha, and Jhalani, 2002) or for investigating heat transfer in specific regions of the stove (Wohlgemuth, Mazumder, and Andreatta, 2009; Urban, Bryden, and Ashlock, 2002; McCorkle, Bryden, and Carmichael, 2003; Bryden et. al., 2003). The lessons learned through these efforts are valuable for creating a zonal model, and are reviewed in Chapter 3.

Pairing experimental data with heat transfer correlations into algebraic models for optimization can be successful, as was shown for a model for predicting cooking pots' efficiency using neural networks in (Hannai et. al., 2006). In that study, a mathematical model was constructed to predict the thermal performance of cooking pots based on experimental data for varying pot radii, height, degree of curvature, material conductivity, and flame diameter. This model was then validated using separate experiments and used to determine the effects of different parameters on efficiency. As a result, the optimal cooking pot could be designed for a given situation, similar to the present goal with cookstoves.

5.2 Model Development

As noted earlier, due to the lack of a suitable and accessible equation set, the current stove design process does not involve the assistance of computational modeling during the conceptual design phase, resulting in a missed opportunity for greater speed and accuracy in arriving at the most efficient design. To fill this gap, this paper presents a validated equation set for prediction of the steady-state thermal efficiency of a cylindrical, shielded-fire household cookstove with a natural draft air supply and flat-bottomed metal pot of diameter larger than the combustion chamber burning a continuous feed of wood sticks as fuel. This general design was chosen as representative of the more common existing improved stove designs today as shown by stove testing catalogs (Jetter et. al., 2012; MacCarty, Still, and Ogle, 2010). While cookstoves using prepared fuels or forced draft may offer good performance, these will require modifications to modeling techniques and data for validation and are therefore left for a later time. The present model is based on a review of past modeling efforts of heat transfer and fluid flow, and validated using 63 data points of experimental results from the literature.

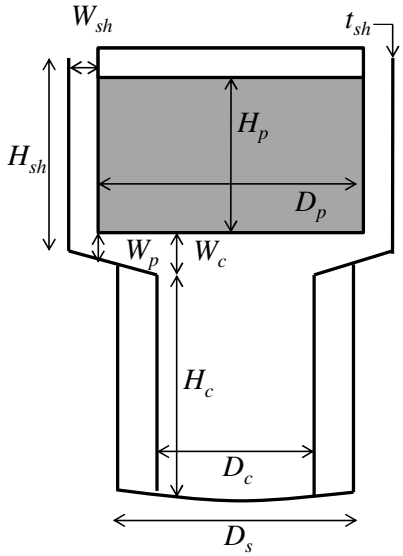

Figure 5.2. Stove geometry

The model utilizes 15 operational, geometrical, and material design variables. The operating conditions include a constant given firepower, fuel heating value and as-received moisture content. The stove material and geometry can in most cases be described by the following 12 design variables (Fig. 5.2):

- D_c – combustion chamber diameter
- H_c – combustion chamber height
- W_c – gap at the edge of the combustion chamber
- W_p – gap at the edge of the pot bottom
- W_{sh} – gap between shield (if included) and pot
- D_p – pot diameter
- H_p – height of water in the pot based on water volume
- D_s – stove combustion chamber body diameter
- k_s – stove body material conductivity
- H_{sh} – height of shield, if included
- t_{sh} – thickness of shield material
- k_{sh} – shield material conductivity

5.2.1 Model assumptions

The following assumptions were made:

- The operation is steady state.
- The firepower is given and sets the combustion rate.

- The fuel bed receives moist wood and underfire air as inputs. The wood is dried and pyrolyzed in the fuel bed producing water vapor, pyrolysis gases, and char. The char is combusted with oxygen to form carbon dioxide. The underfire air is stoichiometric with respect the char combustion.
- The gases leaving the fuel bed leave at the temperature of the top surface of fuel bed.
- The fuel bed covers the entire adiabatic bottom of the combustion chamber.
- Combustion is assumed to be complete (Ragland and Bryden, 2011).
- The thermodynamic properties of the combustion gases except for water vapor from fuel moisture content are the same as air.
- There is axisymmetric, one-dimensional, vertical airflow within the combustion chamber.
- The radial temperature is uniform.
- Radiation heat transfer is idealized with radiant heat transfer only between surfaces with non-participating media. A radiation heat transfer adjustment factor, ϕ, of 0.2 for both the flame and the gas is introduced to account for non-ideal radiative heat transfer between interior surfaces.
- In the cases where the combustion chamber and stove top include multiple layers (such as metal surrounding insulation), the insulative effect of the metal is assumed to be negligible.
- The pot is a flat-bottomed, metal pot.
- Combustion constants and properties are shown in Table 5.1.

The model determines heat transfer and losses via the energy balance in the elements within each of the three zones within the stove.

Table 5.1. Properties and constants

Property	Value	Reference
Wood Combustion	$CH_{1.48}O_{0.65} + 1.05(O_2 + 3.76N_2) \rightarrow CO_2 + 0.74H_2O + 3.93N_2$	(Ragland and Baker, 1991)
	$f_{(s)}$=0.166	
	$AFR_{(s)}$=6.04 (assumed for all experimental comparisons)	
	$LHV = HHV - \left(\frac{m_{H_2O}}{m_f} \right) h_{fg}$ (5.1)	
	$HHV_{f,dry}$=20 MJ/kg (assumed unless specifically provided)	
	$LHV_{dry} = y_{ch} HHV_{ch} + y_v LHV_v$ (5.2)	
Char Combustion	y_{ch}=0.2	(Bussmann 1983, 1986, 1988; Prasad 1985; Ragland 1991)
	HHV_{ch}=32.8 MJ/kg (assuming all carbon)	
	λ_{ch}=1	
	$C + \left(O_2 + 3.76N_2\right) \rightarrow CO_2 + 3.76N_2$ (5.3)	
Pot Details	T_p=373K	
	ε_p=1.0	
	$F_{b\text{-}p}$ calculated per view factor of two parallel discs	
	$F_{stovetop\text{-}p}$=1.0	
	$F_{sh\text{-}p}$=1.0	
Gas Properties	Conductivity: $k = -2 \cdot 10^{-8} T^2 + 8 \cdot 10^{-5} T + 0.0033$ W/mK	(EES, 2011)
	Density: $\rho = \frac{353.09}{T}$ kg/m^3	
	Enthalpy: $h = 0.0725T^2 + 984.49T - 7265.9$ J/kg	
	Specific Heat: $c_p = 0.145T + 984.49$ J/kgK	
	Viscosity: $\mu = -7 \cdot 10^{-12} T^2 + 4 \cdot 10^{-8} T + 8 \cdot 10^{-6}$ kg/ms	

Table 5.1 continued

	Specific heat of water: $c_{p,w} = -7E-11T^3 + 2E-7T^2 + 0.0005T + 1.6786$ kJ/kgK	
Constants	g=9.81 m/s^2	
	T_{amb}=298 K	
	σ=5.67E-8 W/m^{2}K^4	
	h_{fg}=2260 kJ/kg	(Bailis et. al., 2007)

5.2.2 The bed zone

Within the packed bed, the feed rate of wood fuel is set by the assumed firepower. The underfire air is stoichiometric with respect to the char produced. The wood fuel is dried, pyrolyzed, and char combusted at a rate consistent with the feed rate of wood. The mass flow rate and enthalpy of wood, water vapor from fuel moisture, and gases (including air, pyrolysis, and carbon dioxide from char combustion) are tracked separately. The hot gases from the fuel bed enter the flame zone where they are mixed with the overfire air. The gas species except for the water vapor are assumed to have the same thermodynamic properties of air.

An energy balance (Eq. 5.4) in the bed zone of negligible height is used to solve for the temperature of the gases leaving the bed (Bussmann, Visser, and Prasad, 1983; Bussmann and Prasad, 1986) using the bisection method. T_{wall} is guessed for the initial iteration and then taken as the average combustion chamber wall temperature to the 4th power determined in the previous iteration.

$$\dot{m}_{\text{char}}\text{HHV}_{\text{char}} = \sum_i \dot{m}_i \left(h_{bed,i} - h_{amb,i}\right) + \dot{m}_w h_{fg} + \phi_{flame}\varepsilon_{\text{char}}\sigma A_{bed} F_{bed-pot}\left(T_{bed}^4 - T_{pot}^4\right) + \phi_g \varepsilon_{\text{char}}\sigma A_{bed}\left(1 - F_{bed-pot}\right)\left(T_{bed}^4 - T_{wall}^4\right) \quad (5.4)$$

5.2.3 The flame zone

An energy balance (Eq. 5.5) in the flame zone of negligible height, assuming instantaneous and complete combustion and no radiation loss from the flame, is used to determine the gas temperature at the inlet of the combustion chamber using the bisection method.

$$\dot{m}_{\text{v}}\text{HHV}_{\text{v}} + \left[\sum_j \left[\dot{m}_j h_j\right]_{bed} + \left[\dot{m}_{air2} h_{air2}\right]_{amb}\right]_{in} = \sum_j \left[\dot{m}_j h_j\right]_{out} \quad (5.5)$$

5.2.4 The heat transfer zone

Hot gases from the flame zone enter the heat transfer zone, which is divided into five regions (Fig. 5.3). The combustion gases flow up through the combustion chamber (1), to the cooking pot center directly above the fuel bed and flame zone (2), to the cooking pot bottom beyond the edges of the combustion chamber (3), to the pot corner (4) and sides (5). Energy losses through the stove body and heat transfer to the pot are found by discretizing the energy conservation equation for each region. Regions 1, 3, and 5 are discretized into cylindrical or annular control volumes with user-defined thickness, Δx, while regions 2 and 4 are each a single volume. Radiation heat transfer is modeled assuming blackbody radiation between surfaces with non-participating media and a radiation heat transfer adjustment factor fitted from experimental data. Convective heat transfer coefficients in various regions are taken from the existing heat transfer relationships or fitted to published experimental results.

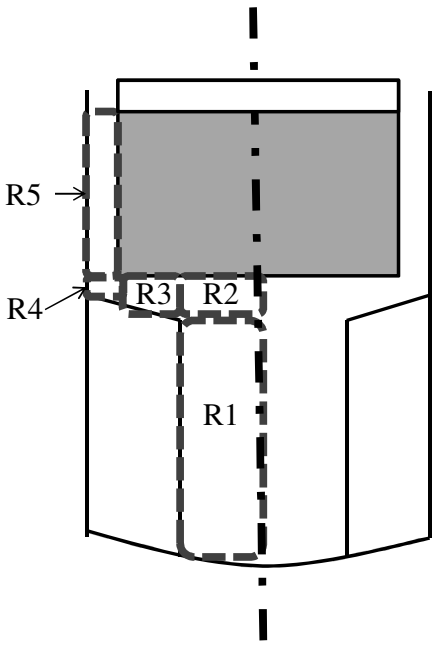

Figure 5.3. Regions of the stove

Region 1: Combustion Chamber

The control volumes in the combustion chamber are a series of stacked discs with vertical flow surrounded by the combustion chamber wall. The wall is represented by a heat flux loss through the analog model of thermal resistance, radiation in from the fuelbed, and radiation out to the pot and to the wall, with the wall-to-wall radiation assumed net zero. Conservation of energy and the bisection method are used to determine the exit temperature of each volume, with the initial inlet temperature equal to the flame temperature (Eq. 5.6).

$$\sum_k \dot{m}_k \left(h_{flame,k} - h_{out,k} \right) = \phi_g \sigma A_{pot,rad} F_{bed\text{-}wall} \left(T_{int}^4 - T_{pot}^4 \right) + \phi_{flame} \varepsilon_{\text{char}} \sigma A_{bed} F_{bed\text{-}wall} \left(T_{int}^4 - T_{bed}^4 \right) + q_{wall} \quad (5.6)$$

The heat flow through the wall is calculated through the thermal resistance analog (Eq. 5.7). Here radiative transport is treated as an equivalent convective term. In the cases of stoves with

metal walled combustion chamber and an exterior filled with insulation, only the insulative layer is considered; however, the thin metal walls could be added to the thermal resistance terms.

$$q_{wall} = \frac{T_{in} - T_{amb}}{R_{int} + R_{cond} + R_{ext}} = \frac{T_{in} - T_{int}}{R_{int}} = \frac{T_{ext} - T_{amb}}{R_{ext}} \tag{5.7}$$

where

$$R_{int} = \frac{1}{\pi D_c H_c \left(10 + \sigma \varepsilon_{\text{char}} A_{bed} F_{bed\text{-}wall} \left[\frac{\beta T_{bed}^4 + T_{pot}^4 - 2T_{int}^4}{T_{in} - T_{int}} \right] \right)} \tag{5.8}$$

$$R_{ext} = \frac{1}{\pi D_s H_c \left(1.42 \left(\frac{T_{ext} - T_{amb}}{H_s} \right)^{0.25} + \sigma \varepsilon_{wall} A_{wall} \left[\frac{T_{ext}^4 - T_{amb}^4}{T_{ext} - T_{amb}} \right] \right)} \tag{5.9}$$

$$R_{cond} = \frac{\ln\left(D_s / D_c \right)}{2\pi H_c \tilde{k}_s} \tag{5.10}$$

Here a constant interior convective heat transfer coefficient of 10 W/m^{2}K is used per (Baldwin, 1987) or this can be calculated using the heated plate equation correlation as in the exterior (Eq. (5.9)) for the combustion chamber height, which, upon investigation, varies between 5.8-13.4 with average 8.6 W/m^{2}K and L2 error of 2.1 W/m^{2}K from 10 W/m^{2}K, representing an average change in predicted efficiency of 0.03% with maximum 0.3%, thus the constant value is used. Heat flow is initially calculated using the interior and exterior wall temperatures from the previous iteration, which are then updated and bisection is used to determine the exit temperature of the gas.

Region 2: Pot Bottom Center

The single cylindrical region directly above the combustion chamber exit is treated as a stagnation point of average heat transfer to the pot only with no losses (Eq. 5.11).

$$\sum_k \dot{m}_k \left(h_{in,k} - h_{out,k} \right) = \tilde{h} \pi \left(\frac{D_c}{2} \right)^2 \left(T_{in} - T_{pot} \right) \tag{5.11}$$

The possible convective heat transfer correlations are presented in Table 5.2, including correlations from the literature (Eqs. 5.11-5.13) or optimization of the form of Eq. 5.14. These correlations were investigated in the model, concluding that $D_{plume}=D_c$ for correlation from (Bussmann, Visser, and Prasad, 1983) gave the best agreement of published options.

Table 5.2. Options for Nu at the pot bottom center

Method	Equation	
Entire pot bottom (Bussmann and Prasad, 1986)	$\mathrm{Nu}_{D_{plume}} = 1.26 \mathrm{Pr}^{0.42} \mathrm{Re}_{D_{plume}} \left(\frac{D_p}{D_{plume}} \right)^{-0.5}$	(5.11)
Entire pot bottom (Shah and Date, 2011)	$\mathrm{Nu} = 0.5 \left(1.65 \mathrm{Re}_{D_c}^{0.5} + 2.733 \mathrm{Re}_{D_c}^{0.59} \right)$	(5.12)
Stagnation region in open fire (Bussmann, Visser, and Prasad, 1983)	$\mathrm{Nu}_{D_{plume}} = 1.03 \mathrm{Pr}^{0.42} \mathrm{Re}_{D_{plume}}^{0.5} \left(\frac{D_c}{D_{plume}} \right)^{-0.65}$	(5.13)
Optimization Form	$\mathrm{Nu} = c_1 \mathrm{Re}_{D_c}^{n_{11}} \left(\frac{D_p}{D_c} \right)^{n_{21}}$	(5.14)

Region 3: Pot Bottom above Stove body

This region consists of a series of coaxial annular rings of width Δx with a potentially sloped bottom which transfer heat to both the pot bottom through convection and radiation and stove body through convection and conduction (Eq. 5.15).

$$\sum_k \dot{m}_k \left(h_{in,k} - h_{out,k}\right) = \tilde{h} A_{pot} \left(T_{in} - T_{pot}\right) + q_{wall} + \phi_g \sigma A_{pot} \left(T_{int}^4 - T_{pot}^4\right) \tag{5.15}$$

The view factor from the stovetop to pot bottom is assumed 1 (for infinite parallel plates), thus the area of the flat pot bottom is used for radiation calculations instead of the slightly sloped area of the stovetop and radiative heat transfer is neglected from the wall loss.

The convective heat transfer at the pot bottom is determined from the same two equation options as the center region (Eqs. 5.11 & 5.12) or a correlation from Bussmann's open fire work (Bussmann, Visser, and Prasad, 1983) beyond the stagnation region (Eq. 5.16).

$$\mathrm{Nu}_{D_{plume}} = 0.32 \,\mathrm{Pr}^{0.33} \,\mathrm{Re}_{D_{plume}}^{0.7} \left(\frac{r}{D_{plume}}\right)^{-1.23} \tag{5.16}$$

Or it is optimized with the form with either the same or different values of c_1, n_1, and n_2 than region 2 (Eq. 5.17).

$$\mathrm{Nu} = c_2 \,\mathrm{Re}_{D_c}^{n_{12}} \left(\frac{D_p}{D_c}\right)^{n_{22}} \tag{5.17}$$

The convective heat transfer coefficient to the stovetop is assumed equal to that of the pot. Heat loss to the stovetop uses the same thermal resistance methods as region 1, with no radiation analog at the interior and conduction through the stove body ends at the cylindrical temperature profile determined at the exit of the combustion chamber (Eq. 5.18) where $r=r_c+i\Delta x$. If the stovetop is sloped, the wall thickness begins at zero and increases to the outside of the stove (Eq.

5.19). In the case of a stove with a body diameter smaller than that of the pot, thermal resistance through the stove wall thickness to ambient is used instead, including convection and radiation terms on each end.

$$T_{body,i} = T_{ext,H_c} - \left(T_{ext,H_c} - T_{int,H_c}\right)\frac{\ln\left(r_s/r\right)}{\ln\left(r_s/r_c\right)} \tag{5.18}$$

$$t_{wall,i} = i\Delta x\frac{W_c - W_p}{r_p - r_c} \tag{5.19}$$

Region 4: Pot Corner

In the single region at the pot corner, there is no heat transfer into the pot but there are losses to the stove body and shield (Eq. 5.20). Heat flux through the body is assumed to be equal to the wall flux in the final element of region 3. Heat flux through the shield, if present, is to be assumed equal to the flux through the first element in region 5 from the previous iteration.

$$\sum_k \dot{m}_k\left(h_{in,k} - h_{out,k}\right) = q_{wall,stovetop} + q_{wall,shield} \tag{5.20}$$

Region 5: Pot Sides

At the pot sides the control volumes are a series of stacked annular rings of height Δx. The calculation of heat transfer ends at the height of the water. If the shield is higher than this level, this additional height is considered in the buoyancy calculations only. The sides of the pot have three possible conditions: 1) completely unshielded 2) within a shield and 3) in an unshielded region past the height of an existing shield. Possible convective heat transfer correlations are shown in Table 5.3, and the energy balance is shown by Eq. (5.21).

$$\sum_k \dot{m}_k\left(h_{in,k} - h_{out,k}\right) = \tilde{h}A_{pot}\left(T_{in} - T_{pot}\right) + q_{wall} + \phi_g\sigma A_{pot}\left(T_{int}^4 - T_{pot}^4\right) \tag{5.21}$$

Table 5.3. Convective heat transfer correlations at the pot sides

Method	Equation	Eq.	Reference
Unshielded Pot			
2-D turbulent wall jet	$\mathrm{Nu} = 0.25\,\mathrm{Pr}\,\mathrm{Re}^{0.75}\left(\frac{z+12}{W_{jet,0}}\right)^{-0.6}$	(5.22)	(Bussmann, Visser, and Prasad, 1983)
Forced convection laminar heated plate	$\mathrm{Nu} = 0.664\sqrt{\mathrm{Re}}$	(5.23)	(Prasad, Sangen and Visser, 1985)
Vertical heated plate as loss	$\tilde{h} = -1.42\left(\frac{T_p - T_{amb}}{H_p}\right)^{0.25}$	(5.24)	(Shah and Date, 2011)
Turbulent flow over isothermal plate	$\mathrm{Nu}_x = 0.0296\,\mathrm{Re}_x^{4/5}\,\mathrm{Pr}^{1/3}$	(5.25)	(Incropera et. al., 2007)
Shielded Region			
Thermally developing flow in parallel plates	$\overline{\mathrm{Nu}} = 1.85\left(\mathrm{Re}\,\mathrm{Pr}\frac{2W_{sh}}{H_{sh}}\right)^{1/3}$	(5.26)	(Bussmann and Prasad, 1986)
Constant Nusselt	$\overline{\mathrm{Nu}} = \frac{\tilde{h}\cdot W_{sh}}{k_g} = \text{constant} = 4.861$	(5.27)	(Baldwin, 1987)
Optimized Format	$\overline{\mathrm{Nu}} = c_3\,\mathrm{Re}^{n_{13}}\left(\frac{2W_{sh}}{D_p}\right)^{n_{23}}$	(5.28)	
Unshielded Region			
Flat plate in turbulent flow	$\mathrm{Nu}_x = 0.0296\,\mathrm{Re}_L^{4/5}\,\mathrm{Pr}^{1/3}$	(5.29)	(Incropera et. al., 2007)

Radiation from shield to pot is considered for the shielded regions with a view factor of 1 using the average interior shield temperature from the previous iteration. Heat flux through the shield wall is calculated using thermal resistance, assuming an equal interior convective heat transfer coefficient as that of to the pot and calculated per the heated plate equation on the exterior. The interior and exterior include a separate radiation term (Eqs. 5.30 and 31) such that they are combined with the convective resistance at the interior or exterior (Eq. 5.32) in parallel (Eq. 5.33) (Baldwin, 1987), which is then combined in series with conduction through the shield in a method similar to that of the combustion chamber walls (Eq. 5.7).

$$R_{rad,int} = \frac{1}{A_{sh,int}\tilde{h}_{rad,int}} = \frac{1}{A_{sh,int}\left(4\sigma\varepsilon\left(\frac{T_{sh,int}+T_p}{2}\right)^3\right)} \tag{5.30}$$

$$R_{rad,ext} = \frac{1}{A_{sh,ext}\tilde{h}_{rad,ext}} = \frac{1}{A_{sh,ext}\left(4\sigma\varepsilon\left(\frac{T_{sh,ext}+T_{amb}}{2}\right)^3\right)} \tag{5.31}$$

$$R_{conv} = \frac{1}{\tilde{h}A_{sh}} \tag{5.32}$$

$$R_{rad+conv} = \frac{R_{rad}R_{conv}}{R_{rad}+R_{conv}} \tag{5.33}$$

5.2.5 Fluid Flow

Fluid flow through the combustion chamber is determined by a momentum balance of airflow due to buoyancy and pressure losses through friction, bends, expansions, and contractions in the flow path (Eq. 5.34) which is used to determine exit velocity and thus total mass flow of gas.

$$\frac{\rho_{exit} V_{exit}^2}{2} = g\left(H_c + W_c + H_{sh}\right)\left(\rho_{amb} - \rho_{exit}\right) - \sum_l \rho_l \frac{V_l^2}{2}\left(\frac{f_l x_l}{D_{h,l}} + K_l\right) \tag{5.34}$$

The exit of the stove for buoyancy calculations is considered to be the point where the flow exits the shield surrounding the pot, or from under the pot in an unshielded stove. The flow path is treated similar to pipe flow and includes pressure drop through 1) the fuel bed, 2) 90° turn under the pot center, 3) gradual contraction or expansion from the combustion chamber along under the pot (the end of region 1 to end of region 3), 4) 90° turn at the pot corner, 5) contraction or expansion to the pot side, and 6) the friction throughout the channels per volume height. Equations for these are shown in Table 5.4. A number of possible correlations for K_{cont} along the bottom and side of the pot were available and are shown in Figure 5.4. The variable pressure drop coefficient in the bed, K_{bed} was assumed zero for all stoves, as stoves of this type have generally been designed to have little air entry resistance with possibly limited flow through the grate but free flow of air above and around the fuel. An additional term of K_{bed}=0.75 was incorporated into the Envirofit stove from (Jetter et. al., 2012) to reflect the effect of the reducer ring within the combustion chamber.

Table 5.4. Fluid flow constants and equations

Property	Equation or Value	Eq.	Reference
Friction factor in channels	Laminar $f_l = \frac{64}{\mathrm{Re}}$ Turbulent f_l=0.02-0.09	(5.35)	(DeLepeliere, 1981) Moody Diagram
90° turn at pot corner	$K_{bend} = 1.0$		(Shah and Date, 2011)
Gradual contraction	[a] $K_{cont} = 0.5 \sin\phi \left(1 - \frac{A_{l+1}}{A_l}\right)$	(5.36)	(Shah and Date, 2011)
	[b] $K_{cont} = 0.2053 \left(\frac{A_l}{A_{l+1}}\right)^2 - 0.152 \frac{A_l}{A_{l+1}}$	(5.37)	(Shaughnessy, Katz, and Schaffer, 2005)
	[c] $K_{cont} = 0.0504 \left(\frac{A_l}{A_{l+1}}\right)^2 - 0.0033 \frac{A_l}{A_{l+1}}$	(5.38)	(Shaughnessy, Katz, and Schaffer, 2005)
	[d] $K_{cont} = 2.0 \left(\frac{A_l}{A_{l+1}}\right)^{1/4} - 2.0$	(5.39)	
Gradual expansion	$K_{\exp} = \left(1 - \frac{A_l}{A_{l+1}}\right)^2$	(5.40)	(Shah and Date, 2011)

[a] ϕ = half-angle of the contraction
[b] curve fit from tabulated values for 90° contraction at the pot side
[c] curve fit from tabulated values for 10° contraction at the pot bottom
[d] correlation that exhibited the behavior needed at the pot side

The mass flow rate of gases is calculated initially assuming stoichiometric combustion to begin the iterative loop, which continually updates the temperature, velocity, and mass flow profiles, until mass flow converges to a specified tolerance, 1E-8 kg/s. A weighted average of the old and new mass flows is used to prevent overshooting in the next iteration, with a factor of 0.6

applied to the old value. Any increase in mass flow rate from the initial guess indicates inclusion of excess air due to the buoyant flow. The solution converges when the difference between mass flow rates between iterations is less than the convergence criteria, 1E-8, requiring 10-20 iterations for most stove designs to converge. Additionally, if the pressure losses through the system are greater than the driving pressure due to buoyancy after at least 10 iterations have been completed, a no-flow error message reported.

5.2.6 Heat Balances

When the solution has converged, thermal efficiency is calculated per the sum of convective and radiative heat transfer into all regions of the pot (Eq. 5.41) divided by the firepower.

$$\eta = \frac{q_{pot}}{q_{wood}} \tag{5.41}$$

Losses include the sum of the heat flow through the combustion chamber wall, stove top, corner, and shield. Sensible heat lost in the exiting gases is calculated in terms of the exit temperature at height of the pot water.

5.3 Model Validation & Verification

The model was mathematically verified by energy balance (accurate within 0.001%), investigating the effects on efficiency of changes in values for element length Δx (1mm showing the optimal grid size), convergence criteria on the mass flow rate of gases (10^{-8} kg/s), and temperature tolerance (0.001 K) in the bisection method.

Based on a literature review of stove studies over the past 30 years, several sets of experimental laboratory results were chosen to develop the needed constants and validate the model (Bussmann and Prasad, 1986; Jetter et. al., 2012; MacCarty, Still, and Ogle, 2010). The studies were chosen based on providing results for the specific type of cylindrical shielded fire stove with flat bottom pot modeled and the publishing or making otherwise available the required level of detail available on stove geometry, fuel properties, and operation. All studies used a water boiling test to measure heat transfer efficiency. This provided a consistent data set of 63 data points which include variation of all of the model design variables summarized in chapter 4. Values predicted by the model were compared to experimental results via the L2 norm error (Eq. 5.42).

$$\varepsilon_{L2} = \sqrt{\frac{\sum_{i=1}^{N} \left(\eta_{i,pred} - \eta_{i,\exp}\right)^2}{N}} \tag{5.42}$$

It should be noted that there is some uncertainty whether the model or the experimental results are the source of any discrepancies. In recent years, several international conferences, working groups, and independent studies have focused on the potential errors (Taylor, 2009), insufficient repeatability between tests (L'Orange, DeFoort, and Willson, 2012) laboratories, and operators, and lack of representativeness of in-field use (Johnson et. al, 2010) of the current dominant WBT protocol (Bailis et. al., 2007). A 2009 analysis of the method error and uncertainty including such factors as fuel ash content, unburned char sorting, and char energy content concluded that "If results of the current UCB [University of California-Berkeley] WBT are being used to compare two stove designs, the relative error in thermal efficiency, specific fuel use, firepower, turn-down ratio, and any emissions factors expressed on a per-energy or per-

mass-of-fuel-consumed basis should be assumed to be ten percent, regardless of that cited as the intra-test error" (Taylor, 2009). As such, the experimental values should be considered with an inherent potential error of at least ±5%.

Additionally, the model is steady-state, while the experimental procedures are not. The WBT begins with the water and stove starting at ambient temperature, whereas the model assumes the pot is already at boiling temperature and the heating effects of the stove body are neglected. Thus, heat transfer to the stove body and pot will both be greater than at steady state during the water and body heating phase while mass flow will likely be reduced due to lower temperature during heating.

5.4 Results

Operation of the model allowed for determination of the constraint space of the model, investigation of radiation transfer and friction factor, and selection of appropriate correlations for free variables and coefficients that most accurately reflect the empirical data. The various combinations are summarized in Table 5.5 and Figure 5.4, with discussion following.

Table 5.5. Comparison of schema

	Schema			
Bottom $_{Correlation}$ Equation	(5.11)	(5.11)	(5.43)	(5.43)
Shield Correlation Equation	(5.27)	(5.27)	(5.27)	(5.44)
ϕ_g, ϕ_{flame}	1	0.2	0.2	0.2
K Correlation Equation	(5.36)	(5.36)	(5.36)	(5.39)
Pressure Loss > Buoyancy	19	2	2	2
Outside +- 5%	24	23	15	2
L2 Norm Error	9.0%	6.5%	5.6%	3.0%
Percent of all points within 5%	32%	60%	73%	94%

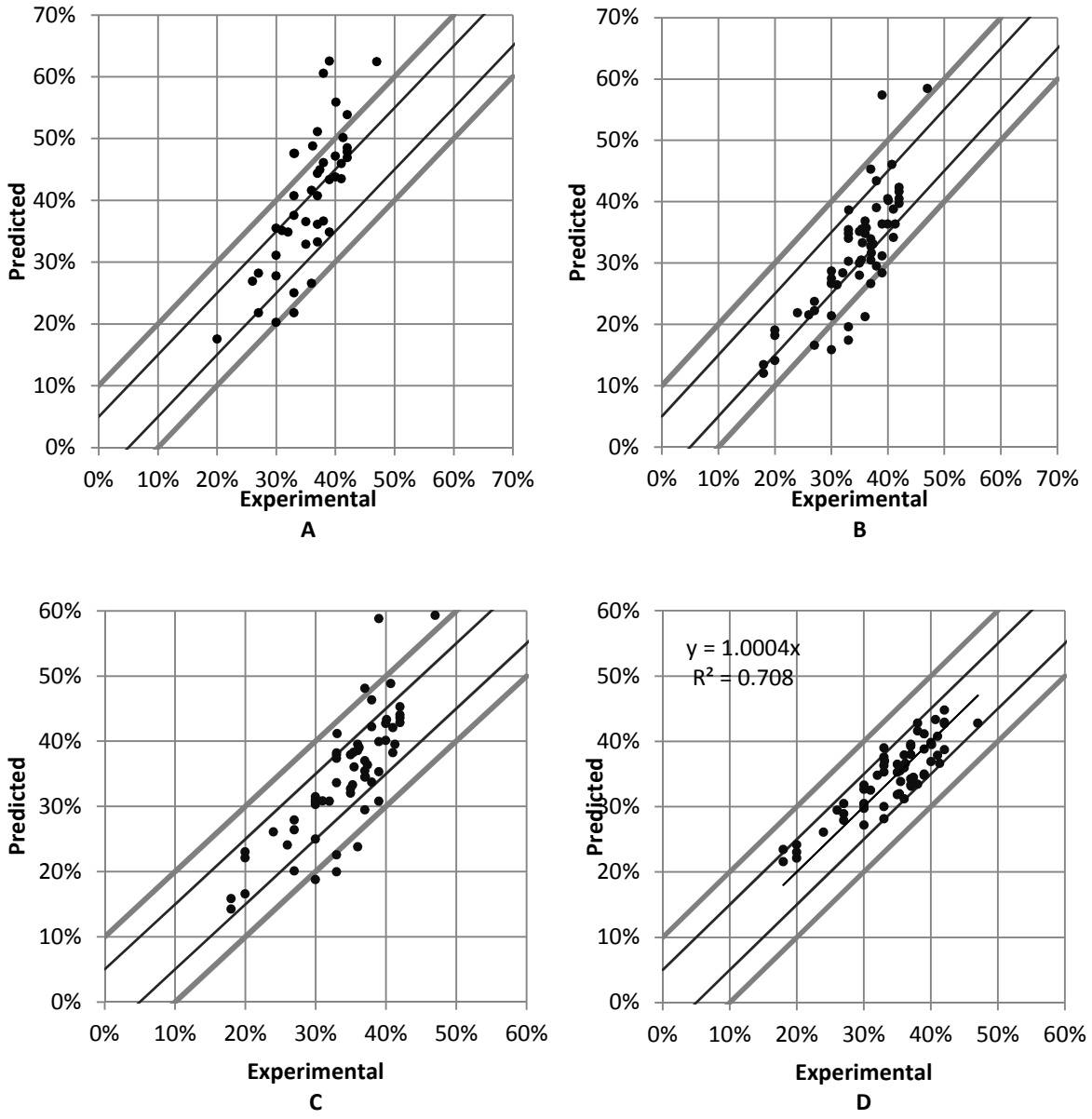

Figure 5.4. Experimental vs. predicted efficiency, with bounds of ±5%, ±10%: (A) Correlations from the literature, (B) Correlations from the literature with radiation tuning factor of 0.2, (C) Correlations from the literature with tuning factor of 0.2 and Nussselt correlation for the pot bottom optimized, (D) Tuning factor of 0.2 and optimized Nusselt correlations for the pot bottom and shield, and pot bottom pressure loss

5.4.1 Geometrical Constraints

The method of fluid flow calculation is not appropriate for all stove geometries. Cookstoves where the diameter of the combustion chamber is greater than that of the pot, such as the Ghana Wood from (MacCarty, Still, and Ogle, 2010) , are not appropriate for the pipe model of pressure loss due to the large cross sectional area of the "pipe" in which the pot was essentially a "plug" at the pipe exit. Nor are those stoves with short combustion chambers (less than 10 cm) and no pot shield through which to develop a buoyant driving force along the flow path. Additionally, extremes in geometry such as small (5 mm) gaps around the pot can create results in which the pressure losses through the system are greater than the draft generated by buoyancy, such that the model could not run.

5.4.2 Radiation adjustment factor, ϕ

Many of the early models in the literature either neglected radiative heat transfer or assumed a constant fractional value of the firepower was transferred to the pot. The present model assumes blackbody radiation heat transfer with nonparticipating media, whereas in reality the view between surfaces will be partially blocked by the flame and gases including CO_2, H_2O and soot. An adjustment factor, ϕ, was added to the radiation transfers from the fuelbed, ϕ_{fl}, and gases, ϕ_g. When this factor was 1, the radiative transfer was clearly too high, shown in Figure 5.4A. As shown in Table 5.5, the most promising pot-bottom correlations from the literature (Bussmann open fire at the pot bottom) (Eq. 5.11) paired with Baldwin's constant Nu at the pot side (Eq. 5.27), full radiation (ϕ=1.0) resulted in an L2 error of 9.0%, whereas a ϕ=0.2 shown in Figure 5.4B resulted in a L2 reduction to 6.5%. More importantly, the number of configurations where the system pressure losses were greater than the buoyancy were also reduced from 19 to 2.

5.4.3 Laminar or Turbulent Friction Factor

The friction factor in channels throughout the stove body was also in question due to Reynolds numbers in the transition region. For laminar flow, the Darcy friction factor is equal to 64/Re, whereas for turbulent flow it can be determined from the Moody diagram, between 0.02 and 0.09, depending on surface roughness. Testing these options in the model showed minor effects on efficiency, with the laminar correlation creating additional no-flow schemes. An optimization of the turbulent factor from 0-0.2 showed the best value to be between 0.086 and 0.1 between several runs, thus the turbulent factor equal to 0.09 was chosen as the default.

5.4.4 Determination and Optimization of Heat Transfer Correlations

There are five areas where multiple heat transfer coefficient correlations must be determined. The correlation for turbulent flow over an isothermal plate was deemed appropriate for both an unshielded pot and the region past an existing shield; whereas, the heat transfer correlation along the entire pot bottom and pot side within the shield were in question. Most correlations from the literature were based on experimental data and did not show suitable agreement with this more comprehensive data set, so it was a natural choice to calculate correlations in these regions based on this larger data set. A standard particle swarm optimization (PSO) was used to determine coefficients in Nusselt correlations of formats used in the literature. The PSO was run to simultaneously minimize the L2 error of predicted efficiency, the quantity of data points greater than ± 5% from the experimental data, and the number of points where the system pressure losses were greater than the draft due to buoyancy.

Several options for the format of the Nu correlation under the pot were investigated, including the formats of Shah (Eq. 5.12) and Bussmann (Eq. 5.11), differentiating correlations

for the pot bottom center and pot bottom above the stovetop (Eq. 5.13 and 5.16), and various possible characteristic lengths, with a single correlation of the form below showing the best results:

$$\overline{\mathrm{Nu}}_{p,bottom} = 0.45\,\mathrm{Re}_{D_c}^{0.736}\left(\frac{D_p}{D_c}\right)^{-0.391} \tag{5.43}$$

After the pot bottom optimization was complete, a second PSO was run for the correlation within the shielded regions of the pot (Eq. 5.28).

$$\overline{\mathrm{Nu}}_{p,side} = 0.001\,\mathrm{Re}_{D_c}^{1.414}\left(\frac{2W_{sh}}{D_p}\right)^{0.122} \tag{5.44}$$

5.4.5 Loss Coefficient for Contractions

Investigation of the loss coefficients, K, for contractions in flow (Figure 5.4) revealed the factor used had a significant impact on whether the pressure losses in the system would be greater than that of the buoyancy, especially for small shield gaps. For the pot bottom, the relationship from (Shah and Date, 2011) (Eq. 5.36) or curve fit from (Shaughnessy, Katz, and Schaffer, 2005) (Eq. 5.38) both gave the same results since there were no drastic contractions under the pot bottom in the stoves tested. However, for the significant contractions at the pot side (on the order of 50% or greater), the K value was critical. It was found that the relationship in (Shah and Date, 2011) gave values that were too low thus overpredicting efficiency and the parabolic curve fit from (Shaughnessy, Katz, and Schaffer, 2005) (Eq. 5.37) gave too high values at these severe contractions, resulting in a no-flow situation. Upon visual investigation, it was noted that the shape of the curve needed to be a root curve, equal to 0 when the area ratio was 1, increasing more rapidly initially from 1-2, then leveling off as the area ratio continued to

increase. Experimentation with values in the code showed the optimal relationship to be that of Eq. (5.39).

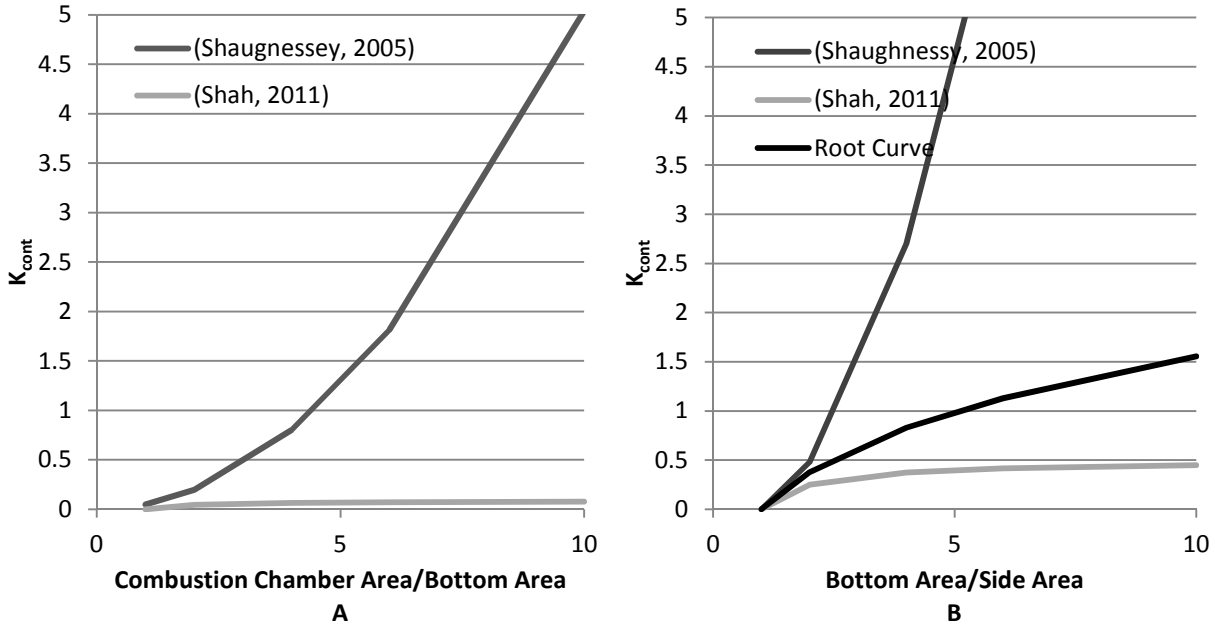

Figure 5.5. K correlations (A) Pot bottom contraction, (B) Pot side contraction

5.4.6 Comparison to Experimental Data

Results comparing the various schemes for the total 63 data points are shown in Table 5.5 and Figure 5.4. The best correlations from the literature, including the Bussmann correlation for the pot bottom (Eq. 5.11), constant Nu of 4.816 (Eq. 5.27) within the pot shield (Baldwin, 1987), and full radiation is shown in Fig. 5.4A, with 19 points missing due to pressure losses greater than buoyancy. Figure 5.4B shows that when reducing the radiation adjustment factor to 0.2 slightly underpredicts efficiency, but most importantly reduces the missing points from 19 to 2 due to greater heat remaining for the buoyant flow. The optimized correlation for the pot bottom reduced the number of outliers (outside +-5%) from 23 to 15 (Figure 5.4C). Optimizing the

correlation for the shielded areas of the pot and applying the improved K factor for the contraction at the side brought all but two data points to within 5%, and only two had system losses greater than buoyancy, for a total of 94% of data points predicted accurately (Figure 5.4D) with an L2 norm error of 3.0%.

5.4.7 Simulation

Once validated as above, the model can be used to simulate effects of design variables and to understand heat flows within the stove.

Table 5.6 shows an example of an energy balance and heat flow analysis for the one-door rocket stove with skirt at high power tested by both Jetter (2012) and MacCarty (2010) and a shielded fire stove (Bussmann and Prasad, 1986). Proportions agree relative to several scantly-detailed heat balances of stoves presented in (Prasad, Sangen and Visser, 1985).

Table 5.6. Energy balance (Watts)

	One-Door Rocket with Skirt, High Power	Fraction[a]	Bussmann D_p=24, W_{sh}=0.01, H_{sh}=0.178	Fraction[a]
Moisture evaporation	87.6		0.0	
Equivalent daf Firepower	4024.0		4000.0	
As-received Firepower	4111.6		4000.0	
Convection:				
Pot center	214.7	*15%*	297.2	*22%*
Pot bottom	699.2	*49%*	190.5	*14%*
Pot sides	390.8	*28%*	557.2	*42%*
Total Convection to Pot	1304.8	*92%*	1044.8	*79%*
Radiation:				
Fire to pot	17.8	*15%*	212.4	*74%*
Wall to pot	12.8	*11%*	17.8	*6%*
Stovetop to pot	56.4	*49%*	15.5	*5%*
Shield to pot	28.0	*24%*	40.4	*14%*
Total Radiation to Pot	115.1	*8%*	286.2	*21%*
Total to Pot	1419.9	**35%**	1331.0	**33%**
Losses:				
Wall	239.2	**6%**	123.8	**3%**
Stovetop	332.9	**8%**	122.1	**3%**
Corner	85.2	**2%**	200.1	**5%**
Shield	249.0	**6%**	302.3	**8%**
Sensible in Exhaust	1698.0	**42%**	1920.7	**48%**
Total Loss	2604.3	**65%**	2669.0	**67%**

[a]*Italic=to pot*, **Bold=total**

Table 5.7 shows flow and temperature data of those two stoves and provides a comparison to rough temperature measurements completed during steady-state operation of the one-door rocket stove, showing good agreement for all except the fuel bed and flame temperatures which were overpredicted and underpredicted, respectively.

Table 5.7. Flow and temperature data

	One-Door Rocket with Skirt, High Power	Measured	Bussmann D_p=24, W_{sh}=0.01, H_{sh}=0.178
Iterations	14		8
Mass flow (kg/s)	0.0049		0.0066
λ	3.7		4.9
Temperatures (°C)			
Fuel bed	1274	790-860	1039
Flame	674	730-830	477
Pot center	470	430-590	451
Pot corner	460	320-360	428
Exit	337	230-330	303
Heat Transfer Coefficients (W/m^2K)			
Pot center	45		26
Pot bottom	44		28
Average pot side	14		25
Velocities (m/s)			
Chamber	1.7		0.6
Pot side	1.5		1.5

Table 5.8 shows a simulation of the standard rocket stove tested in (MacCarty, Still, and Ogle, 2010 and Jetter et. al., 2012), with all variables held constant except the stove body conductivity, except for the metal case which represents a single-walled 0.5 mm metal body with no insulation. Typical stove combustion materials are shown. Studies such as this can help designers to consider the trade-offs between available materials.

Table 5.8. Insulation Study

Material	Conductivity (W/mK)	Predicted Efficiency
perlite	0.05	43.2%
pumice	0.6	36.4%
fireclay brick	1	35.2%
concrete	1.7	34.3%
metal	26.2	35.5%

Table 5.9 shows the effects of varying operating conditions such as fuel moisture content, firepower, and pot diameter on one-door rocket stove efficiency, demonstrating how the model can help to predict the effects of in-field conditions on stove performance. The experimental moisture content variation of (Jetter et. al., 2012) showed essentially no reduction in efficiency between dry (~10%) and wet (~20%) wood for the two rocket stoves, as did the model.

Table 5.9. Effect of moisture content, firepower, and pot diameter

MC_{wood} $\%_{asrecd}$	Efficiency	Firepower (W)	Efficiency	D_p (m)	Efficiency
0%	36.6%	2000	31.0%		
5%	36.2%	3000	34.2%	0.16	36.0%
10%	35.9%	4000	35.9%	0.2	35.8%
15%	35.4%	5000	36.8%	0.24	35.9%
20%	35.0%	6000	37.3%		
25%	34.5%				
30%	33.9%				

Figure 5.6 shows a sensitivity analysis of the five major geometrical variables for that stove, indicating that the pot shield gap has the most significant impact on efficiency while the combustion chamber diameter is the least sensitive of the five variables. These trends are also in agreement with the observations of Chapter 4.

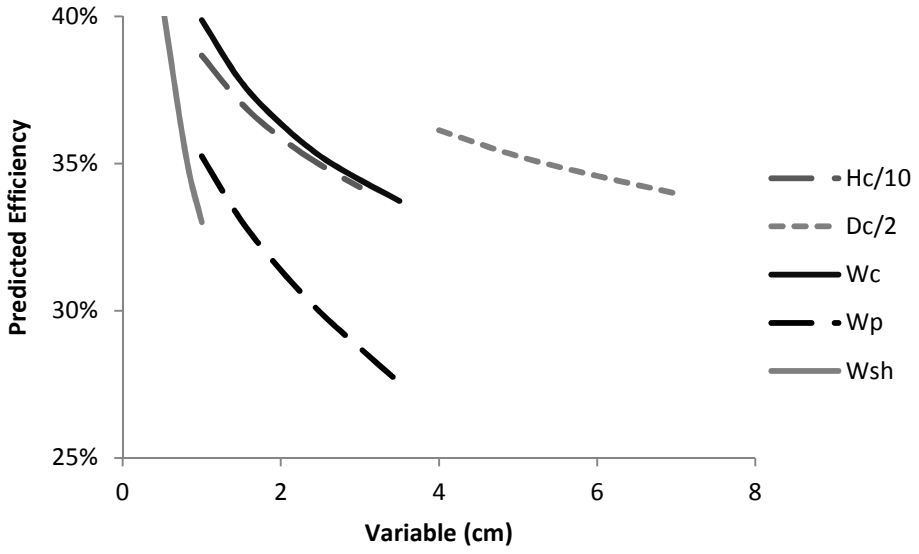

Figure 5.6. Sensitivity analysis of five geometrical design variables

5.5 Conclusions and Future Work

The equation set presented in this paper showed good success at predicting the efficiency of a wide array of stove designs. Pairing standard equations for fluid flow in a pipe successfully indicated the flow behavior for this type of cylindrical shielded-fire stove. Several standard heat transfer correlations paired with empirical Nusselt-format optimizations derived from a large data set for the flat-bottom and shielded pot regions successfully predict 94% of measured heat transfer efficiencies within 5%. The 63 experimental data points used were the only results available with sufficient detail for validating the model, indicating a need for an accepted standard of experiments and reporting methods that are useful for modeling of such stoves.

Although the model is able to predict heat transfer, it does not indicate the resulting combustion efficiency or practicality of the design, thus engineering judgment and experiment should be used to test the utility of any designs based on such a model. Additional research is

needed to include issues of emissions including black carbon and to include models for a broader variety of cookstoves. In many cases, reduction of emissions from a cookstove is as much or more important of a goal in cookstove programs; therefore, to be fully useful the model should be updated to include solid and gas phase combustion and pollutant formation processes paired with relevant experimental data for validation.

Although many of these findings confirm what has been previously known through thumb rules, the model is able to quantify the various stove configurations without the need for extensive experiments. This will enable a broader and more thorough search of the available designs during the conceptual and preliminary design stages. Testing the model's aid in design of a new cookstove given specific constraints for community, material, and cost needs would be a good step toward investigating the power of modeling in design. Any number of design variables can be optimized in conjunction with design variables set based on user needs.

Experiments and CFD can be used to verify convective heat transfer coefficients reported by the model, as well as to verify the heat fluxes through various regions.

Acknowledgements

The authors gratefully acknowledge the financial support of Nordica MacCarty by the United States National Science Foundation Graduate Research Fellowship Program.

CHAPTER 6

CONCLUSIONS AND FUTURE RESEARCH

This thesis presented the tools and data necessary for the computational modeling of a biomass cookstove. The heat transfer and fluid flow processes within a shielded cylindrical single pot cookstove burning wood were expressed and evaluated in terms of 15 design parameters. Methods and findings from the research were presented in three parts: (1) a literature review of previous modeling efforts, (2) an experimental data set from the literature for model validation, and (3) development and use of the model.

The data set includes 63 data points of empirical efficiency encompassing parametric variation of 15 operating, geometrical, and material design variables. The collection is shown to be consistent as evidenced by banded data with no outliers that follow known trends and quantitatively support qualitative thumb rules. The compilation of this data set from the few available articles which offered nearly all of the information required illustrates the need for more detailed experimental reporting of thermal performance characteristics in terms of design characteristics that should include thorough descriptions of all physical and operational variables involved in the experiment. Future work should involve expansion and broadening of the data set and stove types covered. While several variations of each design variable were included in this study, additional data points for unshielded pots, variation of fuel moisture content, and an overall expansion of the design space for this stove type would be useful. In addition, similar data sets should be created for round bottomed pots, and for stoves that utilize charcoal, prepared fuels, and/or forced draft.

The equation set presented in this paper showed good success at predicting the efficiency of a wide array of stove designs. Pairing standard equations for fluid flow in a pipe successfully indicated the flow behavior for this type of stove. Several standard heat transfer correlations paired with empirical Nusselt-format optimizations derived from a large data set for the flat-bottom and shielded pot regions successfully predict 94% of measured heat transfer efficiencies within 5%. Experiments and CFD can be used to verify convective heat transfer coefficients reported by the model as well as to verify the heat fluxes through various regions.

Although the model is able to predict heat transfer, it does not indicate the resulting combustion efficiency or practicality of the design, thus engineering judgment and experiment should be used to test the utility of any designs. Additional research is needed to include issues of emissions including black carbon and to include models for a broader variety of cookstoves. In many cases, reduction of emissions from a cookstove is as much or more important of a goal in cookstove programs; therefore, to be fully useful the model should be updated to include solid and gas phase combustion and pollutant formation processes paired with relevant experimental data for validation.

Although many of these findings confirm what has been previously known through thumb rules, the model is able to quantify the various stove configurations without the need for extensive experiments. This will enable a broader and more thorough search of the available designs during the conceptual and preliminary design stages, allowing for comparison of cost and benefit of various design elements. Testing the model's aid in the design of a new cookstove, given specific constraints for community, material, and cost needs would be a good step toward investigating the power of modeling in design. A number of design variables can be optimized in conjunction with specific design variable requirements based on local user needs.

REFERENCES

Agenbroad J, DeFoort M, Kirkpatrick A, Kreutzer C, 2011a. A simplified model for understanding natural convection driven biomass cooking stoves—Part 1: Setup and baseline validation. Energy for Sustainable Development 15(2):160–68.

Agenbroad J, DeFoort M, Kirkpatrick A, Kreutzer C., 2011b. A simplified model for understanding natural convection driven biomass cooking stoves—Part 2: With cook piece operation and the dimensionless form. Energy for Sustainable Development 15(2):169–75.

Avallone, E., Baumeister III, T., Sadegh, A. 2007. Marks' Handbook for Mechanical Engineers. McGraw-Hill.

Bailis, R., Ezzati, M., Kammen, D.M., 2003. Greenhouse Gas implications of house- hold energy technology in Kenya. Environmental Science and Technology 37 (10), 2051–2059. doi:10.1021/es026058q.

Bailis, R., Ogle, D., MacCarty, N., Still, D., Smith, K.R., Edwards, R. 2007. The Water Boiling Test, Version 3.0. Technical report, University of California, Berkeley. pciaonline.org/node/1048.

Baldwin, S. 1987. Biomass stoves: Engineering design, development and dissemination. Ph.D. thesis, Center For Energy and Environmental Studies Princeton University, Princeton, New Jersey 08544 USA.

Bhandari, S., Gopi, S., Date, A. 1988. Investigation of CTARA wood-burning stove; Part I – Experimental investigation. SADHANA, Proceedings of the Indian Academy of Science, 13:271-293.

Bhattacharya SC, Albina DO, Khaing AM. 2002a. Effects of selected parameters on performance and emission of biomass-fired cookstoves. Biomass and Bioenergy 23:387-395.

Bhattacharya SC, Albina DO, Khaing AM. 2002b. Emission factors of wood and charcoal-fired cookstoves. Biomass and Bioenergy 23:453-469.

Blackshear, P.L., Murthy, K.L. 1965. Proceedings of the Tenth International Symposium on Combustion. Philadelphia Combustion Institute. pp. 911-923.

Bond, T. C., Sun, H. 2005, Can Reducing Black Carbon Emissions Counteract Global Warming? Environ. Sci. Technol., 39, pp. 5921–5926.

Bond, T.C. et al. 2013. Bounding the role of black carbon in the climate system: A scientific assessment. Journal of Geophysical Research-Atmospheres. 118(11):5380-5552. DOI: 10.1002/jgrd.50171

Brewster, J.J. 2006. CFD Design of Improved Cookstoves. University of Strathclyde.

Bruce, N., Rehfuess, E., Mehta, S., Hutton, G., Smith, K. 2006. Indoor air pollution, Disease Control Priorities in Developing Countries 2nd ed. Oxford University Press, New York. doi:10.1596/978-0-821-36179-5/Ch-42, pp. 793–816.

Bryden, K.M., Ragland, K.W., Rutland, C.J. 2002. Modeling thermally thick pyrolysis of wood. Biomass and Bioenergy 22:41-53.

Bryden, KM, Ashlock DA, McCorkle DS, Urban GL. 2003. Optimization of heat transfer utilizing graph based evolutionary algorithms. International Journal of Heat and Fluid Flow 24 pp 267–277.

Bryden, M., Still, D., Scott, P., Hoffa, G., Ogle, D., Bailis, R., Goyer, K., & United States. Environmental Protection Agency. Office of Air and Radiation. 2005. Design principles for wood burning cook stoves. Washington, DC: U.S. Environmental Protection Agency, Office of Air and Radiation.

Burnham-Slipper, H. et al. 2007a. Jet impingement heat transfer for low nozzle-to-plate clearances. In: Proceedings of 10th UK National Heat Transfer Conference. Edinburgh, 10-11 September 2007.

Burnham-Slipper, H. 2007b. A simplified wood combustion model for use in the simulation of cooking fires. Proceedings of the 5th international conference on heat transfer, fluid mechanics and thermodynamics, Sun City, South Africa.

Burnham-Slipper, H. 2008. Breeding a better stove: the use of Computational Fluid Dynamics and Genetic Algorithms to optimize a wood burning stove for Eritrea. PhD Dissertation, University of Nottingham.

Bussmann, P. J. T., Prasad, K. K., 1982. Model predictions of temperature and velocity profiles in turbulent diffusion buoyant flames. Proceedings of the 7th International Heat Transfer Conference EN4.

Bussmann, P.J.T., Visser, P., Prasad, K. 1983. Open Fires: Experiments and Theory. Proceedings of the Indian Academy of Sciences, Engineering Sciences, 6(1):1-34.

Bussmann, P. J. T., Prasad, K. K., 1986, Parameter Analysis of a Simple Wood-Burning Cookstove, Proc. of the 8th International Heat Transfer Conference, San Francisco, CA, 6:3085-3090.

Bussmann, P. 1988. Woodstoves: Theory and Applications in Developing Countries. PhD dissertation, Eindhoven University of Technology.

Clark, S.H., Kays, W.M. 1953. Trans. ASME 75:859.

Cussler, E.L. 1997. Diffusion: Mass transfer in fluid systems (2nd edition). Cambridge: Cambridge University Press.

Daioglou,V., van Ruijven, B.J., van Vuuren, D.P. 2012. Model projections for household energy use in developing countries. Energy 37:601-615.

Date, A. 1988. Investigation of CTARA wood-burning stove. Part II. Analytical Investigation. Sadhana, 13(4):295-317.

Date, A. 2011. Analytic Combustion: With Thermodynamics, Chemical Kinetics, and Mass Transfer. Cambridge University Press.

De Lepeleire, G., Prasad, K. K., Verhaart, P., and Visser, P. 1981. A woodstove compendium. Eindhoven University of Technology.

De Lepeleire, G.; Christiaens, M. 1983. Heat transfer and cooking woodstove modelling. Proceedings of the Indian Academy of Sciences, Engineering Sciences, 6(1): 35-46.

Demirbas. 2004. Combustion characteristics of different biomass fuels. Progress in Energy and Combustion Science. 30:219-230.

Eckert, E.R.G., Drake, R.M. 1972. Analysis of heat and mass transfer. McGraw-Hill, KogaKusha.

Engineering Equation Solver (EES). 2011. S.A. Klein.

Era, Y., Saima, A. 1976. Bulletin J.S.M.E. 19:800.

Gupta, R., Mittal, N.D. 2010a. Flow and Heat transfer in a single-pan wood stove. International Journal of Engineering Science and Technology. 2(9):4312-4234.

Gupta, R., Mittal, N.D. 2010b. Pyrolysis modelling in a wood stove. International Journal of Engineering Science and Technology. 2(10):5088-5098.

Hannani SK, Hessari E, Fardadi M, Jeddi MK. 2006. Mathematical modeling of cooking pot efficiency using experimental and neural network method. Energy; 31:2969–2985.

Hartter, J., Boston, K. 2007. An integrated approach to modeling resource utilization for rural communities in developing countries. Journal of Environmental Management 85:78-92.

Hollman, J.P. 1975. Heat Transfer. London:McGraw Hill-Kogakusha.

Hrycak, P. 1978. Proceedings of the 5th International Heat Transfer Conference 2:EC-11.

Incropera FP. DeWitt DP, Bergman TL, Lavine AS. 2007. Fundamentals of Heat and Mass Transfer, 6th Edition. John Wiley & Sons.

International Energy Agency (IEA), 2010. Energy Poverty: How to make modern energy access universal? World Energy Outlook, Paris.

Jeddi M.K., Hannani, S.K., Farhanieh, B. 2004. Study of Mixed-convection heat transfer from an impinging jet to a solid wall using a finite-element method – Application to cooktop modeling. Numerical Heat Transfer, Part B: Fundamentals: An International Journal of Computation and Methodology, 46(4): 387-397.

Jetter, J.J., Kariher, P., 2009. Solid-fuel household cook stoves: Characterization of performance and emissions. Biomass and Bioenergy; 33:294-305.

Jetter J, Zhao Y, Smith KR, Khan B, Yelverton T, DeCarlo P, Hays MD. 2012. Pollutant emissions and energy efficiency under controlled conditions for household biomass cookstoves and implications for metrics useful in setting international test standards. Environmental Science & Technology. 46(19):10827-10834.

Johnson, M., Edwards, R., Alatorre Frenk, C., Masera, O., 2008. In-field greenhouse gas emissions from cookstoves in rural Mexican households. Atmospheric Environment 42 (6): 1206–1222. doi:10.1016/j.atmosenv.2007.10.034.

Johnson, M., Edwards, R., Berrueta, V., Masera, O., 2010, "New Approaches to Performance Testing of Improved Cookstoves," Environ. Sci. Technol., 44:368–374.

Johnson N.G., Bryden K.M., 2012a. Energy supply and use in a rural West African village. Energy, 43:283–92.

Johnson, N.G., Bryden, K.M., 2012b. Factors affecting woodfuel consumption in household cookstoves in an isolated rural West African village. Energy, 46:310–21.

Joshi, J et al. 2012. Development of efficient designs of cooking systems. II. Computational fluid dynamics and optimization. Industrial & Engineering Chemistry Research. 51:1897–1922

Kausley SB, Pandit AB. 2010. Modelling of solid fuel stoves. Fuel 89: 782-791.

Khummongkol P., Wibulswas P, Bhattacharya SC. 1988. Modeling of a Charcoal Cook Stove. Energy; 13(11): 813-821.

Kumar, R., Lokras, S.S., Jagadish, K.S. 1990. Development, analysis & dissemination of a 3-pan cookstove. Indian Institute of Science, Bangalore.

Legros, G., Havet,I.,Bruce,N.,Bonjour,S. 2009. The Energy Access Situation in Developing Countries. World Health Organization and UNDP.

Lim, S.S., et al. 2012. A Comparative Risk Assessment of Burden of Disease and Injury Attributable to 67 Risk Factors and Risk Factor Clusters in 21 regions, 1990-2010: A Systematic Analysis for the Global Burden of Disease Study 2010. Lancet, 380:2224–60

L'Orange, C., DeFoort, M., Willson, B., 2012, Influence of Testing Parameters on Biomass Stove Performance and Development of an Improved Testing Protocol, Energy Sustainable Dev., 16:3–12.

MacCarty N.A., Still D.K., Ogle D.M. 2010. Fuel use and emissions performance of fifty cooking stoves in the laboratory and related benchmarks of performance. Energy for Sustainable Development. 14:161-171.

McCorkle, D.S., Bryden, K.M., Carmichael, C.G. 2003. A new methodology for evolutionary optimization of energy systems. Comput. Methods Appl. Mech. Engrg. 192:5021–5036.

Prasad, K.K. 1981. Some studies on open fires, shielded fires, and heavy stoves. Eindhoven University of Technology. Eindhoven, the Netherlands.

Prasad, K.K, Sangen. E. 1983. Technical Aspects of Woodburning Cookstoves. Eindhoven University of Technology. Eindhoven, the Netherlands.

Prasad, K. K., Sangen, E., Visser, P. 1985. Woodburning Cookstoves. In Advances in Heat Transfer; Hartnett, J. P., Thomas F., Irvine, J., Eds.; Elsevier: Vol. 17:159-317.

Ragland, K.W., Baker, A.J. 1991. Properties of Wood for Combustion Analysis. Bioresource Technology. 37: 161-168.

Ragland K.W., Bryden K.M. 2011. Combustion Engineering, Second Edition. CRC Press, Florida.

Ravi MR, Kohli S, Ray A. 2002. Use of CFD simulation as a design tool for biomass stoves. Energy Sustain Dev., VI(2):20-27.

Ravi, M.R., Sinha, S., Jhalani, A., and Ray, A., 2002. ‘‘Development of a semi-empirical model for pyrolysis of an annular sawdust bed’’, J. Anal. Appl. Pyrolysis, 71:353-374.

Rehfuess E. 2006. Fuel for life - household energy and health. Geneva, World Health Organization. 2006. Available from: http://www.who.int/indoorair/publications/fuelforlife.pdf [accessed 11.13.12].

Roden, C.A., Bond, T.C., Conway, S., Pinel, A.B.O, MacCarty, N., Still, D., 2009. Laboratory and field investigations of particulate and carbon monoxide emissions from traditional and improved cookstoves. Atmospheric Environment; 43:1170-1181.

Ruiz-Mercado, I., Masera, O., Zamora, H., Smith, K. R., 2011, “Adoption and Sustained Use of Improved Cookstoves,” Energy Policy, 39:7557–7566.

Schlunder, E.U., Gnielinski, V. 1967. Chemie-Ingeniew-Technik 39:578.

Schutte, E. Prasad, Krishna K. (eds) 1989. Woodcombustion Studies, Part I. The Woodburning StoveGroup Eindhoven, University of Technology, Eindhoven (Netherlands).

Schutte, E., Prasad, Krishna K., Moerman, E. 1991. Woodcombustion Studies, Part II. The Woodburning Stove Group Eindhoven, University of Technology, Eindhoven (Netherlands).

Seban, R.A., Black, L.H. 1961. International Journal of Heat and Mass Transfer 3:255.

Seward, F.R., 1970. Prediction of the height of turbulent diffusion buoyant flames. Combustion Science and Technology 2:203-212.

Shah, R.K., London, A.L. Undated. Laminar flow forced convection.

Shah R, Date AW. 2011. Steady-State Thermochemical Model of a Wood-burning cook stove. Combustion Science and Technology; 183(4):321-346.

Shaughnessy, E.J.Jr., Katz, I.M., Schaffer, J.P. 2005. Introduction to Fluid Mechanics. Oxford University Press.

Simmons, G., Lee, W.H. 1965. Fundamentals of thermochemical biomass conversion. Amsterdam: Elsevier.

Smith, K., 1993. Fuel Combustion, air pollution exposure, and health: the situation in developing countries. Annual Review of Energy and the Environment 18 (1):529–566. doi:10.1146/annurev.eg.18.110193.002525.

Smith, K.,Uma,R.,Kishore,V.,Lata,K.,Joshi,V.,Zhang,J.,Rasmussen,R.,Khalil,M., 2000. Greenhouse Gases from Small-scale combustion Devices in Developing Countries, Phase IIA: household Stoves in India, USEPA, Washington, DC (Report no. EPA/600/R-00/052). Available from: /www.epa.gov/nrmrl/pubs/ 600r00052/600R00052.pdfS.

Smith KR, Dutta K, Chengappa C, Gusain PPS, Masera O, Berrueta V, Edwards R, Bailis R, Naumoff Shields K. 2007. Monitoring and evaluation of improved biomass cookstove programs for indoor air quality and stove performance: conclusions from the Household Energy and Health Project. Energy for Sustainable Development;11(2):5-18

Sovacool, B.K. 2012. The political economy of energy poverty: A review of key challenges. Energy for Sustainable Development. 16:272-282.

Taylor, III R. P., 2009, The Uses of Laboratory Testing of Biomass Cookstoves and the Shortcomings of the Dominant U.S. Protocol. M.S. Thesis, Iowa State University. Ames, IA.

Tinney, E.R. 1965. Proceedings of the Tenth International Symposium on Combustion. Philadelphia, Combustion Institute. pp 925-930.

Tiwari, G. N., Yadav, Y.P. 1987. Transient Analysis of Conventional Mud Chullah. Energy Conversion and Management. Vol 27(2):149-152.

Turns, S. 2000. An Introduction to Combustion: Concepts and Applications. McGraw-Hill, USA.

Urban GL, Bryden KM, Ashlock DA. 2002. Engineering optimization of an improved plancha stove. Energy for Sustainable Development; Volume VI (2).

Verhaart, P. 1982. On Designing Woodstoves. Proceedings of the Indian Academy of Sciences, Engineering Sciences. 5(4):287-326.

Visser, P. 1984. Unpublished report. Eindhoven University, The Netherlands.

Weerasinghe, W.M.S.R., Kumara, U.D.L. 2003. CFD Approach for Modelling Of Combustion in a Semi-Enclosed Cooking Stove. Proceedings of the International Conference on Mechanical Engineering 2003, Bangladesh. ICME2003.

Wohlgemuth A, Mazumder S, Andreatta D. 2009. Computational Heat Transfer Analysis of the Effect of Skirts on the Performance of Third-World Cookstoves. ASME Journal of Thermal Science and Engineering Applications; Vol. 1 / 041001-1-10.

World Health Organization (WHO), 2004. Addressing the links between indoor air pollution, household energy, and health. WHO/HDE/HID/02.10.

Zhang, J., Smith, K., Ma, Y., Ye, S., Jiang, F., Qi, W., Liu, P., Khalil, M., Rasmussen, R., Thorneloe, S.A., 2000. Greenhouse gases and other airborne pollutants from household stoves in China: a database for emission factors. Atmospheric Environment 34(26): 4537–4549. doi:10.1016/S1352-2310(99)00450-1.

Zube, D.J. 2010. Heat transfer efficiency of biomass cookstoves. M.S. Thesis, Colorado State University, Fort Collins, Colorado.